CONTRACT NO. 04-319
FINAL REPORT
MAY 2009

Particle Phase Peroxides: Concentrations, Sources, and Behavior

CALIFORNIA ENVIRONMENTAL PROTECTION AGENCY

AIR RESOURCES BOARD
Research Division

PARTICLE PHASE PEROXIDES: CONCENTRATIONS, SOURCES, AND BEHAVIOR

FINAL REPORT
CONTRACT NO. 04-319

PREPARED FOR:

CALIFORNIA AIR RESOURCES BOARD
RESEARCH DIVISION
CALIFORNIA ENVIRONMENTAL PROTECTION AGENCY
1001 I STREET
SACRAMENTO, CALIFORNIA 95814

PREPARED BY:

S.E. PAULSON, PRINCIPAL INVESTIGATOR

UNIVERSITY OF CALIFORNIA
LOS ANGELES, CALIFORNIA 90089-0029

MAY, 2009

For more information about the ARB's, Research Division's research and activities, please visit our Website:

http://www.arb.ca.gov/research/research.htm

Table of Contents

1. Executive Summary

Recent epidemiological studies have shown a strong relationship between particulate pollution and health outcomes, including increased mortality. Determining the 'causative agent' in particles responsible for damaging health is the subject of increasing research activity, but many questions remain. A class of biologically active species known collectively as reactive oxygen species (ROS) is a candidate for part of the adverse health effects caused by particle inhalation. In particles, hydrogen peroxide, H_2O_2, is the dominant ROS, and the only one that can be measured directly. Ambient particulate peroxide levels exceed those expected from gas-particle partitioning by factors of 200-1000 (Arellanes et al., 2006). This indicates particles *generate* peroxide in aqueous solution (Hasson and Paulson, 2003, Arellanes et al., 2006).

In numerous *in vitro* studies, hydrogen peroxide at levels well below those measured in ambient samples has been shown to damage lung epithelial cells (Oosting et al., 1990, Holm et al., 1991, Brown et al., 2004, Li et al., 2002). Recently, an *in vivo* study showed that two-hour exposures to particulate hydrogen peroxide produced symptoms associated with respiratory distress, while gas-phase peroxides or ammonium sulfate particles alone elicited on minimal responses (Morio, et al., 2001). Morio et al. (2001) used elevated PM levels and gas phase H_2O_2 in their study in an effort to create an exposure environment with elevated H_2O_2 dissolved in ammonium sulfate particles, but they were not able to measure particulate peroxide concentrations. As part of this project we duplicated the particle generation system used for the *in vivo* study in our laboratory and found that because ambient particles generate H_2O_2 while ammonium sulfate particles do not (they simply take up H_2O_2 from the gas phase according to Henry's law), the peroxide concentrations used in that study were well within the normal range for particulate peroxide levels in polluted areas. The *in vivo* results combined with our understanding of peroxides in the study's particles and in ambient air indicates that very short term exposures (2 hours) to peroxide levels generated by ambient particles produces measurable changes in lung physiology related to inflammation and respiratory distress.

At this time, the underlying mechanism by which particles generate H_2O_2 is not known. The most likely candidates are redox reactions mediated by transition metals and quinones (Hasson and Paulson, 2003, Arellanes et al., 2006). Transition metals are generally present in sufficient concentrations that they, especially if combined with organics that prolong the lifetimes of their photo-oxidized forms, could account for the observed generation of H_2O_2. Quinones are generally

not present in particles at concentrations sufficient to account for the observed H_2O_2 unless there is a suitable but unknown electron donor in the particles.

In this study, particles were collected on Teflon® filters using impactors to create size cuts, for periods of 1-30 hours for ambient samples or minutes for source materials. The filters were extracted within 30 minutes of sampling completion, using pH adjusted water with ethylene diamine tetra-acetic acid (EDTA) added, and gentle agitation. H_2O_2 was monitored in the samples using high pressure liquid chromatography (HPLC) with fluorescence detection.

In order to further understand the phenomenon of H_2O_2 generation by particles and its relevance to particle health effects, we carried out a series of studies to elucidate H_2O_2 generation activity as a function of pH, and in solutions designed to partly mimic physiological fluids. We also monitored the time dependence of H_2O_2 generation both when particles are in solution and when they are aged on a filter after collection.

The pH of the extraction solution has a different effect on coarse and fine mode particles. Coarse mode particles (>2.5 μm) generate maximum H_2O_2 at pHs between 1 and 3; H_2O_2 generation monotonically decreases between pH 3 and 6, and flattens out again above pH 6 up to 8, at a level that is about 30% of the maximum (low pH) value. This behavior is consistent with H_2O_2 production by transition metals, particularly iron, for which the rates of several redox reactions have been observed to be enhanced by low pHs.

In contrast to coarse particles, fine mode particles (<2.5 μm) generated maximum H_2O_2 at pH 4.5, and lower H_2O_2 generation at both lower and higher pHs. H_2O_2 generation at pH 7.4 was about half of the maximum observed at pH 4.5. This behavior may be consistent with contributions from more than one mechanism to H_2O_2 generation, such as a combination of transition metal and quinone activity.

H_2O_2 generation was either unaffected or significantly enhanced by extraction solutions made to partly mimic lung lining fluid or other physiological fluids. Gamble's and Ringer's solutions, two 'physiologically relevant' solutions from the literature, have ionic strengths of 0.15-0.19 M, pHs of 7.4 and a mixture of inorganic salts. In the case of Gamble's solution, sodium citrate and glycine are also added. Ringer's solution produced larger enhancements to H_2O_2 production (relative to extraction in pH 7.4 waters, by factors averaging 6.5 (4.7 to 7.3) and 3.2 (1.8 to 4.2) for the fine and coarse modes, respectively. Gamble's solution had a smaller effect: fine mode particle H_2O_2 production was enhanced by an average factor of 3.4 (with a range of 2 to 4.2), while the coarse mode exhibited no significant change (average 1.2, range 0.5 to 1.5). There was a reasonably large

degree of variability in this response between samples, so it is not clear that this effect will necessarily be the same for all samples. These results, however, point in the direction of significant generation of H_2O_2 by ambient particles *in vivo*.

Ambient particles were aged to investigate the decay of H_2O_2 generation activity. For the first day or so, particles retain 80 to 90% of their initial activity. By 120 hrs, particles exhibited H_2O_2 activity that was less than 10% of the initial value. Measurements of H_2O_2 production by secondary organic aerosols generated in the laboratory suggests that H_2O_2 generation is an even more labile property of these aerosols; H_2O_2 generation dropped to 15% of the original signal after 45 hours. These reductions in H_2O_2 activity highlight the importance of using fresh particles to study the health effects of ROS. Particles older than a week or two presumably induce effects that are due to something other than their intrinsic ability to generate H_2O_2 and ROS.

Once particles are extracted, the rise of H_2O_2 in solution is fastest in the first 15 or so minutes. The rate of H_2O_2 production declines continuously, reaching an inflection point after about 100 minutes and continuing at a low rate for several hours to several days. Eventually, some particles start to consume ROS. As the process is likely a mixture of reaction kinetics and particle dissolution, it is difficult to compare the process to pure reaction kinetics, but it indicates that after inhalation, this aspect of particle toxicity may taper off after a day to several days.

More finely size fractionated aerosols were collected with a Micro Orifice Uniform Deposition Impactor (MOUDI) for longer periods of 24-30 hours. H_2O_2 generation collected with the MOUDI were in good agreement with the results collected with the virtual impactors, consistent with the aging result above, indicating that particles maintain most of their ability to generate H_2O_2 for durations of about a day. Fine, coarse, and ultrafine fractions exhibited noticeably different behavior for most samples. Overall averages of H_2O_2 generation normalized to particle mass are similar between the size cuts for the UCLA site. The ultrafine size cut has a very small mass of particles, and as a result frequently does not produce signals that are above the detection limit.

A variety of source materials and additional test aerosols were analyzed for ROS generation, including fresh particles from conventional diesel, biodiesel, and biogenic secondary organic aerosols generated in the laboratory, and a standard reference material, NIST SRM 1649a. NIST SRM 1649a was collected in the 1970s, and as expected, showed no ROS generation activity. Diesel PM was investigated repeatedly, both from on-road engines on a chassis dynamometer and from a diesel generator, and showed variable activity depending on load. However, in all cases except one, the H_2O_2 generation activity was well below average ambient activities normalized to particle mass.

Because conventional diesel particles are not very soluble, however, it is unclear if analysis of very fresh diesel particles provides a full picture of the ability of diesel particles to generate ROS. A small number of biodiesel PM samples indicate that biodiesel has significantly higher ROS activity, but the difference may be due in part to their increased solubility in the aqueous extraction solution relative to conventional diesel. Biogenic secondary organic aerosols generated in the laboratory exhibit variable, but generally high ROS generation activity, relative to diesel and ambient aerosols.

This report details many measurements made on ambient aerosols, several of which were collected using a pair of virtual impactors (VIs). The impactors were chosen because they accommodate a high sample flow rates of 55 LPM, while making a single size cut at 2.5 μm, which in turn allows a reasonably high measurement time resolution of 1-3 hours. Measurements made in Riverside in August 2005 had shown highly variable fine mode H_2O_2 levels, and sporadic very high levels of copper, zinc and lead, leading us to suspect either an unusual local industrial source of Cu/Zn/Pb, or sample contamination. Initial investigations did not turn up a contamination source, so we continued to use the VIs in some cases. More recently we have determined that the VIs are indeed releasing Cu and Zn, into the fine mode channel. Similar results have been reported in high velocity inlets (Murphy et al., 2004). As a result, several sets of fine mode results are not reported here. They may be reported later if they are corroborated by results from repeated measurements made with new sampling equipment.

Field campaigns were conducted in Riverside at two different sites: a parking lot on the UC Riverside campus downwind of the 60 freeway during August 2005, and an orange grove on the UC Riverside campus upwind of the 60 freeway during July-August 2008. Because of the contamination issue, only coarse mode results are included in this report. Both campaigns point to metals as the cause of ROS generation in the coarse mode. Correlations between H_2O_2 generation and iron content in the aerosols were significant at the parking lot site, and strong in the orange grove. The orange grove results also showed a significant correlation between ROS generation and aluminum, which was not measured in the earlier study. Additionally, while coarse mode H_2O_2 generation per unit mass was lower at the Riverside site than at UCLA or at the 110 freeway site, because of the very high mass loadings in Riverside, total H_2O_2 generation by coarse mode aerosols in Riverside are higher than at UCLA or the 110 Freeway site. In all of the measurements at Riverside, H_2O_2 activity had little or no significant correlation with particle mass, consistent with the notion that chemical composition plays a more significant role in H_2O_2 generation than does particle mass.

2. Introduction

2.1 Background

2.1.1 Particle Health Effects

Tiny solid or liquid particles in the air have long been known to obscure visibility, damage materials, and adversely affect human health. During recent years, research in this area has escalated due to recognition of the role of aerosols, particularly those smaller than 2.5 microns ($PM_{2.5}$), in delivering potentially toxic compounds deep into the lungs. Recent epidemiological studies indicate that increases in human morbidity and mortality due to lung cancer, cardiopulmonary disease, and asthma are associated with significantly lower concentrations of fine particles ($PM_{2.5}$) than those previously thought to affect human health (Tolbert et al. 2000; Pope et al. 2002; Samet 2002) . Ultrafine particles (< 0.1 μm) and smaller fine particles (< 0.3 μm) may be especially toxic (Salvi and Holgate 1999; Utell and Frampton 2000) and have recently been shown to be able to penetrate through cell walls, entering both lung epithelial cells and macrophages, and potentially leading to mitochondrial damage (Li et al. 2003). Coarse particles (generally >2.5 μm, <10 μm) are clearly not free of toxic effects, however. Several recent studies have found them to be more toxic than fine mode particles (Kleinman et al. 2003; Schins et al. 2004) .

The origins of particle toxicity are beginning to be unraveled. Particulate matter contains a large variety of chemical components, including metals, organic carbon of both primary and secondary origin, soot, inorganic acids and bases, salts, water, reactive oxygen species such as H_2O_2, hydroxyl radical, and the superoxide ion, and biological material such as endotoxins. Increasing evidence supports the notion that particles themselves, as well as compounds adsorbed to their surfaces, are toxic; much of particle activity remains even after washing with organic and aqueous solvents (Sagai et al. 1993; Utell and Frampton 2000; Murano et al. 2002) . Reactive oxygen species (ROS, oxygen centered free radicals and their metabolites) play a clear role in inflammatory responses, which are implicated in both respiratory distress diseases such as asthma, and in carcinogenesis. Because of this, aerosol-borne compounds that elicit formation of ROS, as well as ROS themselves, have been the subject of intense investigation (Gurtner et al. 1987; Oosting et al. 1990; Holm et al. 1991; Sporn et al. 1992; Crim and Longmore 1995; Sagai et al. 2000; Li et al. 2002; Brown et al. 2004; Vidrio et al., 2008).

2.1.2 Reactive Oxygen Species

Generally the most biologically consequential reactive oxygen species (ROS) are H_2O_2, hydroxyl radical, and the superoxide ion ($O_2^{\cdot}$-). H_2O_2, which is extremely soluble, has the potential to dissolve in the liquid phase of particles and experience enhanced delivery into lungs (Friedlander and Yeh 1998) . Superoxide, hydrogen peroxide and the hydroxyl radical are closely coupled via a series of redox reactions. Of the coupled ROS, $O_2^{\cdot}$-, H_2O_2 and $HO^{\cdot}$, H_2O_2 is a fairly stable intermediate, and the only one that may be monitored directly.

Superoxide results from a single electron addition to molecular oxygen:

$$O_2 + e^- \rightarrow O_2^{\cdot}- \quad (1).$$

Superoxide is generated in small amounts as a byproduct of metabolic consumption of oxygen:

$$O_2 + 4\,H^+ + 4\,e^- \leftrightarrow 2\,H_2O \quad (2).$$

Superoxide is also produced in atmospheric water (i.e., cloud and fog drops as well as, presumably, water associated with aerosol particles) by Fe^{2+} in reaction (9) below, and by other mechanisms that are enhanced by sunlight but not well established (Anastasio et al. 1997 ; Finlayson-Pitts and Pitts 2000). Particularly at low pH, superoxide reacts spontaneously to form H_2O_2. *In vivo*, the enzymes superoxide dismutase and glycolate oxidase catalyze this reaction.

$$2\,O_2^{\cdot}- + 2\,H^+ \rightarrow O_2 + H_2O_2 \quad (3).$$

Superoxide can also react with HO_2 to generate H_2O_2:

$$O_2^{\cdot}- + HO_2 \rightarrow O_2 + HO_2^- \ (+ H^+) \rightarrow H_2O_2 \quad (4).$$

Superoxide itself is easily converted to HO_2 particularly at low pH:

$$O_2^{\cdot}- + H^+ \rightarrow HO_2 \quad (5).$$

HO_2 also disproportionates to generate H_2O_2. The analogous gas-phase reaction is a dominant source of H_2O_2 in the gas phase.

$$HO_2 + HO_2 \rightarrow H_2O_2 + O_2 \quad (6).$$

Reduction of hydrogen peroxide results in production of the reactive hydroxyl radical:

$$H_2O_2 + e^- \rightarrow HO^{\cdot} + OH^- \quad (7).$$

When this transformation is catalyzed by iron or another transition metal, it is known as the *Reaction* (Fenton 1894) :

$$H_2O_2 + Fe^{2+} \rightarrow HO^{\cdot} + OH^- + Fe^{3+} \quad (8).$$

Fe^{2+} also catalyzes the formation of H_2O_2:

$$Fe^{2+} + O_2 \rightarrow O_2^{\cdot}- + Fe^{3+} \quad (9),$$

$$Fe^{2+} + O_2^{\cdot}- + 2\,H_2O \rightarrow H_2O_2 + 2\,OH^- + Fe^{3+} \quad (10),$$

$$Fe^{2+} + HO_2 + H^+ \rightarrow H_2O_2 + Fe^{3+} \quad (11).$$

In water in equilibrium with the atmosphere, Fe^{2+} tends to reduce oxygen via reaction (9), rather than destroy H_2O_2 via reaction (8), due to the high concentration of dissolved O_2 coupled with the ratio of reaction rates of (8) and (9).

Hydrogen peroxide is a common gas in the atmosphere, and it is moderately elevated in polluted air. Unlike other ROS such as O_3, H_2O_2 is extremely soluble in water, so substantial concentrations are anticipated in the aerosol phase. The transport of hydrogen peroxide into the alveolar portion of the lung can arise via transfer from the gas or particle phases. As a result of its high solubility and diffusivity, the gas-phase peroxides are expected to be absorbed in the upper airways and thus be unable to penetrate into the lower lung (Wexler and Sarangapani 1998) . In their study of the effects of H_2O_2 and aerosols on rats, however, Morio et al. (2001) found that gas phase H_2O_2 generated the same suite of changes that were observed for the combination of aerosols and H_2O_2 but to a lesser degree, indicating that there was some transport of gas-phase peroxides into the lower lung. This was confirmed using ^{18}O-labeled H_2O_2, which was found to deliver the isotope into the lavage fluid (Morio et al., 2001). Both coarse-mode and ultra-fine particles also tend to deposit in the upper airways, where they play a role in upper airway-related diseases such as asthma and other allergic responses. The fine mode aerosol particles, on the other hand, have a low diffusivity and penetrate more effectively into the lower lung, where 20 - 30% of the particles deposit (Hinds 1982) . In principle, as the gas-phase peroxides are absorbed in the upper airway, some of the aerosol peroxides may desorb from the particles. In practice, the evidence indicates that particles do enhance delivery of H_2O_2 (Morio et al., 2001). Desorption may be inhibited by other solutes that enhance the solubility of the peroxides, or, as appears to be the case for urban aerosols, peroxides may be continuously generated by the particles once they deposit in the lung.

2.1.3 The Role of H_2O_2 in Cell Injury

Several studies have investigated the effects of H_2O_2 on respiratory tract cells, and their results form part of the framework supporting the hypothesis that oxidative stress, caused by elevated levels of ROS, results in substantial cell damage (Gurtner et al. 1987; Oosting et al. 1990; Holm et al. 1991; Sporn et al. 1992; Crim and Longmore 1995; Dellinger et al. 2001; Li et al. 2002). One of the ways in which particles appear to induce health effects, including many pulmonary diseases, is to change the level of generation of ROS by lung tissues (Kehrer 1993 ; Morio et al. 2001; Kleinman et al. 2003 ; Brown et al. 2004). Alveolar macrophages (the first line of

immunological defense against inhaled particles), neutrophils, and bronchial epithelial cells generate ROS and other mediators in response to foreign substances such as particles (Laskin and Pendino 1995; Li et al. 2002). Excessive ROS, from either endogenous or exogenous sources, can overwhelm the anti-oxidant capabilities of tissues, such that a state of oxidative stress is created (Kehrer 1993) . Oxidative stress is a 'biological emergency' that in turn initiates airway inflammation and a range of cellular responses (Li et al. 2003).

It has been demonstrated that the exposure of respiratory tract cells to aqueous H_2O_2 solutions at concentrations ranging from 20 pM to 1mM results in significant amounts of cell damage (Gurtner et al. 1987; Oosting et al. 1990; Holm et al. 1991; Sporn et al. 1992; Crim and Longmore 1995; Geiser et al. 2004). These concentrations are significantly lower than those we have measured in urban aerosols, which fall in the 10-100 mM range (below). The effects of the hydrogen peroxide solutions include inhibition of the conversion of ADP to ATP at 75 μM H_2O_2 (Crim and Longmore 1995), the destruction of the alveolar epithelium, including DNA strand breaking and decrease in lung surfactant biosynthesis at concentrations starting at 50-500 μM H_2O_2 (Oosting et al. 1990; Holm et al. 1991; Sporn et al. 1992), and the inhibition of alveolar epithelial wound repair at 100-300 μM H_2O_2 (Geiser et al. 2004). Additionally, ROS may be generated via reactions of other particle-borne pollutants, such as semiquinone radicals in the lung itself (Dellinger et al. 2001).

One animal study has been performed specifically to assess the effects of H_2O_2 in aerosols (Morio et al. 2001). In this study, Morio et al. (2001), exposed Sprague-Dawley rats to: a) laboratory-generated $(NH_4)_2SO_4$ aerosols at high concentrations of 215 or 430 $\mu g/m^3$, b) high concentrations (relative to ambient) of H_2O_2 of 10, 20 or 100 ppb, or c) a combination of the high concentration H_2O_2 and $(NH_4)_2SO_4$ aerosols. Relative humidity was maintained at 85% and animals were exposed for short time periods (relative to typical ambient exposures) of 2 hours. These levels of both particle mass and H_2O_2 are higher than typical ambient levels (5-100 $\mu g/m^3$ and 0.1-10 ppb in urban air, respectively), but exposure times are short. At the time of that study, little was known about measuring particulate H_2O_2, and this parameter was not measured by the researchers. A number of responses that are associated with inflammation in lung tissues were assayed. $(NH_4)_2SO_4$ aerosols or H_2O_2 alone were observed to induce slight responses; in the case of H_2O_2 they were noticeable. For rats exposed to a combination of aerosols and H_2O_2, the responses were pronounced. Electron microscopy of lung tissues both immediately and 24 hours after exposure revealed increased numbers of neutrophils in pulmonary capillaries adhered to the vascular endothelium, as well as

increased tumor necrosis factor-α production by alveolar macrophages. As discussed by Morio et al., (2001), neutrophil influx and adherence is the first step in the inflammatory response to tissue injury (Wagner and Roth 2000), and neutrophil adherence has been reported to stimulate the release of tumor necrosis factor-α from macrophages (Sredni-Kenigsbuch et al. 2000). Tumor necrosis factor-α is an early response proinflammatory cytokine known to activate neutrophils and macrophages (Brouckaert and Fiers 1996). The response was moderate, however, since changes in bronchoalveolar lavage fluid cell number, viability, or protein content or lactate dehydrogenase levels were not observed. Exposure to combined aerosol and H_2O_2 also revealed a transient increase in production of superoxide anion by alveolar macrophages, followed by an eventual reduction in superoxide production. Nitric oxide production was decreased by exposure to H_2O_2 either alone or in combination with aerosol, which Morio et al. (2001) suggested may be due to superoxide anion-driven formation of peroxynitrite. Finally, Morio et al. (2001) found that expression of the antioxidant enzyme heme oxygenase-1 was increased in rats exposed to the combination of aerosol and H_2O_2. Cells respond to oxidative stress by generating heat shock proteins, including heme oxygenase-1 (Bierkens 2000).

Each of these responses has been observed to be associated with cellular responses to particulate matter. Increases of tumor necrosis factor-α were observed following exposure to PM10 and PM2.5 (Li et al. 1996 ; Imrich et al. 1999). Increases and subsequent decreases of superoxide production have also been correlated with inhaled PM (Li et al. 1996 ; Kleinman et al. 2003) . Increased expression of heme oxygenase-1 by alveolar macrophages has been observed by Li et al. (2000) following *in vitro* exposure of alveolar macrophages to diesel exhaust.

In choosing $(NH_4)_2SO_4$ as the matrix aerosol, Morio et al. (2001) may have unknowingly generated aerosols that did not deliver H_2O_2 to the test animals that was enhanced relative to ambient aerosols. Since Morio et al.'s 2001 study, we have measured H_2O_2 in ambient aerosols and have found them to exceed levels predicted by gas-particle partitioning (Henry's Law, described below) by at least a factor of 300. Ammonium sulfate is a major component of many ambient aerosols, but it contains none of the complexities of ambient aerosols. Here, we report measurements of H_2O_2 by $(NH_4)_2SO_4$ aerosols, and as expected, the results are consistent with gas-liquid partitioning governed by Henry's law. We also discuss the implication of these results.

2.1.4 Peroxides in Particles: Atmospheric Chemistry

Gas-phase hydroperoxides are formed in the atmosphere via two routes: (1) gas-phase reactions of HO_2 with itself and with RO_2 (e.g., Lightfoot et al. 1992) , and (2) water reacting with the 'Criegee intermediate' product of alkene ozonolysis (Hasson et al. 2001a, b) .

Hydroperoxides are expected to partition between the gas-phase and liquid water according to their Henry's law constants:

$$A_{(g)} \Leftrightarrow A_{(l)} \quad (12)$$

$$H_A \times P_A = [A] \quad (13)$$

where H_A is the Henry's law constant (M atm^{-1}), [A] is the liquid-phase concentration of A (M), and P_A is the gas-phase partial pressure of A (atm). H_A for H_2O_2 is 1.0×10^5 M atm^{-1} at 25 °C (Sander 1999). For a "typical" urban scenario, with a gas phase H_2O_2 concentration of 2 ppb and an aerosol mass loading of 50 $\mu g/m^3$, of which 50% is water, Henry's law predicts an aerosol hydrogen peroxide concentration of 0.16 ng/m^3, or 0.18 mM in the aerosol liquid water.

Numerous measurements of gas phase H_2O_2 concentrations have been made using some twenty methods. Maximum H_2O_2 concentrations of 10 ppb have been observed with a strong dependence on NO_x, location, and season (Jackson and Hewitt 1999; Lee et al. 2000) . Measurements of organic hydroperoxides in ambient air, which have been much less common, indicate that organic hydroperoxides comprise from 10% up to 60% of the total hydroperoxide loading in the gas phase (Heikes et al. 1987; Hellpointner and Gäb 1989; Hewitt and Kok 1991). Methyl hydroperoxide, hydroxymethyl hydroperoxide, ethyl hydroperoxide, 1-hydroxyethyl hydroperoxide, and peracetic acid have all been observed (e.g., Heikes et al. 1987; Hellpointner and Gäb 1989; Hewitt and Kok 1991; Junkermann and Fels 1993).

Previous measurements of gas- and particle-phase H_2O_2 have demonstrated high levels of H_2O_2 associated with ambient particles. Hewitt and Kok (1991), using the same detection method employed here, briefly mention aerosol phase H_2O_2 levels of <0.1 -10 ng m^{-3} at Niwot Ridge, Colorado. Hasson and Paulson (2003) measured both gas- and particle-phase H_2O_2 with mass loadings ranging from <0.1 – 13 ng m^{-3} and roughly estimated that particle phase H_2O_2 levels exceed Henry's Law predictions by a factor of 10, however no particle mass was recorded. Hung and Wang (2001) measured ROS in size segregated aerosols collected on a sidewalk adjacent to a major thoroughfare using a dichlorofluorescein assay calibrated with H_2O_2. They reported an average H_2O_2 equivalence of 21 ng m^{-3} and an inferred H_2O_2 activity defined as ng of H_2O_2 per μg of particle mass

between 0.15 – 0.35 ng μg^{-1}, depending on the size fraction. Sonication was used to extract the aerosols, a process that appears to induce the formation of H_2O_2 and which may have resulted in the high background levels they reported (Hasson and Paulson 2003). They also aged aerosols in ambient air and saw a significant decrease (>60%) in ROS levels over a time period of 110 hrs (Hung and Wang 2001 data recalculated by Hasson and Paulson 2003). Arellanes et al. (2006) reported fine and coarse mode H_2O_2 concentrations of 5.4 ± 6 and 10 ± 7 ng m^{-3}, respectively, and H_2O_2 normalized to aerosol mass levels of 0.58 and 0.51 ng μg^{-1}, respectively, on the campus of UCLA. Additional measurements taken near the heavily traveled 110 freeway had fine and coarse mode H_2O_2 levels that were 12 ± 9 and 20 ± 9 ng m^{-3}, respectively, and measured H_2O_2 normalized to aerosol mass levels of 0.58 and 1.05 ng μg^{-1} in the fine and coarse modes. At all locations sampled, it was shown that particle phase H_2O_2 exceeded levels predicted using Henry's Law by two to three orders of magnitude in both the fine and coarse modes, respectively, demonstrating that particles generate substantial quantities of H_2O_2 in solution for hours after they are collected. Finally, Venkatachari et al. (Venkatachari et al. 2005; Venkatachari et al. 2007) investigated summer and winter concentrations of particle bound-ROS collected in two locations: Rubidoux, CA and Flushing, NY; using the dichlorofluorescein assay and extracting filters with sonication. PM collected in the summer months at Rubidoux was reported to have an average ROS content of 243 ng m^{-3}, a much higher value than observed by any of the four other studies (Hung and Wang, 2001, Hasson and Paulson 2003, Arellanes et al. 2005, Venkatachari et al. 2007). Winter levels of particle associated ROS in Flushing, NY contained an average ROS concentration of 40.2 ng m^{-3}, still high but in much closer agreement with other studies. An evaluation of H_2O_2 activity (ng of H_2O_2 per μg of aerosol mass) was not possible as PM masses were not reported.

Hydrogen peroxide and its related redox species, hydroxyl radical and the superoxide ion have long been recognized as key species in the aqueous phase reactions that take place in water suspended in the atmosphere. They are important in understanding cloud processing of air, and are at the center of acid formation in clouds and of dimethyl sulfide processing in marine environments (Seinfeld and Pandis 1998, Finlayson-Pitts and Pitts 2000). As such, the chemistry of H_2O_2 and related species contributes to the aerosol indirect effect, which is among the most important uncertainties in climate science.

2.1.5 Does Henry's Law Govern Aerosol H_2O_2?

Our initial hypothesis was that H_2O_2 in particles is governed by partitioning of gas phase H_2O_2 into the particulate aqueous phase, or possibly that aerosol peroxide concentrations would be lower than Henry's law predictions because of destruction or consumption of H_2O_2 by co-solutes in the aerosols, such as metals. Several lines of evidence from our field measurements, however, indicate that Henry's law exerts little control over particulate H_2O_2 concentrations; instead H_2O_2 levels in particles far exceed that predicted by Henry's law. The simplest explanation of our results is that peroxides are actively generated or released by particles, at least once they are suspended in aqueous solution, in remarkable quantities. Several lines of evidence support this hypothesis, as follows.

2.1.6 Simultaneous Measurements of Particle and Gas-Phase H_2O_2 and Relative Humidity

Our first study, published in 2003 (Hasson and Paulson 2003), showed that particulate peroxide levels are much higher than predicted by Henry's law. However, since we were not able to collect PM mass data at that time, we could not accurately quantify the degree of deviation from Henry's law. Since this study, we have begun to measure PM mass together with H_2O_2 levels in both gas and particulate phase. Fig. 2-1-1 shows the relationship between the hydrogen peroxide concentration measured in the particle phase and the particulate concentration calculated from the measured gas-phase concentration and Henry's law.

The calculation from Henry's law is arrived at by multiplying the measured gas-phase H_2O_2 by H_A. To calculate the actual concentration of H_2O_2 in aerosol liquid water from measured peroxide levels, we considered two cases: a) that water makes up 50% of particle mass, regardless of the relative humidity (RH), or b) that the aerosol liquid water content (LWC) is determined by RH in a manner that accounts for the non-linear uptake of water by mixed salts, according to the method described by Sloane and Wolff (1985). In these calculations we assumed that a particle density of 1 g/cm^3, which is likely only a slight underestimation given that we measured wet particle mass which has a lower average density than dry particle mass. Since the RH was usually below 55%, the point at which LWC = ~50% according to Sloane and Wolff's (1985) model, the calculation that accounts for RH results in higher calculated concentrations for H_2O_2 in aerosol liquid water.

In all cases, measured particle-borne H_2O_2 greatly exceeds the Henry's law value. Using the assumption that the LWC is 50% of the measured aerosol mass, the measured concentrations

exceed Henry's law by an average of about 300%; assuming the LWC calculated based on measured aerosol mass and RH, the measured concentrations exceed Henry's law by an average of about 700%. The concentrations of H_2O_2 calculated for the aerosol liquid water are very high, up to 50mM or more. Figure 2-1-1 shows the relationship between particulate-phase H_2O_2, in ng/m^3 and the aerosol LWC in μg/m^3. Although the data are limited, no correlation is observed in the coarse mode, and a weak negative correlation is observed for the fine mode.

2.2 Methods of Collection and Analysis of Hydrogen Peroxide and Organic Peroxides

Unless otherwise specified, throughout this report we use the methods detailed here for collection and analysis of H_2O_2 generation by particulate matter and gas phase peroxide concentrations.

2.2.1 Collection of Gas Phase Samples

Gas-phase hydroperoxides were extracted into the aqueous phase using a helical coil collector of the design of Hartkamp and Bachausen (1987), as used in previous laboratory studies by this group (Hasson et al. 2001a, b). Ambient air was drawn through the stripping coil at 4.5 L min^{-1}, while 10 mL of stripping solution (10^{-4} M Na_2EDTA adjusted to pH 3.5 with sulfuric acid) was simultaneously circulated through the coil at a flow rate of 1 ml min^{-1}. The coil is constructed from a 1 m × 2 mm ID glass tube, in which the stripping solution forms a thin, continuously flowing layer on the inside of the walls of the coil. The collection efficiency of the coil is found to be ≥ 92 % for samples containing 1×10^{13} molecules cm^{-3} of H_2O_2 and peracetic acid (Hasson et al. 2001a). These levels are well above ambient levels, which rarely exceed 3×10^{11} molecules cm^{-3}.

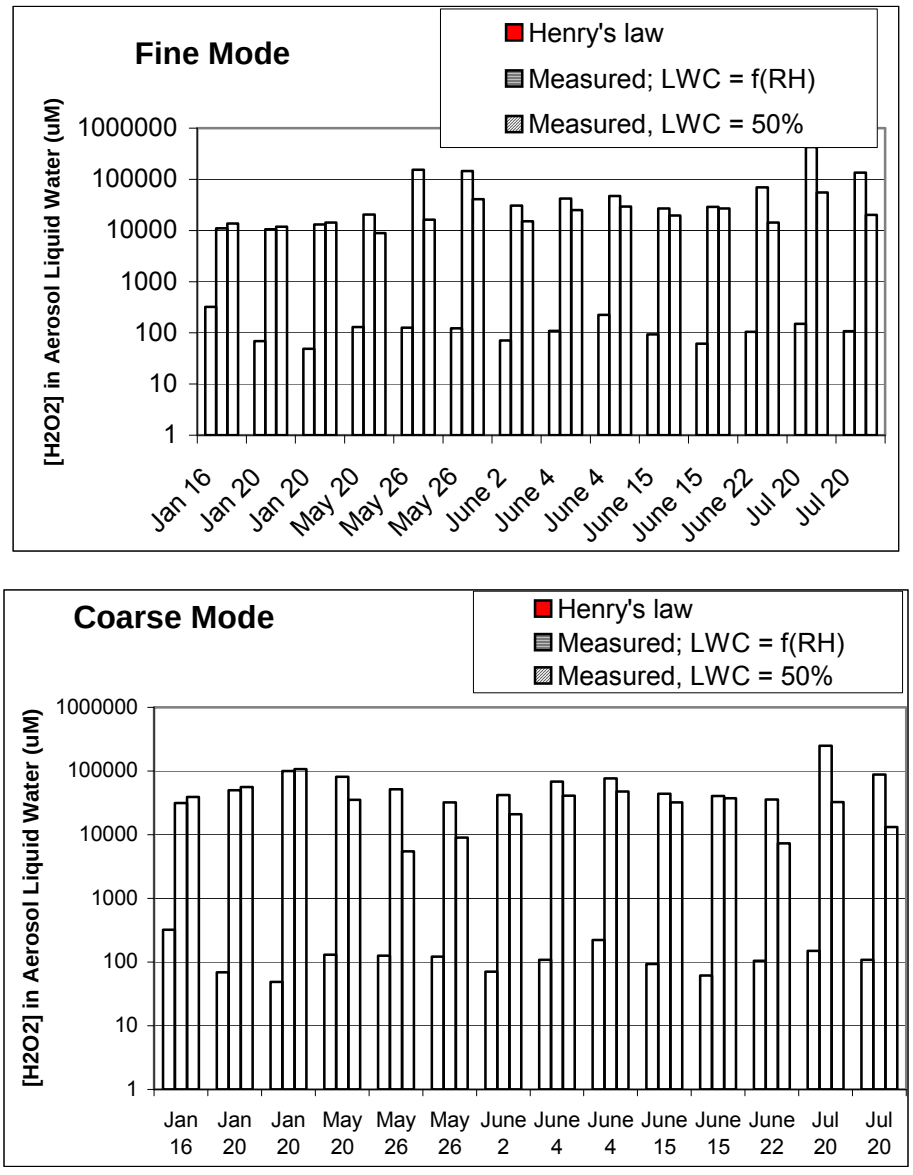

Figure 2-1-1 Particulate H_2O_2 in aerosol liquid water (top panel, fine mode, lower panel, coarse mode). Units are μM to allow comparison on a log scale. The first bar (solid) indicates the concentration predicted by Henry's Law, calculated from the gas-phase concentration. The second (horizontal stripes) and third (diagonal stripes) bars indicate the particulate H_2O_2 concentration derived from the measured particulate H_2O_2 loading. The middle bars result from assuming the aerosol liquid water content (LWC) scales with measured particle mass and relative humidity as described in the text. The right hand bars result from assuming that the LWC equals 50% of the measured particle mass, regardless of RH.

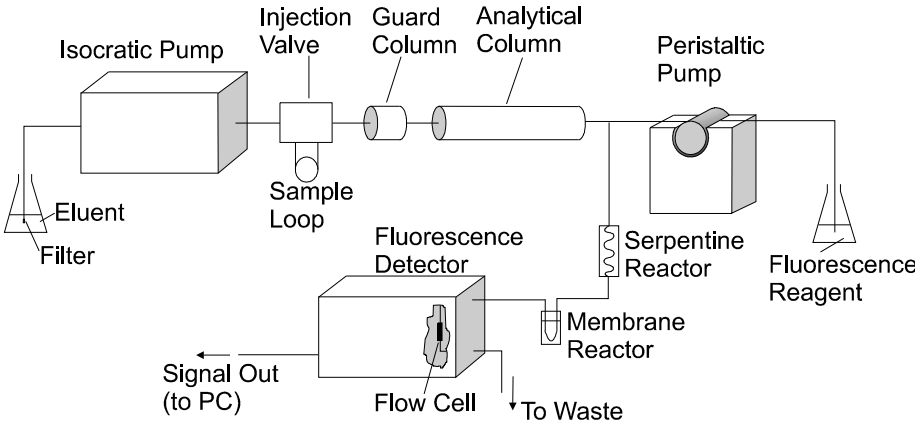

Figure 2-2-1 Schematic of HPLC-fluorescence detector for hydroperoxides.

This sampling technique strips both gas- and aerosol-phase hydroperoxides from the air sample, thus the measured gas-phase hydroperoxide concentration will be systematically higher than its true value. Since total hydroperoxides in PM are less than 1% of the gas-phase, however, the systematic errors introduced by sampling particles with the gas phase are negligible. Following sampling, the stripping solution contains both hydrogen peroxide and carbonyl compounds, as well as other species absorbed from the gas. Peroxides and carbonyls are known to react with each other in solution to form hydroxyalkyl hydroperoxides and dihydroxyperoxides. These species are also measured with our analysis technique, however, and do not form at measurable concentrations under our sampling conditions. Gas-phase samples are generally collected for 30 minutes. Since aerosol samples are collected for 90 minutes or more, several gas-phase samples are typically collected to obtain an average gas-phase concentration that corresponds to the aerosol concentration.

2.2.2 Collection and Extraction of Aerosol Samples

Aerosol samples were collected on 47 mm, 2μm pore-size Teflon filters (Pall Corporation) supported on stainless steel filter holders. Size segregation of the coarse and fine aerosol was achieved using a virtual impactor (VI) unless otherwise specified. The VIs were fabricated at the University of Southern California, under the direction of Prof. C. Sioutas. One is constructed from anodized aluminum and the other from Teflon-coated aluminum. They were each operated with a total flow rate of 55 L min^{-1}, corresponding to a size cut of 2.5 μm.

Unless otherwise specified, samples were collected at the UCLA site, which is located on the roof of the Math Science Building at UCLA. The site is 8 km from the Pacific coast, has annually

averaged PM2.5 levels that slightly exceed the national annually-averaged PM2.5 standard of 15 $\mu g/m^3$, and apart from the presence of some sea-salt, is reasonably representative of urban aerosol. During the day, when there is a persistent on-shore flow at about 5 m/s, the rooftop site receives slightly aged air from two major thoroughfares: the 405 freeway and Wilshire Boulevard (Chung et al. 2003), both 1 km away. During the evening, night, and early morning, the flow is offshore, which brings air from the more populated Los Angeles area, although the immediate fetch is a relatively low-density hillside area (Chung et al. 2003). From 2004 to 2008, the Building was adjacent to a construction site.

The aerosol-phase hydroperoxides were extracted into the aqueous phase by adding 3 or 4 ml of stripping solution (18 MΩ water with 0.1 mM EDTA added and adjusted to pH 3.5 unless otherwise noted). It was initially hoped that the hydroperoxides could be rapidly extracted from the filters using a sonic bath. It was found, however, after 15 minutes of sonication of pure, deionized water, that high levels of hydrogen peroxide were created, at concentrations an order of magnitude larger than the levels expected in the sample solutions (Hasson and Paulson, 2003). The samples were, therefore, gently agitated every few minutes. The rise of H_2O_2 in the extraction solution is not instant, but proceeds over a time span of hours (Sections 3 and 4). The time to reach the maximum value varies from sample to sample, and can be as long as a day. All samples investigated generated H_2O_2 in solution significantly more slowly after the first 100 minutes, so in the interests of practicality and convenience (recognizing samples need to be analyzed very soon after collection), we recorded H_2O_2 values at 120 minutes unless otherwise specified. The value at 100 minutes is generally about 70% of the maximum amount of H_2O_2 production, or H_2O_2 concentration in the extraction solution (Hasson and Paulson, 2003 and below) but it can be as little as 55% or as much as 90%.

2.2.1 Hydroperoxide Analysis

Quantification of the hydroperoxides present in aqueous solution is performed using the HPLC-fluorescence technique first reported by Hellpointner and Gab (1989) as described in detail by Hasson et al. (2001a,b), and shown schematically in Figure 2-2-1. In brief, hydroperoxides are first separated on a reversed-phase C18 analytical column. At the end of the column, a mixture of the reagents horseradish peroxidase and *para*-hydroxyphenyl acetic acid (POHPAA) is added. The horseradish peroxidase enzyme catalyzes the stoichiometric reaction between hydroperoxide and

POHPAA, resulting in the formation of one POHPAA dimer for every hydroperoxide molecule present. This dimer is detected by fluorescence. The hydroperoxides are identified by comparison of their retention times with those of hydroperoxide samples synthesized in the laboratory. Because the same species is detected regardless of the peroxide involved, the signal response per molecule of any peroxide is the same. Pure peroxides (which are explosive) are not required for calibration standards (see also Hasson and Paulson 2003 and Arellanes et al., 2006).

3. Laboratory Investigations & Method Development

3.1 Uptake of H_2O_2 by ammonium sulfate particles and its relationship to Henry's Law

3.1.1 Experimental Design

Measurements of H_2O_2 uptake by pure ammonium sulfate (AS) particles were made as follows. AS particle were generated by passing zero generated air through a Collison Nebulizer (BGI Inc., MRE CN-24) containing a 0.2% (w/v) AS solution. Under these conditions, the resulting aerosol has a log-normal size distribution with a geometric mean of 416 ± 20 nm. Ammonium sulfate particles were mixed with gas phase H_2O_2 that was generated as follows. First, zero air (Thermo Environmental Instruments zero air generator) was passed through a bubbler containing 200 mL of 0.005 to 0.1 M H_2O_2. Depending on the desired gas phase H_2O_2 concentration, both the H_2O_2 concentration and the zero air flow were varied. Resulting gas phase H_2O_2 concentrations were between 13 – 7900 ppb. The H_2O_2 airstream was conditioned by mixing with water-saturated air to obtain a final RH of 95%. The conditioned gas phase H_2O_2 air-stream was finally mixed with the airstream containing AS particles (Fig 3-1-1) and the flow directed into 20 cm corrugated Teflon tubing followed by a 35 cm mixing tube, followed by a second 20 cm corrugated Teflon tube. A filter housing unit was placed directly after the second corrugated Teflon tube to collect the AS particles.

Gas phase H_2O_2 levels were measured prior to mixing into the aerosol flow, point A of Fig 3-1-1, by directing flow to a stripping coil designed to concentrate H_2O_2 from the gas phase into the aqueous phase (Hartkamp et al., 1987, Hasson and Paulson 2003). The conditioned air/water vapor/gas phase H_2O_2 flow was collected for 5 – 10 min into water adjusted to pH 3.5. Next, the H_2O_2 air-stream was reconnected to the AS generation line and the RH and particle distribution were measured just upstream of the filter holder using a hygrometer and an SMPS, respectively (Point B of Fig 3-1-1). After a sampling event, the combined AS and conditioned H_2O_2 airstreams were again measured for RH and particle size distribution to determine the drift that had occurred during the experiment (point B of Fig 3-1-1). In calculations, the average of initial and final RH was used and did not differ more than 10% in all experiments. Similarly, gas phase H_2O_2 levels were measured after sampling without the aerosol stream at the point where AS particles were collected

(Point B of Fig 3-1-1) and the average of initial and final H_2O_2 concentrations was used in subsequent calculations. Samples were collected on tared Teflon filters (Pall Corp.) for 20 – 60 min and after sampling were weighed and extracted in a pH 3.5 solution for 2 hrs, and the extract analyzed for H_2O_2.

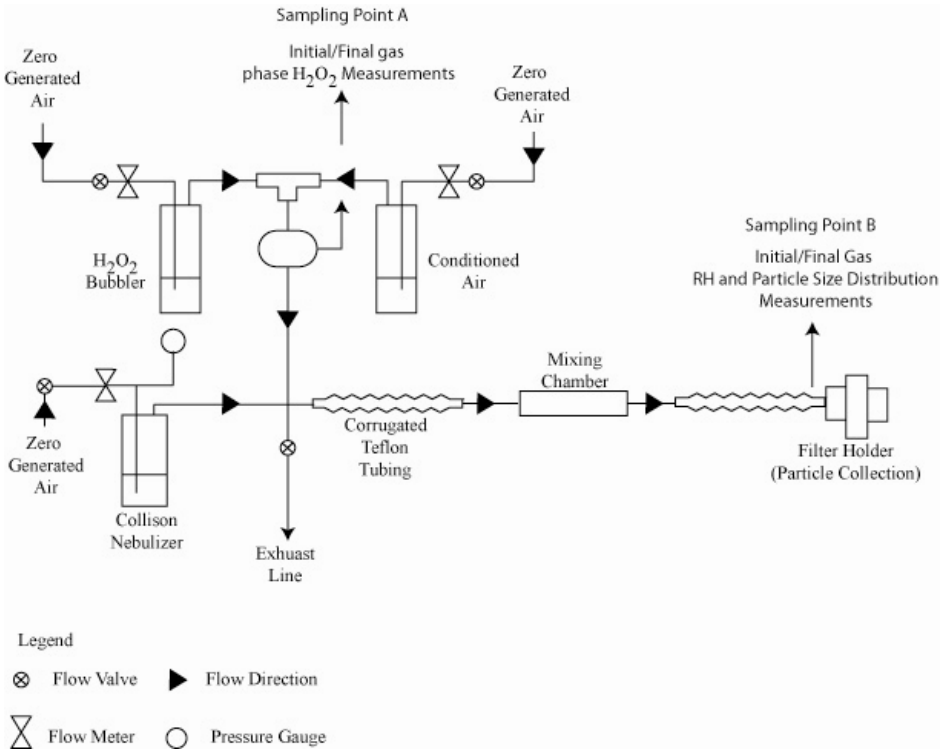

Figure 3-1-1 Schematic of the ammonium sulfate/H_2O_2 generation line

3.1.2 Results

Nine sets of measurements were made to investigate uptake of H_2O_2 by ammonium sulfate (AS) particles. To promote the partitioning of H_2O_2 from the gas to the particle phase, the PM liquid water content was elevated by maintaining a relative humidity (RH) throughout measurements above the deliquescence point of AS particles (RH = 79.9%, Finlayson-Pitts and Pitts, 2000). The amount of H_2O_2 taken up by AS particles was studied over a wide range of gas phase H_2O_2 levels (0.01 – 8 ppm). Particles had mass concentrations in the range of 5 – 19 μg m^{-3} and a log-normal size distribution with a geometric mean of 416 ± 20 nm.

Gas- to particle phase partitioning can be described using Henry's Law, which governs gas-liquid partitioning for gasses (Eq. 1).

$$M_{H_2O_2} = H_A \times P_{H_2O_2} \qquad \text{Eq. 1}$$

In Eq. 1 M_{H2O2} is the aqueous concentration [M], P_{H2O2} the gas phase concentration [atm] and H_A [M atm^{-1}] the effective Henry's Law constant for H_2O_2. H_A is dependent primarily on temperature and chemical composition of the aqueous phase. Several measurements of H_A have been made using various temperatures and chemical compositions and for dilute solutions at room temperature, and a value of 10^5 M atm^{-1} is generally accepted (Sander et al., 1999) . Chung et al. (2005) have reported that in the presence of high concentrations of ammonium sulfate common in ambient aerosols, H_2O_2 solubility can increase by as much as a factor of two.

Generated AS particles were exposed to various gas phase H_2O_2 concentrations, 10 – 170 ppb in seven instances, and concentrations as high as 8 ppm on two occasions. Measured relative humidity was used to estimate the mass fraction of water and ammonium sulfate, using an empirical relationship (Eq. 2) that assumes that AS and water particles have densities of 1.8 and 1.0 g cm^{-3}, respectively (Li et al., 2000).

$$\text{AS Mass fraction} = 2.27 - 11.15(RH) + 36.34(RH)^2 - 64.21(RH)^3 + 56.83(RH)^4 - 20.09(RH)^5 \qquad \text{Eq. 2}$$

Once the AS mass fraction is determined, the mass fraction of water can be found and the aerosol liquid water calculated. The H_2O_2 concentration determined analytically is compared to expected values determined from the aerosol liquid water, combined with Henry's Law using a $H_A = 1.7 \times 10^5$ M atm^{-1} (Chung et al., 2005) for concentrated $(NH_4)_2SO_4$ solutions (Table 3-1-1). Average RH levels measured were 82 ± 0.4%, which is expected to result in an AS and water mass fractions of 40 and 60%, respectively (Li et al., 2000). The ratio of predicted to actual H_2O_2 levels was on average 1.0 ± 0.3, indicating (as expected), that ammonium sulfate aerosols do not generate H_2O_2 (as do ambient aerosols), and simply take up H_2O_2 from the gas phase according to Henry's Law.

Table 3-1-1 The Uptake of H_2O_2 by Ammonium Sulfate Particles

Run	Gas Phase H_2O_2 (ppb)	Expected Particle Phase H_2O_2 Concentration Using Henry's Law (μM)[a]	Measured Particle Phase H_2O_2 Concentration (μM)	Particle Phase H_2O_2 Compared to an Unadjusted Henry's Law[b]
1	7,900	134,300	180,000	1.34
2	7,900	134,300	195,000	1.45
3	170	2,890	4,300	1.49
4	120	2,040	1,800	0.88
5	15	255	260	1.02
6	12	204	150	0.74
7	17	289	260	0.90
8	13	221	170	0.77
9	13	221	150	0.68
Ave ± SD				1.0 ± 0.31

[a] Expected particle phase H_2O_2 concentration is calculated using an effective Henry's Law constant (H_a) for concentrated salt solutions

[b] Calculated as the ratio of Henry's Law predictions to measured particle phase H_2O_2

Morio et al. (2001) intended to test aerosols containing concentrated H_2O_2 relative to ambient. Because ambient aerosols *generate* H_2O_2, however, the aerosols they generated and tested contained similar amounts of H_2O_2 as that found associated with ambient aerosols (this work, Arellanes et al., 2006, Hasson and Paulson 2003). According to Henry's law, and our measurements of aerosols generated in the same manner, these aerosols contained 10-180 ng m^{-3} H_2O_2. Ambient fine mode aerosols average 5 – 40 ng m^{-3} H_2O_2, combined coarse and fine average 20-75 ng m^{-3}, and peak at ~170 ng m^{-3}.

3.2 Ethanol in the Extraction Solution

3.2.1 Motivation

Because the composition of the extraction solution may affect the observed H_2O_2 levels, we are investigating the influence of a number of components are be added to the extraction solution. Prior to the work described here, a small amount of ethanol (EtOH) has been added to the extraction solution with the motivation that it might enhance the solubility of particles and "wet" the Teflon filters (Pall Corp.), but had not to date been validated either for this purpose or as a potential source of contamination. Here we investigate its merits.

3.2.2 Experimental Description

HPLC grade 200 proof ethanol from Sigma-Aldrich was used for this study. Earlier work used 200 proof EtOH from the Gold Shield Chemical Co., however this was discovered to contain more H_2O_2 than the HPLC grade EtOH, so its use was discontinued.

For this study, pairs of filters loaded with fine mode ambient aerosols were collected using the virtual impactors. One filter was extracted with water adjusted to pH 3.5 with 0.1 mM Na_2EDTA (referred to as "stripping solution" because it is the same solution as that used to strip H_2O_2 from the gas phase in the stripping coil, section 2) with 0.2 mL of EtOH, and the other was extracted with stripping solution alone. Both were extracted in Teflon Petri-dishes. In addition, two unused filters were placed in separate Teflon Petri-dishes and extracted with the same two solutions. 100 μL aliquots of extract from alternating extraction solutions were injected into the HPLC at intervals of 4 minutes.

3.2.3 Results

Undiluted EtOH contained 2.2×10^{-6} M H_2O_2. When 0.2 mL of ethanol is diluted with stripping solution to 3 mL, a concentration of 3×10^{-7} M results. In comparison, H_2O_2 concentrations in stripping solution without EtOH ranges from $0.5\text{-}2.0 \times 10^{-7}$ M, so clearly ethanol increases the blanks, and is highly undesirable from this point of view. To determine if EtOH is actually aiding in the dissolution of aerosols from Teflon filters (Pall Corp.), EtOH ranging from 0 to 1 mL was added to the extraction solution while the total extract volume was held at 3 mL. Figure 3-2-1 shows the results for samples and blanks extracted with and without 0.2 mL ethanol. The general time-dependent behavior is typical—the rate of H_2O_2 formation decreases continuously from its initial value, dropping off significantly after the first 100 minutes. The extraction solution containing EtOH maintained an H_2O_2 level with a constant offset above the EtOH from free solution. Blank H_2O_2 levels are higher for the extract solution with EtOH and the concentration rises with time, going from 0.9 to 5×10^{-7} M. In contrast, the blank without EtOH stays relatively constant.

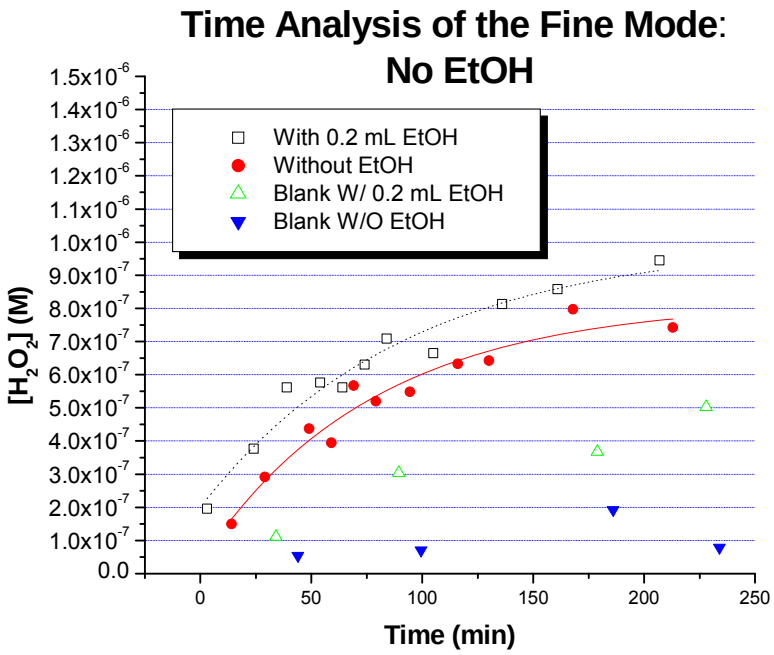

Figure 3-2-1 Time profile of the extraction process for fine mode aerosols

As shown in Figure 3-2-1, the EtOH does not seem to greatly increase the H_2O_2 levels when compared to the extract solution without it. This could be interpreted to indicate that EtOH does not benefit the dissolution of fine mode aerosols from Teflon filters (Pall Corp). This is more evident in Figure 3-2-2, which displays the H_2O_2 concentration normalized to the final concentration, which shows that stripping solution with and without EtOH have indistinguishable rise rates. Additional tests using extract solutions with 0.1 to 1.0 mL of EtOH were also performed (Figures 3-2-3 and -4). The results are very similar to the 0.2 mL results. Fig. 3-3-3 appears to indicate that ethanol could inhibit H_2O_2 formation in the extraction solution eventually; the 0.1 mL solution produces more H_2O_2 as time goes on, compared to the 0.2 mL solution; but this isn't clearly reproduced by the other solutions. Differences for the aerosol samples are modest and generally within the scatter of the data, however the larger amounts of ethanol appear to result in a slightly more rapid initial rise of H_2O_2 in the extraction solution.

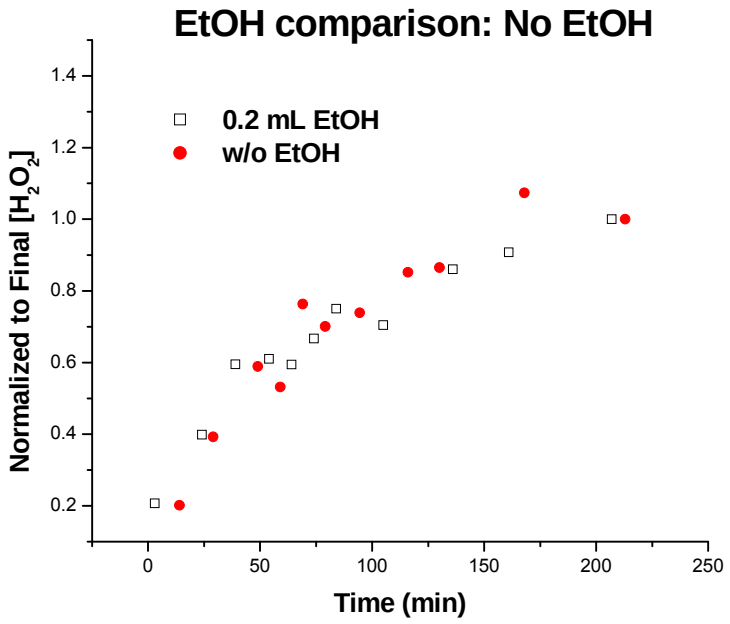

Figure 3-2-2 Time dependent H_2O_2 normalized to the final concentration for each sample.

Because of the contamination problems commonly associated with commercially available EtOH, and its apparent limited value in the analysis, the use of EtOH as part of the aerosol extraction process has been discontinued.

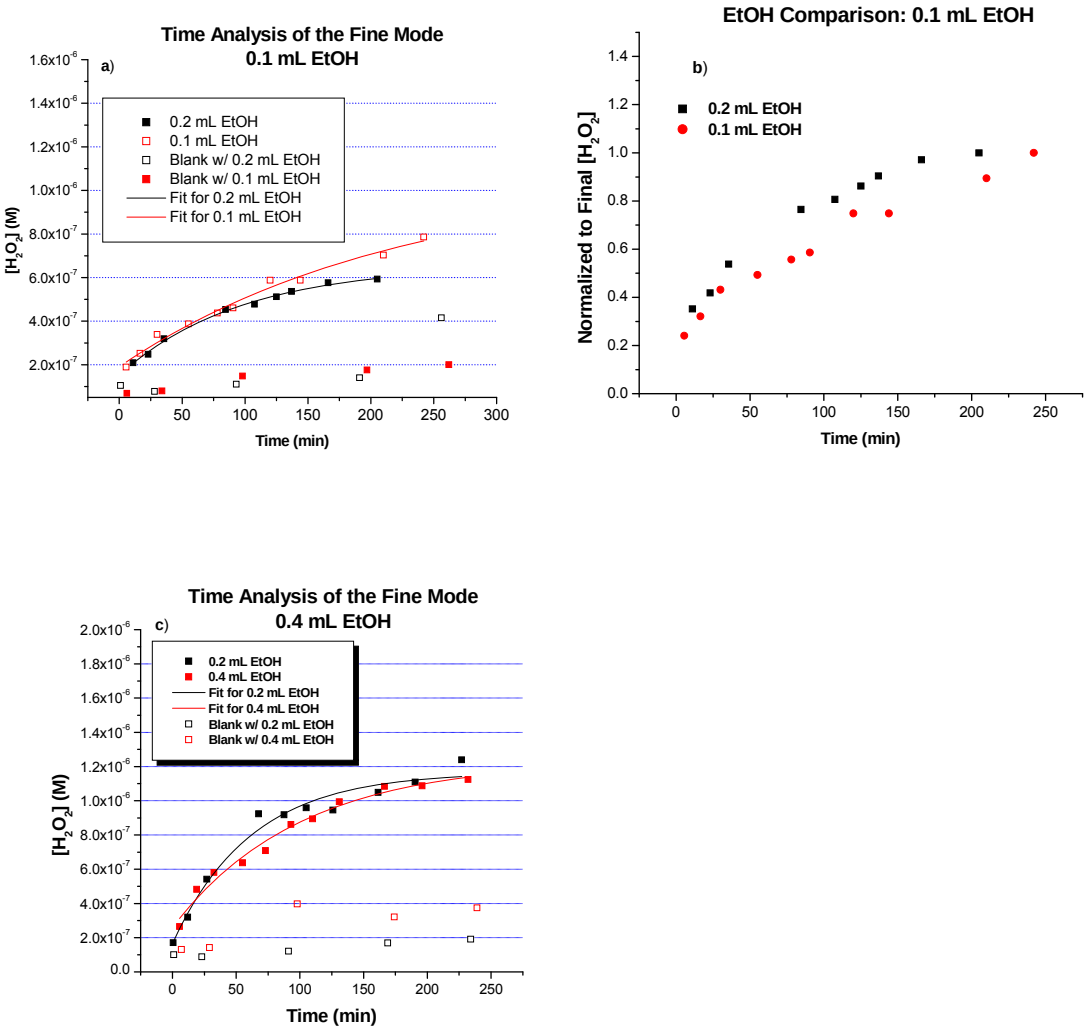

Figure 3-2-3 a) time profile comparison of 0.1 and 0.2 mL of EtOH. B) 0.1 and 0.2 mL EtOH data normalized to the fine H_2O_2 concentration. C) time profile comparison of the extraction process of 0.2 to 0.4 mL EtOH.

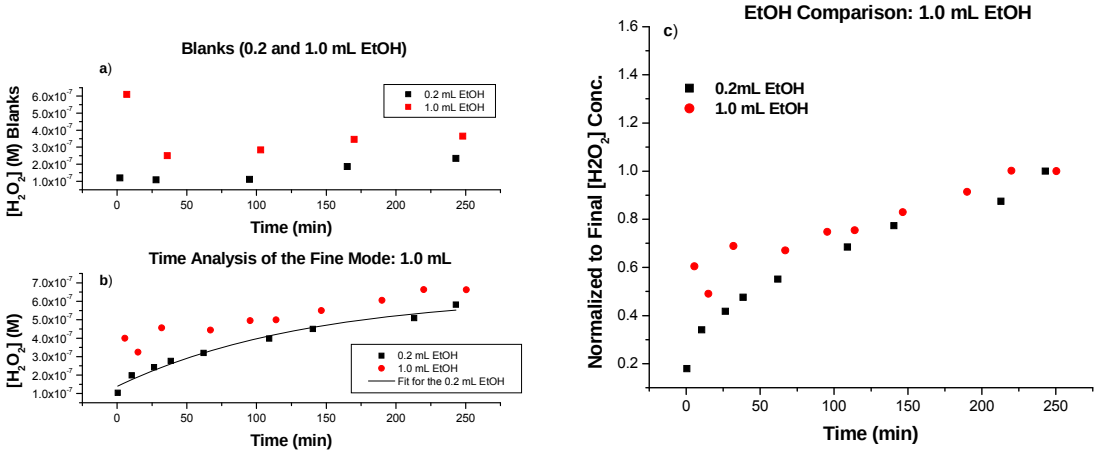

Figure 3-2-4 1 mL and 0.2 mL EtOH extract solution compared. A) Blank solutions of 0.2 and 1 mL EtOH. B) Time profiles of the two extract solutions. C) The H_2O_2 concentration normalized to the respective final H_2O_2 concentrations.

3.3 Metal Contamination from Virtual Impactors

3.3.1 Introduction

In an on-going effort to understand the source of H_2O_2 formation in particles, we started analyzing metals in particulate matter samples in the summer of 2005, coinciding with the Secondary Organic Aerosols at Riverside Study (SOARS) I field campaign in Riverside. Metal samples were collected using a parallel sampling train alongside H_2O_2 sample collection. The sample trains were randomly assigned to each analysis, and changed frequently, and their equal performance verified in terms of both aerosol mass collection and H_2O_2 generation. H_2O_2 samples were always measured on site within minutes of finishing collection, while metals (as well as mass) samples were stored and analyzed later. During SOARS I, we observed several phenomena that suggested there might be either a source of metal contamination in our sampling train or an unusual local industrial source of high Cu/Zn. Evidence included occasional very high H_2O_2 levels and much more variability than previously observed, only in the fine mode. Additionally, we observed occasional very high levels of copper and zinc, and in samples for which lead was included as an analyte, lead as well. The high Cu and Zn levels in fine mode PM further were extraordinarily well correlated with one another, with r^2

values of 0.95 or higher. The high Cu and Zn levels were sometimes, but not always correlated with high H_2O_2 levels.

3.3.2 Virtual Impactors

Initial efforts to locate such a source of contamination focused on brass fittings and tubing, and were not conclusive (below). Figure 3-3-1 shows the concentrations of metals in filter extracts (in ppb in the extract solution) for field blanks collected in the following manner. New Teflon filters (Pall Corp.) are loaded into the filter holders used for sampling, and the pump is turned on for 30 s (normal sampling takes 1-4 hours). The filter is removed and analyzed as usual. There are 3 sets of measurements shown. In each case, fresh filters were placed in the filter holder and the pump was turned on for 30s. The 'open' filters were placed in the filter holder with nothing in front of it. The 'line' filters were downstream of the complete sample train (e.g., all fittings and inlet lines, about 30 cm long), with the virtual impactor removed. 'VI' filters had the complete sampling train including the virtual impactors. There are two virtual impactors, and each collects a fine and coarse mode sample. Only the filters connected to the fine mode using the VI showed highly elevated Cu and Zn. Sodium and potassium are also shown and exhibit no significant differences. Next, a Teflon chamber filled with particle free air was used as a sample. Cu and Zn were not significantly elevated in the 2 hour clean air sample compared to the 30 second 'field blank' (Fig. 3-3-1). The results indicate that the Cu/Zn/Pb contamination source accumulates on VIs and is mostly removed by the first few seconds of air flow once the pump is turned on. When the VIs were first purchased from USC/Prof. Sioutas, we did not observe the random high values in H_2O_2 generation by particles, and the average H_2O_2 in the fine mode collected with VIs was reasonably consistent with the equivalent size cut sampled with a MOUDI impactor (Section 4, and Arellanes et al., 2006). As part of our recent field campaign in Riverside, we collected a large number of field blanks for metal analysis. While it may be possible in future to perform metal analysis on the same filter as H_2O_2 analysis, to date we have used a randomly assigned filter from one of the VIs for metal analysis, and have analyzed the other for H_2O_2. Many, but not all of the fine mode metal blanks exhibited highly elevated levels of Cu, Zn and Pb, and the metals were also very well correlated with one another. High levels of Cu and Zn were not observed on coarse mode filters. Clearly the Cu/Zn/Pb contamination from the VIs does not affect all samples. It also seems likely that this is a problem that has developed as the VIs have aged, and it may be exacerbated by the very high temperatures in Riverside, which often exceed 100 F.

In studies of aircraft inlets used for particle sampling, Murphy et al. (2004) found evidence of ablation of the inlet by ice and large dust particles. The phenomenon produced sub-micron sized metal particles composed of elements present in the inlet material, but not necessarily in the same ratios as found in inlet material. The gas speed through parts of the aircraft inlet, about 200 m s^{-1}, are higher but comparable to the speeds experienced by gasses passing through the VIs, which reach about 115 m s^{-1} at sample flow rates of 55 Lpm. While we do not sample ice particles, we do expose the VIs to dust.

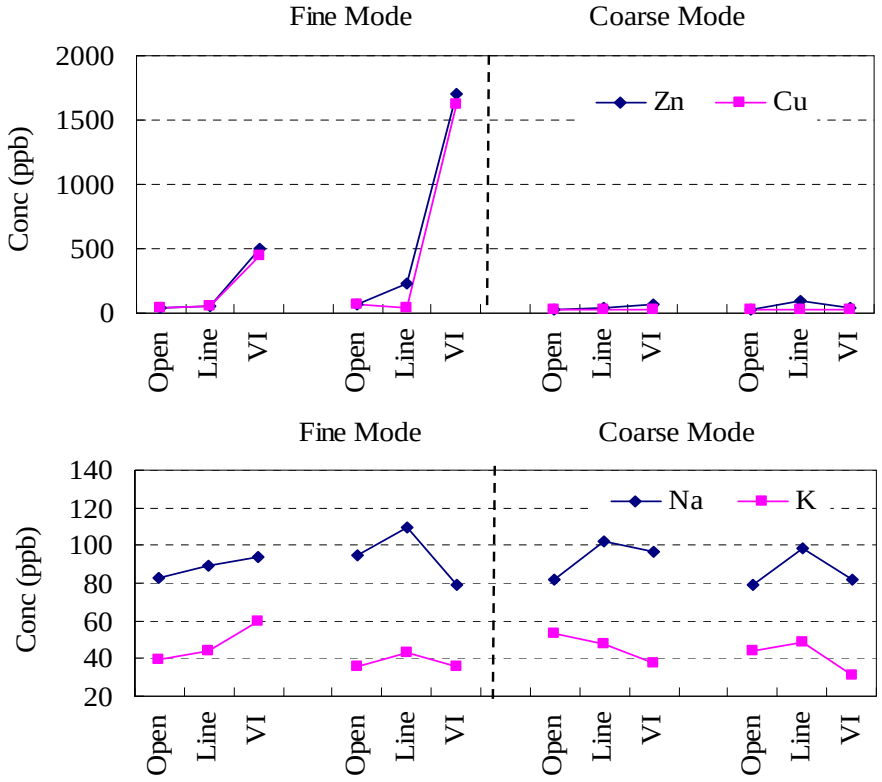

Figure 3-3-1 Concentrations of Zn, Cu (top) and Na, K (below) in 5 mL of extract (ppb) for blanks collected with filter holder directly open to the air (Open), with filter holder connected to copper tubing (Line), and with filter holder connected to VI inlet (VI) for fine and coarse mode aerosols.

Most fine mode results using the virtual impactors are omitted from this report. pH-related behavior has been repeated, and data collected with a new sampling system are completely consistent with the virtual impactor data, so these data are included. The virtual impactors were used only for ambient aerosols, so that many of the results are not affected. This includes all coarse mode data, data collected with the MOUDI impactor, source aerosol data (diesel, biodiesel and secondary organic aerosol) and laboratory generated ammonium sulfate aerosols.

3.3.3 Brass Fittings

To check for possible contamination, a representative brass fitting used during the SOARS campaign was submersed in the same solution used to extract filters designated for metal analysis (Section 4). A 4 mL aliquot of the extract was filtered in the same manner as SOARS samples, while another 4 mL was left unfiltered, and the results are shown in Table 3-3-1. In both filtered and unfiltered brass fitting samples, zinc is the most abundant metal, even though generally brass alloys are predominately composed of copper. This may be a result of the pH of the extraction solution leaching zinc more effectively than copper (Deguillaume et al., 2005).

Table 3-3-1 Analysis of a brass fitting used on the aerosol sampling line.

	Brass Fitting Composition (ng)[a]		
metal	Filtered	Unfiltered	Percent Composition of Unfiltered Sample
Ba	30	35	<1
Ca	9345	9010	7
Cu	22670	22145	18
Fe	200	13090	11
Pb	19715	19860	16
V	ND[b]	ND[b]	0
Zn	70475	68175	56

[a] Units are ng of metal found per 5 mL of solution
[b] Not detected

Filter housings were also checked for contamination from the dust that can accumulate on the gasket used to seal the housing units. It was not possible to remove the gasket, thus 10 mL of HNO_3 at pH 3.5 was used to flush the gasket. Half of the solution was filtered. Results are shown in Table 3-3-2. Filtration has little effect on the metal concentrations, and metal levels were similar among the three filter holders.

Table 3-3-2 Metal analysis of filter housing units used during the SOARS campaign.

Metal	VI 2 [1] Fine		VI 2 Coarse		VI 1 [2] Coarse	Average Percent Composition [3]
	Filtered (ng mL^{-1})	Unfiltered (ng mL^{-1})	Filtered (ng mL^{-1})	Unfiltered (ng mL^{-1})	Filtered (ng mL^{-1})	
Ba	4.6	3.7	0	7.5	6.5	0.27 ± 0.2
Ca	820	776	1270	1290	837	57 ± 3
Cu	183	227	301	310	229	14 ± 1
Fe	178	163	273	284	136	12 ± 2
V	3.5	<MDL [4]	<MDL	<MDL	<MDL	< 1
Zn	179	248	275	288	352	16 ± 4

[1] VI 2 is virtual impactor 2; both fine and coarse mode aerosols collected were designated for metal analysis
[2] VI 1 is virtual impactor 1; which collected fine and coarse mode aerosols, both designated for H_2O_2 analysis.
[3] percent composition is determined by taking the average metal levels found for all samples and comparing to the average total.
[4] below method detection limit
Note: unfiltered VI 1 coarse and VI 1 fine (unfiltered and filtered) samples were analyzed. However, no metals were detected, likely an error with the ICP-OES (see Section 6 text).

Ratios of metals in SOARS samples are shown in Table 3-3-3 together with those for the brass fitting extractions. It is clear that there is no correlation involving the metal ratios, indicating that the brass fittings are not the source of the contamination. The dust on the filter holders is more similar to the SOARS ratios, but it still a poor match for two of the four ratios.

Table 3-3-3 Metal ratios for brass sample and SOARS

Sample	**Cu/Fe**	**Pb/Fe**	**Zn/Fe**	**Zn/Pb**	**Ca/Fe**	**Cu/Zn**
SOARS	7.0	0.60	7.8	5.4	5.6	1.2
Brass Filtered	112	97	348	3.6	46	0.3
Brass Unfiltered	1.7	1.5	5.2	3.5	0.69	0.3
Avg. Filter holders (filtered)	1.2	-	1.4		5.0	0.88

4. H_2O_2 Dependence on Aerosol Age and Extraction Solution Composition

4.1 Aerosol Aging

4.1.1 Aging Protocol

To elucidate the temporal characteristics of H_2O_2 generation in an aqueous medium, we performed the following analyses. Samples were collected from June 6 – 14, 2007 with each sampling event lasting a minimum of 3 hrs using two virtual impactor sample pairs in parallel to produce pairs of fine and coarse mode samples. To monitor the time evolution of H_2O_2 within the extraction solution, a 100 μL sample was analyzed every 2 – 5 minutes during the first 60 min of the extraction process and every 10 – 15 min thereafter, creating a time profile of H_2O_2 levels generated by particles over 3 hrs of extraction. Field blanks were also monitored for H_2O_2 at the same time intervals over the course of 3 hrs.

Fine and coarse mode aerosols were collected in a similar manner using two virtual impactor sampling trains to obtain two sets of fine and coarse mode particles. For every sampling event two field blanks were also recorded by placing unused filters into fine and coarse mode filter holders. From a single sampling event, the two sets of filters loaded with fine and coarse mode particles were cut in half, yielding four filter halves per mode. Immediately after a sampling period one filter half was analyzed for H_2O_2, which represents the initial reference activity at time = 0 hr. The remaining filters were allowed to age in ambient room air while stored in Petri dishes open to the surrounding environment. After 19 hrs has passed, another filter half is analyzed for H_2O_2 and the process repeated at 26, 42, and 120 hrs. Field blanks were also analyzed at each aging time and used to correct observed H_2O_2 levels in the samples.

Sampling was conducted on the campus of the University of California, Los Angeles (UCLA) which is located 8 km from the Pacific Ocean at 34.07° N, 118.45° W, 150 m elevation. The sampling site was also 24 m above ground level on the roof of the Math Sciences building. During the day there is a persistent on-shore flow (5 m s^{-1}), delivering slightly aged air from two major thoroughfares; the 405 Freeway and Wilshire Blvd are located 1.5 km away (Chung et al., 2003). Sampling was conducted intermittently between Nov 2004 and Jun 2007 and always during

daylight hours. Sampling times ranged from 2 – 6 hrs depending on the ambient aerosol concentration and type of analysis.

Fine (≤ 2.5 μm) and coarse (≥2.5 μm) mode particles were collected with virtual impactors operated at minor and major flows of 2.5 and 55 Lpm, respectively. Both fine and coarse mode particles were collected on Teflon filters (Pellman, 47 mm, 2 μm pore) housed in stainless steel filter holders. To determine particle mass, filters were tared prior to sampling and then re-weighed immediately afterwards with a micro-balance (Sartorius, ME-5, ± 1 μg). In some instances, filters were cut in half using a Ni-plated scalpel, allowing for multiple analyses of fine and coarse mode particles from the same sampling event. For each sampling event, a minimum of one field blank was recorded by placing a tared filter randomly into one of the filter holders used to sample either fine or coarse mode particles, and turning on the sampling line for 30 sec. Field blank filters were then analyzed in the same manner as other filters, and the observed H_2O_2 was used to correct H_2O_2 for the corresponding ambient samples.

Collected particles were extracted into the aqueous phase by immersing filters into a known volume of extract solution for 2 hrs, after which the extract solution is analyzed for H_2O_2 using an HPLC/fluorimeter as described below. In the series of experiments where either the extraction pH was varied or physiologically relevant extract solutions were used, all results are presented relative to a common extract solution containing 0.1 mM Na_2EDTA with an adjusted pH of 3.5 using 0.1 N H_2SO_4 (hereafter referred to as stripping solution [SS] 3.5). Extract solutions with varying pHs (1.5 – 7.6) were made by adjusting the pH with either 0.1 M NaOH or 0.1 N H_2SO_4. Two physiologically relevant extract solutions comprised of saline dispersions were investigated; Gamble's and Ringer's solutions (Table 4.1) (Kanapilly, 1973, Jung et al., 2006). Both solutions mimic the ionic strength and pH of lung lining fluid and were freshly made every two weeks. As a reference, an aqueous solution with a pH of 7.4 was used to measure H_2O_2 as well.

4.1.2 Results

Coarse mode ambient particles were aged to investigate the decay of H_2O_2 generation. Filters halves were allowed to age for 19, 26, 42 or 120 hrs indoors in the dark, and the H_2O_2 associated with the particles was measured. The results are shown in Fig. 4-1-1. The H_2O_2 content associated with one half filter, measured immediately, was used as a reference to compare H_2O_2

activity in aged aerosols. Fig. 4-1-1 shows the aging profile of the H_2O_2 activity (measured as ng of H_2O_2 per unit of particle mass) as the particles age. Coarse mode activity dropped steadily, although not monotonically, reaching about 50% of the initial signal by 40 hrs. By 120 hrs, both particle fractions had H_2O_2 activity that was less than 10% of the initial value. Field blanks recorded at each sampling time were used to correct measure H_2O_2 levels. H_2O_2 associated with field blanks were constant throughout the time period, ranging from 20% of the sample values initially, up to about 70% after 120 hours (at which time the sample signal had decayed away substantially).

Hung and Wang (2001) performed a limited aerosol aging study in which the H_2O_2 activity of size fractionated particles was measured at 1 and 115 hr after sample collection. They observed a drop off in activity of about 60% in all size fractions investigated. This is less decay than observed here (90-100%). The difference in results is unclear; it may due to differences in the particles themselves, or to the sonication step employed as part of the ROS analysis protocol used by Hung and Wang (2001). A reduction in H_2O_2 activity indicates that chemical species within particulate matter able to generate H_2O_2 are depleted with time, and highlights the importance of using fresh particles when studying the health effects of ROS. Particles older than a week presumably induce effects (e.g., in toxicity studies) that are due to something other than their intrinsic ability to generate ROS.

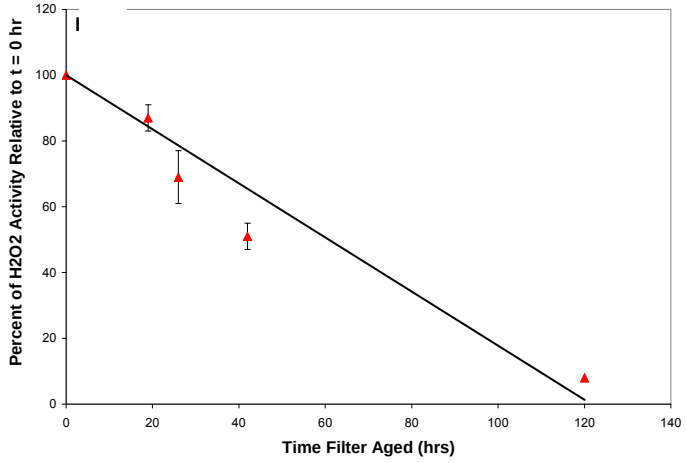

Figure 4-1-1 Coarse mode H_2O_2 activity as a function of aerosol aging. Data is presented as a percentage relative to the activity of H_2O_2 at time = 0 hrs. The error bars at 19 and 42 hrs represent the standard deviation and at 42 and 120 hrs it shows a range.

4.2 Time Analysis of the Extraction Process

The evolution of H_2O_2 levels during the extraction process was studied in fine and coarse mode aerosols. Based on the time evolution of H_2O_2 levels it may be possible to obtain kinetic-like information regarding the generation of H_2O_2 within extract solutions. The observed time dependence of H_2O_2 levels are likely due to several processes including the dissolution of species that generate H_2O_2 from particles, chemical reactions that generate H_2O_2, as well as a minor contribution from the dissolution of existing H_2O_2 in particles. Regardless of the source, the kinetic-like information gathered in these experiments is representative of chemical and physical processes that lead to H_2O_2 formation. Thus, a direct comparison to a chemical rate constant for reactions known to generate H_2O_2 is difficult to make.

Time analysis data were corrected for the changing volume of the extraction solution as successive aliquots are removed, as well as for H_2O_2 levels measured in field blanks. Volume corrections are made by totaling H_2O_2 moles for each measurement made, including the previous measurement. A fine and coarse mode field blank was recorded for each sampling event and was used to make corrections to observed H_2O_2 levels. Both fine and coarse mode field blank H_2O_2 levels were linear with time. Thus, field blank corrections were made, specific to the time of sampling, by interpolating H_2O_2 levels with respect to time. Temporal H_2O_2 profiles for fine and coarse mode particles are presented as the number of H_2O_2 moles, corrected for both volume and field blanks, for a total of five sampling events taken over four days in June, 2007 (Figs. 4 2.1 and 4-2-2). Throughout, the term formation/dissolution is used and represents the amount of H_2O_2 observed in the extract solution due to dissolution from particles and chemical formation within the extract solution. Each data set was fit with logarithmic curve to guide the eye. Both fine and coarse mode associated H_2O_2 showed a rapid rate of increase within the first 15 min, after which the rate of H_2O_2 formation/dissolution decreased and a final H_2O_2 level was approached.

Initial H_2O_2 measurements, within 15 min, were used to develop an H_2O_2 formation/ dissolution rate by using a linear fit, the slope of which is equivalent to the rate of H_2O_2 formation/dissolution per min, or alternatively H_2O_2 molar production per min. Fine mode associated H_2O_2 levels had an initial rate of H_2O_2 formation/dissolution of $(4 \pm 1) \times 10^{-11}$ moles min^{-1}, or $(1 \pm 0.3) \times 10^{-9}$ M min^{-1}. Coarse mode H_2O_2 rates were $(1 \pm 0.1) \times 10^{-10}$ moles min^{-1} or alternatively $(3 \pm 0.3) \times 10^{-8}$ M min^{-1}. Coarse mode H_2O_2 rates are 2.5 times faster and generally exhibit rates that decrease as a function of time faster than fine mode H_2O_2 rates.

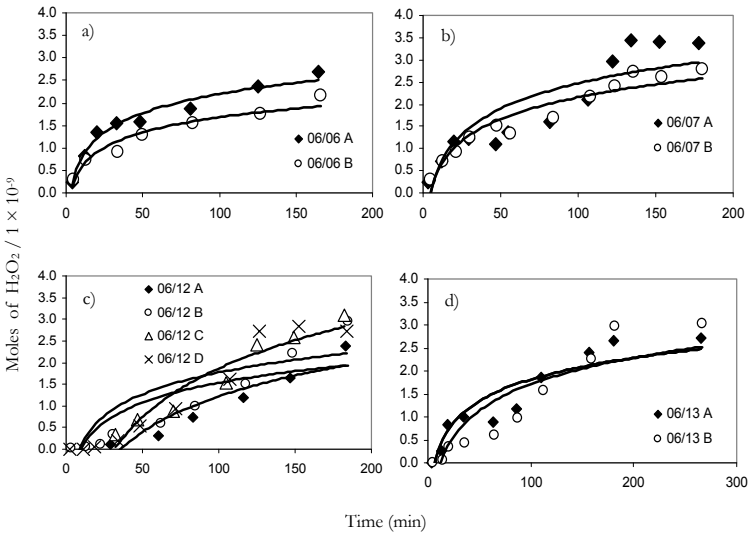

Figure 4-2-1 H_2O_2 time profiles of the extraction process for fine mode particles. Moles of H_2O_2 are corrected for changes in extraction volume as aliquots are drawn for analysis and field blank H_2O_2 levels. Sampling dates are indicated in each panel. Letters after the date indicate different samples collected at different times on the same day.

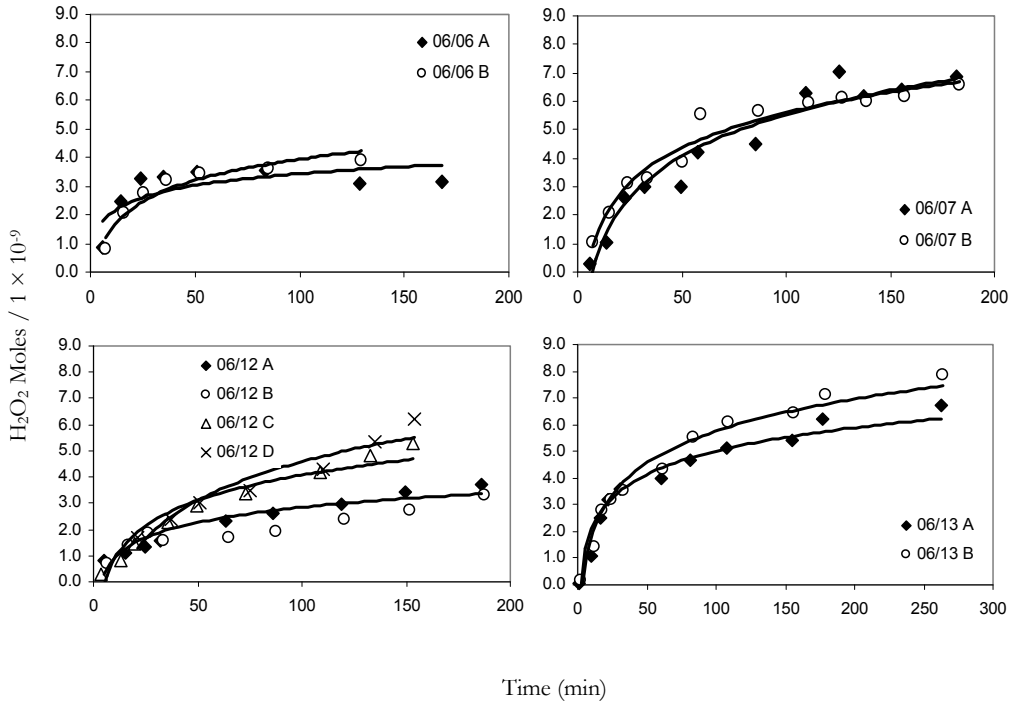

Figure 4-2-2 Time analysis of coarse mode H_2O_2 levels during the extraction process. The moles of H_2O_2 are adjusted by volume and field blank corrections. Sampling dates are indicated in each panel. Letters after the date indicate different samples collected at different times on the same day.

H_2O_2 formation rates derived from these data can be compared to controlled investigations of the formation of H_2O_2 in aqueous solutions with chemical species known to exist in ambient particles. Two relevant studies are those conducted by Chung et al. (2006) and Zuo and Hoigne (1992) which investigated production of H_2O_2 mediated by quinone and Fe(III)-oxalato species, respectively (Zuo and Deng, 1997, Chung et al., 2006). Chung et al. (2006) showed that in the presence of excess dithiothreitol, an electron donor, H_2O_2 formation is well correlated with three quinones, phenanthraquinone, 1,2-naphthoquinone and 1,4-naphthoquinone, but not several others. Dithiothreitol is not present in ambient aerosols, but it may be a proxy for sulfhydryl groups present in biological systems (such as glutathione). Chung et al. (2006) showed that the rate of H_2O_2 formation in the presence of a large excess of dithiothreitol was linearly dependent on aqueous quinone concentrations in the range 10^{-7} to 10^{-6} M, and the observed rate is 1-2 orders of magnitude larger than what was observed for the fine and coarse mode production of H_2O_2 in aqueous solution. This indicates there are (as expected) much lower levels of electron donors in ambient aerosols compared to the DTT levels added (the molar ratio was not reported by Chung et al. (2006) but there appears to have been a large excess). Additionally Chung et al. (2006) reported that the concentrations of the active quinones were very low in the summer months, or generally when temperatures exceeded about 30 ºC, which is not consistent with this mechanism playing a major role in ROS generation, or particle toxicity, in the summer.

When a solution of Fe(III) and oxalic acid, at pH 4, was exposed to sunlight, Zuo and Deng (1997), H_2O_2 formation at a rate of 220 nM min^{-1} was observed. This is around an order of magnitude faster than what we observe; about 15 and 30 nM min^{-1}, respectively for fine and coarse particles. Initial Fe(III) and oxalic acid concentrations were 1 and 5 μM, respectively and are realistic particle concentrations (Deguillaume et al., 2005, Chebbi and Carlier, 1996). It is reasonable to assume that iron in ambient particles is less available than dissolved iron used by Zuo and Hoigne, but our measurements take place in dim room light and partially opaque Petri dishes, so a different mechanism is required. The H_2O_2 temporal profiles in both fine and coarse modes display two parts; the initial, rapid appearance of H_2O_2 followed by a slower rate of H_2O_2 appearance

It has been shown that transition metals also have a two part dissolution temporal profile; a rapid first dissolution step, followed by a slower rate of dissolution (Desboefs et al., 2005). Transition metals associated with the outer portion and surface of ambient particles is quickly released in an aqueous solution. The inner portion of ambient particles, containing solid phase Fe, will be dissolved at a slower rate (Deguillaume et al., 2005). The two-step dissolution process for Fe

and H_2O_2 along with similar H_2O_2 formation rates, is consistent with the involvement of redox reactions involving speciated Fe and the production of H_2O_2 in extract solutions.

4.3 The Effect of Extraction Solution Composition and pH on H_2O_2 Generation by Ambient Aerosols

4.3.1 pH

Nine Sets of four fine and coarse mode aerosols were collected at UCLA on Teflon filters (Pellman) using parallel virtual impactor sampling trains. Each filter was cut in half, resulting in four half-filters each for the fine and coarse modes for each aerosol sample. Extraction solutions are made with MilliQ water (18MΩ cm^{-1}) filtered through polyethersulfone, 0.22 μm pore filters. 0.1 mM was added, and finally the pH is adjusted using 0.1 N H_2SO_4 or 0.1 M NaOH.

The first few sets of filters were cut by hand, using a nickel plated scalpel. The resulting four filter halves were extracted at pH 1.95, 2.94, 3.5 and 6.00 (Table 4-3-1). All other filters were cut using a ceramic blade that was attached to a guillotine-like cutter. One half of each of these latter samples was extracted at pH 3.5, and the second half at one of the following pHs: 3.97, 4.13, 4.5, 5.0, 6.0 or 7.6. Data for pH 3.97 and 4.13 were averaged.

Table 4-3-1. Sample and Analysis Data Points

	Fine Mode		Coarse Mode	
Extraction Solution pH	Number of data Points used for Average	Number of Different Ambient Aerosol Sampling Events	Number of data Points used for Average	Number of Different Ambient Aerosol Sampling Events
1.94	3	3	2	2
2.94	3	3	2	2
4.06*	5	4	5	4
4.51	4	3	5	4
5.02	5	4	5	4
6.00	2	2	2	2
7.62	4	2	4	2

*Average of measurements made at pH 3.94 and 4.13.

Particle-associated H_2O_2 levels as a function of pH are plotted relative to pH 3.5 measurements, and are shown in Fig. 4-3-1 (a-b). Both fine and coarse mode H_2O_2 were affected by changes in the pH. For the fine mode, particle-associated H_2O_2 levels peaked at pH 4.5, 25% above

the reference pH 3.5 measurements. At the acidic pH of 1.5, H_2O_2 generation decreased to 28% of pH 3.5 levels. As the pH is increased to 5.5 and above, H_2O_2 generation decreased to levels that ranged from 50 to 75% of the levels observed at pH 3.5. For the coarse mode, H_2O_2 production is at a maximum at the most acidic pHs tested, 1.5 – 2.5, where it exceeded the pH 3.5 reference solution by 25% (Fig 4-3-1 b). H_2O_2 monotonically decreases at pHs above 2.5, reaching roughly 30% of pH 3.5 levels at pH 6.5, after which it remains fairly constant as the pH was increased further.

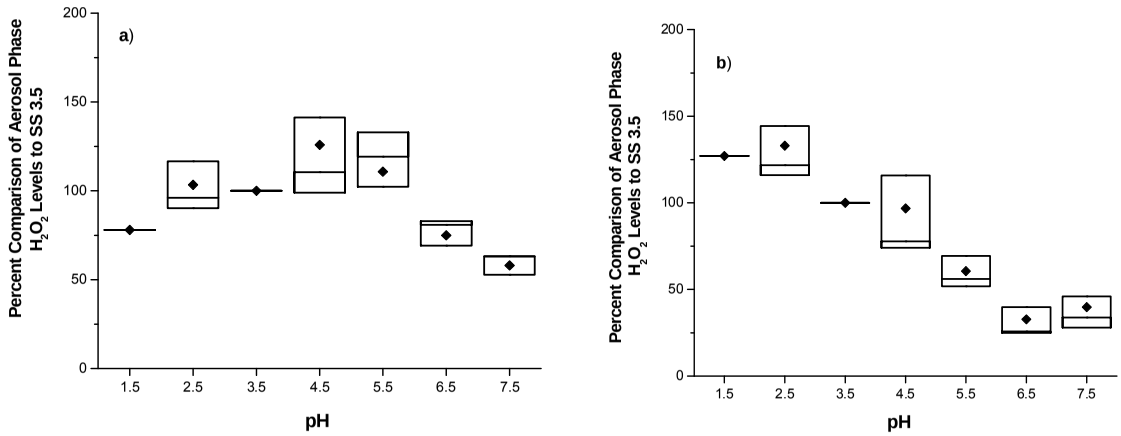

Figure 4-3-1 Peroxide responses to changes in pH.

a) Fine and b) coarse mode H_2O_2 responses to variations in extract solution pH. All results are presented relative to H_2O_2 levels measured in the pH 3.5 extract solution. The black diamonds indicate the average, the horizontal bar represents the median, and upper and lower boundaries of the boxes represent the standard deviation of the mean. Data for pH 3.5 is set to 100% and is included as a visual guide. In both fine and coarse modes the data point for pH 1.5 is an average of three measurements, hence the lack of a box.

Differences in how fine and coarse mode H_2O_2 levels respond to pH changes may offer insight into chemical mechanisms responsible for formation of ROS by particles. Zuo and Hoigne (1992) explored a potential mechanism for H_2O_2 formation in atmospheric waters (such as cloud and fog drops and water associated with aerosol particles) and postulated that Fe(III) complexed to mono-, di-, and tri-oxalato (oxalic acid) ligands were responsible for the formation of H_2O_2. The basis of their mechanism is that Fe(III)-oxalato complexes absorbs UV and visible light (200 – 420 nm) more strongly than any other Fe(III) complexes and is thus able to photo-reduce (Zuo and Hoigne, 1992). In laboratory controlled experiments, solutions containing Fe(III) and oxalate were irradiated and the formation of H_2O_2 monitored. It was found that H_2O_2 production was linear with respect to initial concentrations of oxalate and Fe(III). Their proposed mechanism for H_2O_2

formation from Fe(III)-oxalato involves the photoreduction of Fe(III)-oxalato to Fe(II)-oxalato which dissociates, yielding Fe^{2+} and an oxalate radical. Both $Fe^{2+}$and the oxalate radical can be oxidized by molecular oxygen to yield the superoxide anion that will equilibrate with HO_2 radical. Both HO_2 and $O_2^{\cdot-}$ radicals can react with Fe(II) to generate H_2O_2 (R-1). Zuo and Hoigne (1992) also observed that the Fe(III)-oxalato photoreduction mechanism proposal for H_2O_2 formation is sensitive to changes in pH. At acidic conditions, pH 1 – 4, H_2O_2 generation remains relatively high and constant. At pHs greater than 4, a sharp decline in H_2O_2 production was noted, reaching 20% of the value at pHs between 1 and 4 by pH 6. The reduction in H_2O_2 formation is due to two reasons, the first being that Fe(III)-oxalato complexes are unstable at pH 5 or greater (Zuo and Hoigne, 1992). Second, it is noted that the reaction of Fe(II) with $HO_2^{\cdot}$ /$O_2^{\cdot-}$ is three orders of magnitude faster than the corresponding reaction with Fe(III) at pHs less than 5, due to the $HO_2^{\cdot}$ pKa being 4.8 (Zuo et al., 1992). In a related regime, Siefert et al. (1994) investigated the availability of Fe(II) for participation in photochemical redox reactions by collecting ambient particles, adding oxalate and irradiating solutions with UV-light (320 – 390 nm). Irradiated solutions were monitored for 25 hrs, and in all cases, H_2O_2 production was rapid during the first 5 hrs then gradually approached a final concentration. Similarly, measurements of Fe(II) formation with respect to time were shown to rapidly increase within the first 5 hrs, and then taper off to a final concentration.

In both experiments the availability and speciation of Fe played a critical role in the amount of H_2O_2 generated. In the absence of Fe(II), very little H_2O_2 was observed, giving evidence that the Fe(III)/Fe(II) photoreduction cycle is capable of generating H_2O_2. The availability of chemical species is dependent on the solubility of aerosols being extracted which is in turn dependent on the extraction solution pH. Additionally, the availability of speciated transition metals, like Fe(II) and Fe(III), in aqueous solutions is greater at acidic pH (<5); whereas at more basic pHs, precipitation is likely to occur. Dissolved Fe(III) can be complexed to several ligands which include: water, hydroxides, inorganic and organic species. Fe(III) hydroxide species are prevalent at pHs less than 3 and rapidly decrease as the pH is increased to 6. On the other hand, Fe(III)-hexaaquo complexes become more prevalent as the pH approaches 6 (Deguillaume et al., 2005). In contrast, Fe(II)-hexaaquo complexes are favored at pHs less than 5 while $Fe(OH)^+$ is favored at pHs greater than 5 (Deguillaume et al., 2005). Measurements of speciated Fe in atmospheric waters have demonstrated Fe(II) concentrations ranging from 20 – 80% of total Fe concentrations with maximums occurring during the day and declining in the evening hours (Erel et al., 1993). The availability of Fe(II) is determined by the presence of oxidizing compounds, the dissolution of Fe-containing solids and the

pH (Deguillaume et al., 2005). In the presence of organic species like oxalic acid, Fe(III)-oxalato complexes form easily, provided the pH is less than 5, and are dominant compounds due to greater stability constants. In this pH variation study, H_2O_2 production from fine mode particles displayed a trend similar to what Zuo and Hoigne (1992) observed, which was relatively constant H_2O_2 production levels at pHs less than 4.5 followed by a decrease when the pH is increased past 4.5 (Zuo and Hoigne, 1992). The H_2O_2 associated with the fine mode displays a maximum H_2O_2 production at pH 4.5. At this pH, Fe^{3+} and Fe^{2+} are present and available to participate in reactions; in particular, Fe(III) will complex to organic ligands that were extracted from collected aerosols. The pH is suspected to play two roles, first by affecting the dissolution rates of chemical species from aerosols which in turn dictates their ability to participate in chemical reactions. Second, the pH will determine what form of Fe is available by shifting the Fe(III)/Fe(II) equilibrium constants, as well as affect what form either Fe(II) or Fe(III) exists as in solution. Subsequently, this affects the aqueous phase chemistry taking place in the extraction solution. One aspect of H_2O_2 production not considered is heterogeneous reactions, where Fe compounds at the surface of solids with aerosols can participate in reactions similar to homogeneous ones. Heterogeneous H_2O_2 production would likely be occurring in the coarse mode extracts due to their composition, i.e., rich in soil minerals (Deguillaume et al., 2005). However, it is suspected that heterogeneous reactions would decline as the basicity is increased, a phenomena that is attributed to a relative strengthening of Fe-O bonds (Deguillaume et al., 2005). This could be an explanation for the sudden decrease in H_2O_2 production in coarse mode extracts as the pH is increased passed 3.5. These pH measurements corroborate the notion that transition metals, in particular Fe, are at least partly responsible for the generation of H_2O_2 in extract solution. In an acidic extraction medium (pH < 4.5), the production of H_2O_2 is favored, indicated by the trends observed in Fig 4-3-1, for both fine and coarse mode extract solutions. Zuo and Hoigne (1992) explored the effects of pH variations on H_2O_2 production from the Fe(III)-oxalato photoreduction in the presence of oxygen. They observed that between pH 1 and 4, the H_2O_2 production rate was relatively constant, dropping off by 80% when the pH was increased to 5 or above. This trend was observed in our pH variation experiments in fine mode extraction solutions, thus it is possible that Fe(III)-oxalato complexes are participating in reactions that can generate H_2O_2 as a byproduct. There are other routes that can generate H_2O_2, such as the analogous Cu(I)/Cu(II) redox cycle, and the reduction of quinoids, and they are not ruled out by these experiments. Instead, it is likely that several ROS-generating chemical reactions occur in solution to produce the observed H_2O_2.

4.3.2 Extraction in Physiologically Relevant Solutions (PRS)

Generation of H_2O_2 by ambient particles may be affected by other solutes in the extraction solution. Similarly, the composition of lung lining fluid may substantially impact release of H_2O_2 by ambient particles deposited in the lungs. Recognizing that lung lining fluid is considerably more complex than solutions generated in the lab, we attempted to assess the impact of the increased ionic strength and buffering ability found in physiological fluids. Two fluids have been used over the years for this purpose: Gamble's and Ringer's, and while their composition is different, they mimic the pH (7.4) and ionic strength of lung lining fluid (~0.17 M) (Kanapilly et al., 1973). The chemical composition of both PRSs and their respective ionic strengths are presented in Table 4-3-2. Two additional solutions at pH 3.5 and 7.4 were also used to extract collected aerosols and served as reference solutions to compare H_2O_2 levels measured in the PRSs. Particle-associated H_2O_2 production measured in PRS extract solutions and the pH 3.5 solution was compared to measurements made in the pH 7.4 (SS 7.4) solution and are presented relative to SS 7.4 (Fig. 4-3-2). As a reference, fine mode H_2O_2 levels and activity measured in SS 7.4 were 1.9 ± 0.2 ng m^{-3} and 0.10 ± 0.02 ng μg^{-1}, respectively. Fine mode H_2O_2 production in Ringer's and Gamble's solution was a factor of 6 and 3, respectively, greater than H_2O_2 production in SS 7.4. Coarse mode H_2O_2 concentration and activity measured in SS 7.4 were 4.2 ± 0.5 ng m^{-3} and 0.10 ± 0.02 ng μg^{-1}, respectively. Coarse mode H_2O_2 production in Gamble's and Ringer's was not similar to what was observed in the fine mode. H_2O_2 production in Ringer's extract solution was a factor of 3 greater than what was measured in SS 7.4. No change was observed for H_2O_2 production in Gamble's when compared to SS 7.4. In the coarse mode, the SS 3.5 extract solution resulted in H_2O_2 production that was a factor of 6.5 greater than what was found in SS 7.4. Measured H_2O_2 activity, defined as ng of H_2O_2 per unit mass of aerosol collected, mirrored the trends observed in fine and coarse mode H_2O_2 mass loadings.

Table 4-3-2 Gamble's and Ringer's solution compositions.

	Molar Concentration (mM)	
Chemical	Gamble's	Ringer's
NaCl	116	114
NH_4Cl	10	--
$NaHCO_3$	27	31
NaH_2PO_4	1.2	2
Na_2HPO_4	--	14.6
Na_3citrate	0.2	--
glycine	6	--
$CaCl_2$	0.2	--
pH	7.4	7.4
Ionic Strength (M)	0.15	0.19

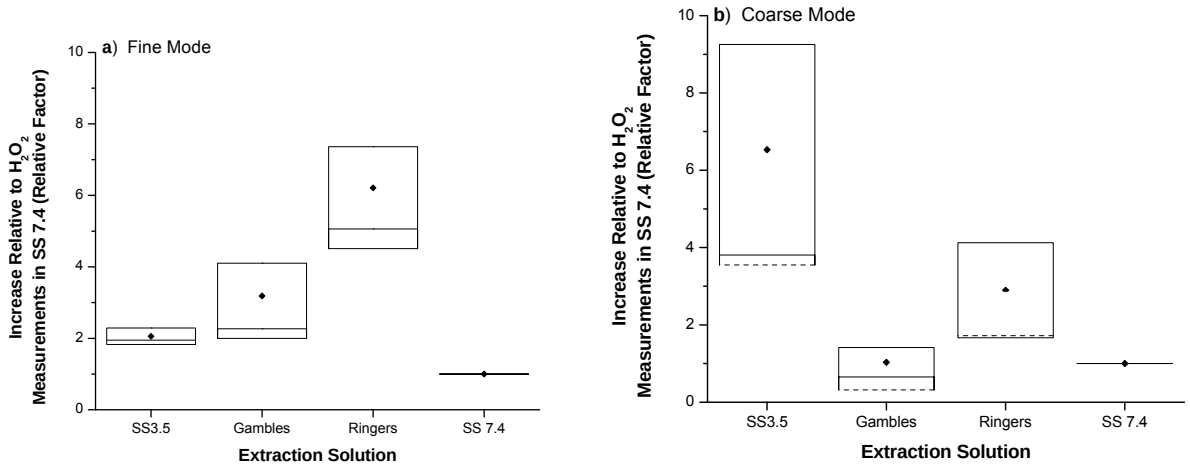

Figure 4-3-2. Peroxide responses to PRSs. a) Fine mode and b) coarse mode associated H_2O_2 levels found in PRSs and pH 3.5 solutions to the SS 7.4 reference solution. H_2O_2 levels measured in the PRSs and SS 3.5 are presented relative to the amount of H_2O_2 measured in the SS 7.4 solution and are presented as a ratio. H_2O_2 levels found in the SS 7.4 solution are presented as a visual aid and represent the control, with an 'increase factor' of 1. The black diamond represents the average, the horizontal bar within the box is the median and the upper and lower limits of the box indicate the standard deviation of the mean.

With the exception of the coarse mode H_2O_2 measured in Gamble's solution, the amount of H_2O_2 generated in extract solutions exceeded H_2O_2 levels observed in the SS 7.4 solution (again, both Gamble's and Ringer's solutions are at pH 7.4). The SS 3.5 and SS 7.4 were included in the pH variation analysis discussed here and demonstrate that H_2O_2 levels at a physiologically relevant pH 7.4 were decreased by 60%, relative to what was measured in the SS 3.5 solution. Despite similar

pHs, Ringer's and Gamble's solutions increased H_2O_2 production in the fine and coarse mode extract solutions. The ionic strength of Ringer's and Gamble's was 0.019 and 0.016 M, respectively, and may have played a role in observed H_2O_2 production levels measured. Fe(III) monomer complexes (Fe^{3+}, $Fe(OH)^{2+}$, and $Fe(OH)_2^{+}$) co-exist in various mole fractions dependent on the pH and ionic strength. At pHs greater than 5, the $Fe(OH)_2^{2+}$complex is dominant even when oxalate is present because the Fe(III)-oxalato stability constant begins to decrease after pH 5.5 (Deguillaume et al., 2005; Zuo and Deng, 1997). In the SS 7.4, the ionic strength is near zero; whereas in the PRSs the ionic strength is close to 0.02 M which has the effect of decreasing Fe(III) hydrolysis equilibrium constants in such a way that $Fe(OH)^{2+}$ is the dominant Fe(III) complex (Flynn, 1984). In a manner analogous to Fe(III)-oxalato, the $Fe(OH)^{2+}$ complex can participate in redox reactions in the presence of dissolved O_2 to generate H_2O_2. This is further supported by the observed trend in coarse mode H_2O_2 levels: a decrease in relative concentrations and activities.

4.4 H_2O_2 Measurements in Size Fractionated Particles

Here we discuss measurements made with a Micro Orifice Uniform Deposition Impactor (MOUDI) used to fractionate ambient aerosol into more fractions than possible using the virtual impactors.

4.4.1 Sampling and Analysis of Size Fractionated Aerosols

Ambient aerosols were sampled at UCLA from May to June, 2004 and again from May to September, 2006. The MOUDI (Model 110, MSP Corporation) is a 10 stage cascade impactor operating on the premise of inertial impaction. Ambient air was drawn at 30 Lpm into an inlet with an 18 μm size cut using a rotary vane pump (GAST, 300-GX). Particle laden air travels through ten stages each with a unique particle size cut (Table 4-4-1). As particles traverse the MOUDI, those with smaller inertial masses are impacted on later stages, and particles with larger inertial masses are collected on the upper stages (Fig. 4-4-1). Collection of particles at each stage is accomplished with a Teflon filter (47 mm, 2 μm pore, Pall Scientific). Each stage has a plate which holds the filter and has specifically engineered holes through which the airstream flows. For each progressive stage the holes become smaller and more numerous. The pattern and number of holes per stage has been optimized to achieve the desired size cut (Marple et al., 1991) .

Table 4-4-1 MOUDI size cuts

MOUDI Stage	Size Cut (μm)	Size Fraction Collected (μm)
Inlet	18	
1A	10	18 – 10
2A	5.6	10 – 5.6
3A	3.2	5.6 – 3.2
4A	1.8	3.2 – 1.8
5A	1	1.8 – 1.0
6A	0.56	1.0 – 0.56
7A	0.32	0.56 – 0.32
8A	0.18	0.32 – 0.18
9A	0.1	0.18 – 0.1
10A	0.056	0.1 - 0.056
After Filter (AF)	<0.056	0.056 – 0.01*

*Estimated lower end range

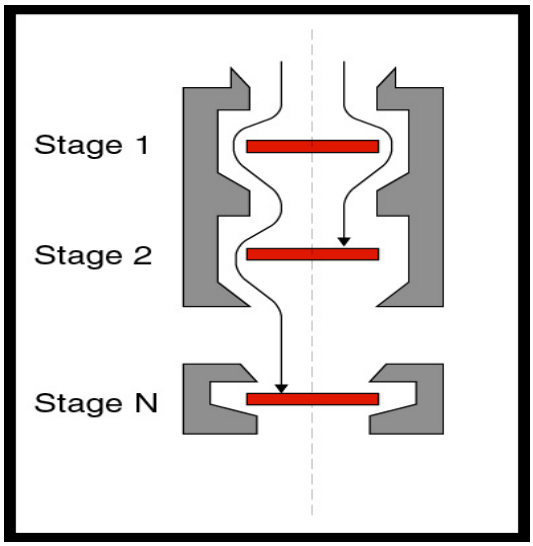

Figure 4-4-1 MOUDI schematic.
The arrows indicate the air flow. Particles with low mass will traverse further into the MOUDI. Larger particles with more inertia will be impacted in upper stages. Teflon filters are used as the aerosol collection medium.

Sampling times ranged from 20 – 30 hrs and typically began in the morning hours (7-11 AM) continuing until the next day. Long sampling times were required to obtain enough aerosol mass for H_2O_2 analysis, especially at lower size cuts. MOUDI sampling occurred in three phases. Phase I was

conducted from May to June of 2004 at UCLA with a MOUDI configuration that was altered from its normal operational set-up. A configuration that used stages 2A – AF eliminated stage 1A, meaning that stage 2A consolidates particle sizes ranging from 5.6 – 18 μm. Phase II, conducted in May 2006, used a different MOUDI stage configuration (2A – 8A and AF), so that the AF stage collected particles in the size range of 0.18 – 0.01 μm. Note, the 0.01 μm lower end of the particle size range is an estimation made for data analysis purposes and is not an exact size cut. In both phase I and II, a pH 3.5 solution (SS 3.5) was used to extract aerosols from filters. Phase III, conducted from August to September, 2006, involved using the MOUDI in another configuration: stages 1A – 5A and 9A – AF, in which stage 9A consolidates particles with a size range of 1.0 – 0.1 μm. During phase III, filters were cut in half and extracted in either a physiologically relevant solution (PRS) or SS 3.5 for a comparison of H_2O_2 levels and activities.

All filters were extracted for 2 hrs with gentle agitation and the extract analyzed for H_2O_2 using the HPLC/fluorimetric method described in detail in Section 2. In all three phases, aerosol mass concentrations were recorded using a microbalance (± 1 μg, Sartorius, ME-5). During phase III, tared filters were weighed after a sampling event and then cut in half with a Ni-plated scalpel. Filter halves were weighed to determine the amount of aerosol mass per half filter.

During phase I, filter blanks were obtained by placing an unused Teflon filter (Pall Corp.) in SS 3.5 for 2 hrs then analyzing for H_2O_2. The amount of H_2O_2 found was used to correct all H_2O_2 levels measured in size fractionated aerosols for a particular sampling event. During phase II, field blanks were incorporated into the sampling regime and conducted in the following manner. At the conclusion of a sampling run, two tared Teflon filters were loaded onto MOUDI stages. Once loaded, ambient air was drawn through the MOUDI for 30 sec, and the filters were removed, extracted, and analyzed. The moles of H_2O_2 measured in each filter blank extract were averaged and used to correct measured H_2O_2. In phase III, field blanks were taken in the same manner, except that field blank filters were cut in half and extracted in both SS 3.5 and a PRS. Again the average of H_2O_2 moles found in each extract was used to correct observed H_2O_2 levels.

A small study on background H_2O_2 was conducted by comparing H_2O_2 levels measured in field blanks, to H_2O_2 levels measured in SS 3.5 that was pulled from a stock solution, and SS 3.5 that had been left in a sealed Teflon Petri-dish for 2 hrs (Fig. 4-4-2). H_2O_2 levels in stock SS 3.5 averaged 0.87×10^{-7} M, and when left on a Petri-dish rose to 1.18×10^{-7} M. The average H_2O_2 concentration found in field blanks was 1.52×10^{-7} M, a slight increase compared to the SS 3.5 H_2O_2 content

measured in the stock and some that had been left in a Petri-dish. Thus, the amount of H_2O_2 measured in field blanks comes mainly from background sources. Average field blank H_2O_2 levels when extracted in 3 mL of SS 3.5 were $1.05 \pm 0.3 \times 10^{-7}$ M. PRS field blank H_2O_2 levels were similar to pH adjusted water at 1.10 ± 0.2 and $0.9 \pm 0.4 \times 10^{-7}$ M for Gamble's and Ringer's solutions, respectively.

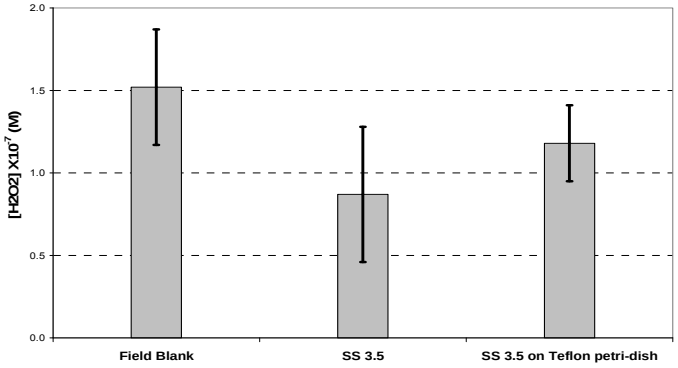

Figure 4-4-2 Average H_2O_2 levels found in field blanks, compared to H_2O_2 in the extraction solution. Error bars represent the standard deviations. Volume used in all analysis was 4 mL.

Field blank contributions to observed H_2O_2 levels varied with the particle size fraction (Fig. 4-4-3 and 4-4-4). Aerosols larger than 1.8 μm have relatively large H_2O_2 signals thus field blank H_2O_2 contributions to measured levels were small. As particle size decreases, both particulate mass and measured H_2O_2 drop so that field blank contributions rise. The H_2O_2 levels in particles less than 1.0 μm dropped significantly, resulting in many samples for which field blank H_2O_2 was 70% or more of the sample signal. In phase III, field blank contributions were not as large due to a change in the MOUDI configuration which resulted in more particles of smaller sizes being collected and few samples being excluded from further analysis.

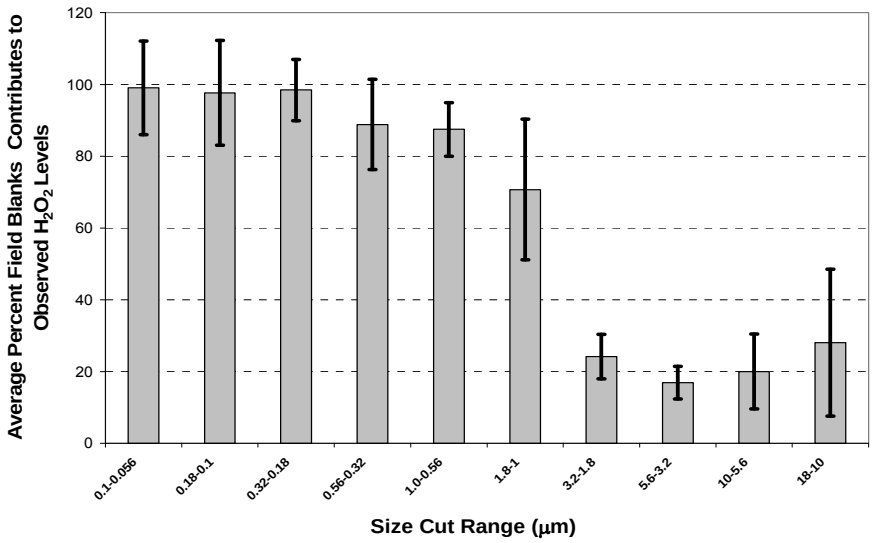

Figure 4-4-3 Average field blank contributions for Phase I and II to observed H_2O_2 levels by size range. Error bars represent the standard deviations.

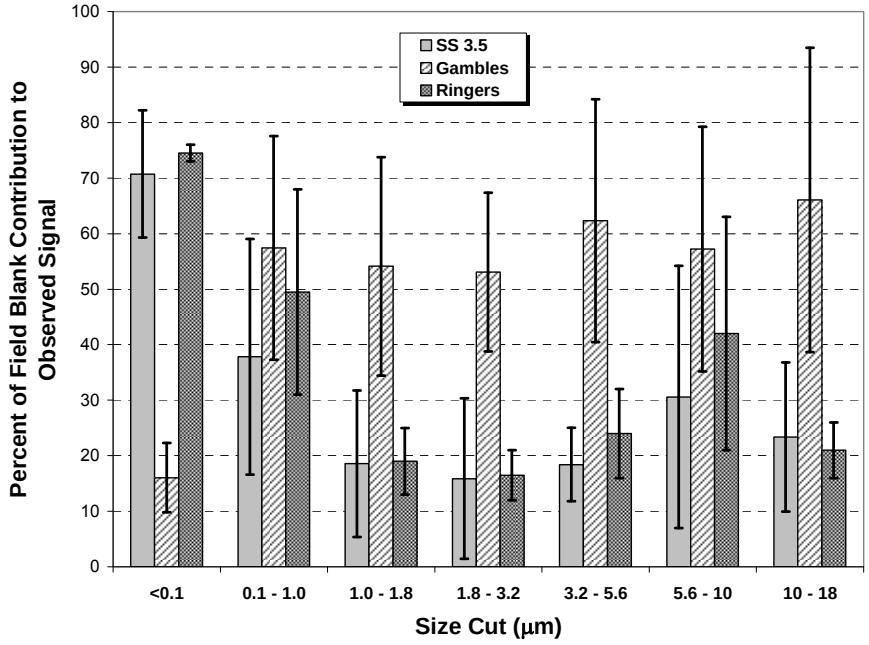

Figure 4-4-4 Field blank H_2O_2 contributions to measured H_2O_2 levels. For SS 3.5 and Gamble's extract solutions, the error bars represent the standard deviation. For Ringer's extract solution, the error bars represent a range.

4.4.2 Results

H_2O_2 levels, activities, and aerosol mass concentrations are graphically presented below in the following format: the x-axis represents the particle size range midpoint in a $\log_{10}$ format because midpoint sizes can cover three orders of magnitude. The y-axis represents the parameter measured normalized to the log of the size range (ΔLogD). Normalized aerosol mass concentrations are presented as a function of size for phase I and II (Fig. 4-4-5). Summing individual average mass concentrations yields 42 μg m^{-3} (fine and coarse mode particle combined), very similar to previous measurements made at UCLA which averaged 39 μg m^{-3}. Particles in the 1.78 – 3.18 μm range had the highest average mass concentration, 8.4 ± 0.8 μg m^{-3}, and particles collected in the last stage (≤0.18 μm) had the lowest mass concentration of 0.81 μg m^{-3} (Table 4-4-2).

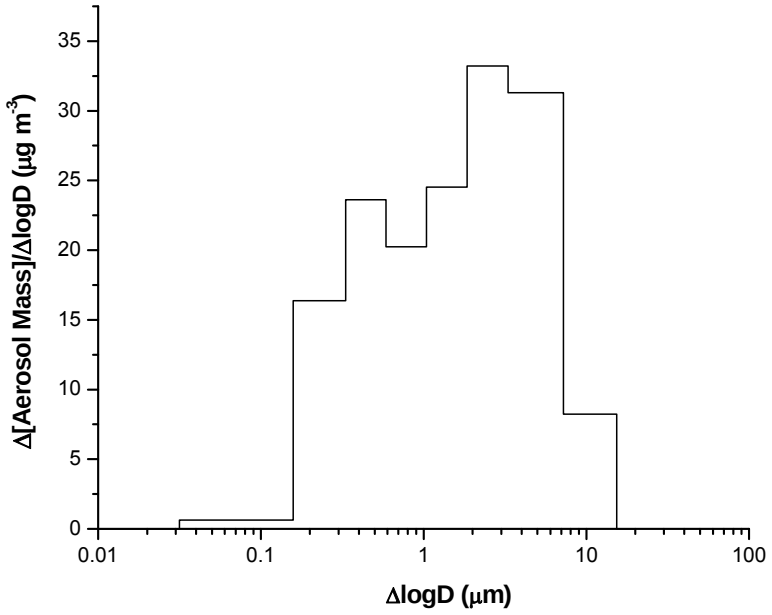

Figure 4-4-5 Average aerosol mass concentrations found during phase I and II. Data used to create this plot are presented in Table 4-4-2.

Table 4-4-2 Average aerosol mass concentration per MOUDI size range.

Stage	Size Range	Ave. [Mass] ($\mu g\ m^{-3}$)	SDOM	N
AF	<0.18	0.81	(0.42-1.02)*	3
8A	0.32 – 0.18	4.09	0.9	5
7A	0.56 – 0.32	5.74	(0.94-10.29)*	3
6A	1.00 – 0.56	5.10	1.18	7
5A	1.78 – 1.00	6.14	0.57	11
4A	3.18 – 1.78	8.37	0.77	11
3A	5.62-3.18	7.74	0.93	11
2A	18-5.62	4.16	0.38	11
Total		42.15		

*represents a range which is used due to a small sample set. SDOM represents the standard deviation of the mean.

H_2O_2 levels normalized by the size range are presented in Fig. 4-4-6. Table 4-4-3 shows H_2O_2 associated with each size fraction falls in the range of 0.4 – 3 ng m^{-3}, with larger quantities in the size fractions above 1 μm. The sum of all the fractions averages to 11 ng m^{-3}, similar to averages for measurements made with virtual impactors at UCLA (at other times) of about 15 ng m^{-3}. The peroxide associated with fine mode (< 2.5 μm) and coarse mode (>2.5 μm) particles is also similar to the virtual impactor measurements. In the MOUDI measurements, H_2O_2 is measured to be 4.2 and 7 ng m^{-3} for fine and coarse aerosols, while the virtual impactor values are 5.4 ± 6 and 10 ± 7 ng m^{-3}. The differences may be attributed to several factors: errors, especially in the sample flow rates, which are more likely to be systematic, and the decay of the ability of particles to generate peroxide with time. Virtual impactor samples are typically collected over 2 hrs or so, while MOUDI samples are collected over 24 hrs. Other measurements (above) indicate that peroxide generation decays by about a factor of 10% over 24-30 hrs, which may also be responsible for some of the difference. Fig. 4-4-7 and Table 4-4-5 show particle-associated H_2O_2 normalized to particle mass. Normalized activity is highest in the ultrafine and coarse modes and lowest in the accumulation mode (0.1 – 1 μm).

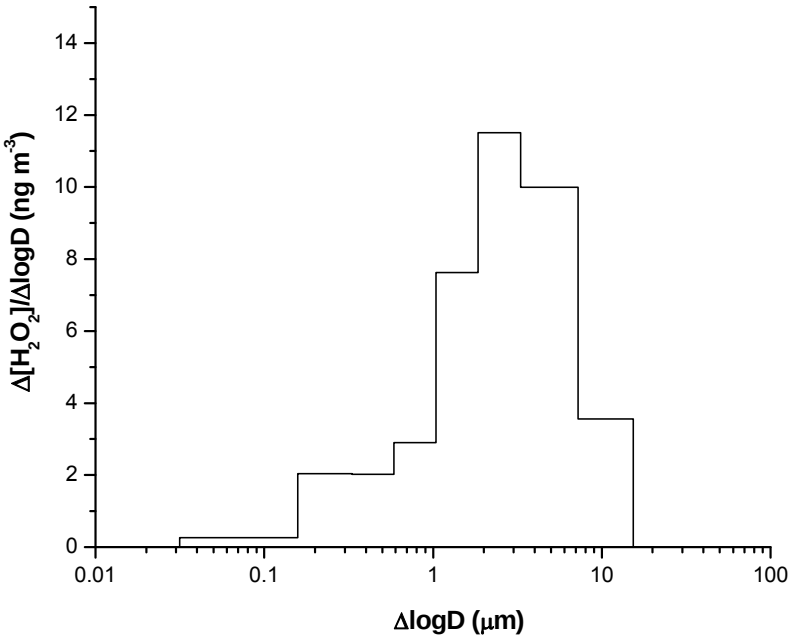

Figure 4-4-6. Average H_2O_2 levels per size fraction normalized to ΔLogD. Data and associated statistical information are presented in Table 4-4-3

Table 4-4-3 Average H_2O_2 levels per size fraction.

Stage	Size Range (μm)	Average $[H_2O_2]$ (ng m^{-3})	$\Delta[H_2O_2]/\Delta logD_P$	SDOM/ Range
AF	<0.18	0.33	0.68	0.32 – 0.57
8A	0.32 – 0.18	0.50	2.01	0.6
7A	0.56 – 0.32	0.37	1.53	0.10 – 1.27
6A	1.00 – 0.56	0.73	2.91	1.0
5A	1.78 – 1.00	2.03	8.11	1.1
4A	3.18 – 1.78	3.03	12.04	1.1
3A	5.62 – 3.18	2.60	10.50	1.4
2A	18 – 5.62	2.13	4.21	0.9
Total		11.7		

Error reported is standard deviation of the mean. If the sample set is too small (N<5) a range is reported.

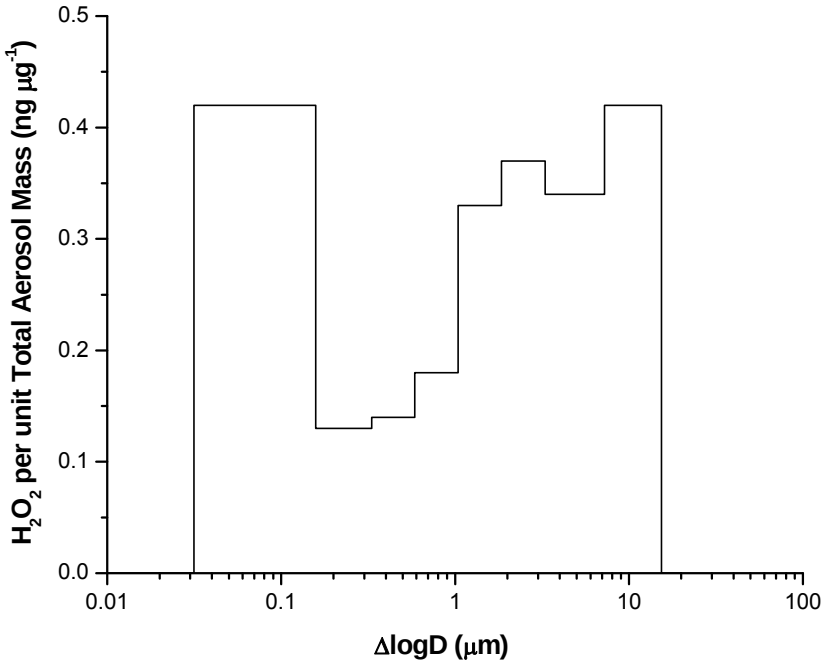

Figure 4-4-7 Average H_2O_2 activity found per size fraction. Associated data and statistical information are presented in Table 4-4-5.

Table 4-4-5 Average H_2O_2 activities per size fraction.

Stage	Size Range (μm)	Ave H_2O_2 /Total Aerosol Mass	SDOM/ Range
AF	<0.18	0.41	0.15 – 0.24
8A	0.32 – 0.18	0.10	0.02
7A	0.56 – 0.32	0.11	0.01 – 0.11
6A	1.00 – 0.56	0.18	0.05
5A	1.78 – 1.00	0.36	0.06
4A	3.18 – 1.78	0.41	0.05
3A	5.62 – 3.18	0.35	0.04
2A	18 – 5.62	0.46	0.08

Error reported is standard deviation of the mean. If the sample set is too small (N<5), a range is reported.

Further sampling was conducted with the MOUDI in which collected aerosols were extracted in SS 3.5 or a PRS such as Gamble's or Ringer's solution. The amount of H_2O_2 measured in each extract solution was compared to observe the effects that the PRSs had on the ability of particles to generate H_2O_2. During this phase, filters were cut in half to make comparisons so the

MOUDI configuration was changed to consolidate several size fractions (Table 4-4-6). Stage 9A collected aerosols in the size range of 0.1 – 1.8 μm, consolidating four size fractions (Table 4-4-1). In previous measurements, these size fractions consistently picked up the least amount of aerosol mass and had the lowest H_2O_2 levels. Also the new consolidated size fraction was similar to the accumulation mode size definition of 0.1 – 2.0 μm.

Table 4-4-6 MOUDI configuration used during phase III testing

Stage	Size Cut (μm)
1A	18-10
2A	10-5.6
3A	5.6-3.2
4A	3.2-1.8
5A	1.8-1.0
9A	1.0-0.10
AF	0.1-0.056

Five and two runs were conducted comparing particle activity in Gamble's and Ringer's solutions to SS 3.5, respectively. Total H_2O_2 levels, determined by summing the H_2O_2 for all size fractions, were similar for SS 3.5 and Gamble's solutions at 12.3 and 15.3 ng m^{-3}, respectively. Ringer's' results were significantly lower at 5.3 ng m^{-3}. Despite the similarity between total particle-associated H_2O_2 production in SS 3.5 and Gamble's extract solutions, there were differences for individual size fractions. The largest difference observed was H_2O_2 for ultrafine particles in the various extract solutions. Ultrafine H_2O_2 levels were measured at 0.7, 6.1 and 2.3 ng m^{-3} for SS 3.5, Gamble's and Ringer's, respectively (Table 4-4-7). The ultrafine fraction made up 6, 60 and 60% of the total peroxides found in SS 3.5, Gamble's and Ringer's respectively (Fig. 4-4-8). The peroxide measurements in Gamble's and Ringer's are also elevated compared to SS 3.5 for the accumulation mode (0.18 – 1 μm). In the coarse mode, H_2O_2 levels measured using Gamble's and Ringer's were much lower compared to SS 3.5. This is consistent with the results in section 4.3, except that Ringer's lowered the relative activity more than Gamble's in that case. Given the sample to sample variations observed (above) this difference may be sample specific.

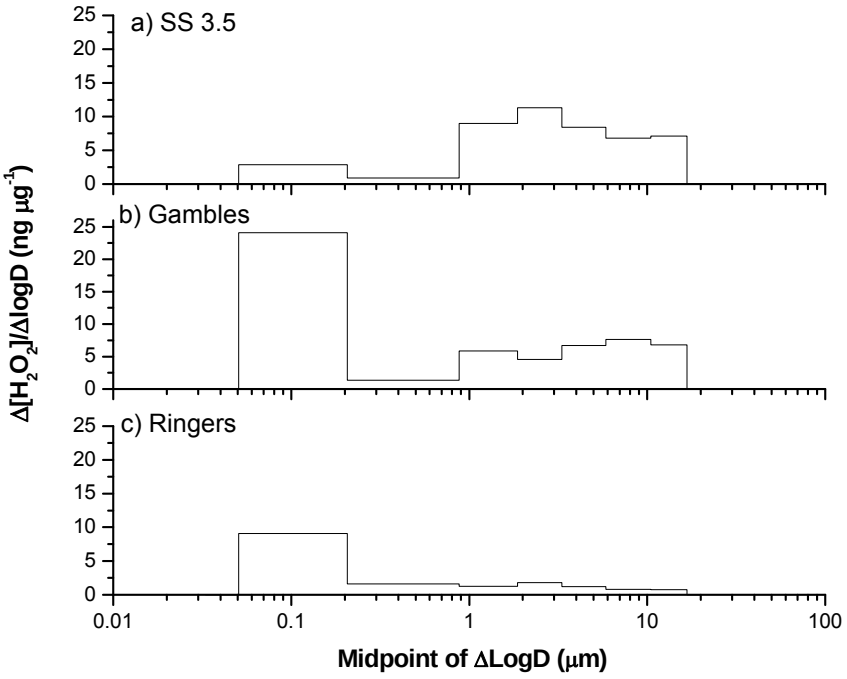

Figure 4-4-9 Measured particle phase H_2O_2 levels normalized to ΔLogD. Data and associated statistical information are presented in Table 4-4-7

Table 4-4-7 Average particle phase H_2O_2 levels measured

Size Range (μm)	$[H_2O_2]$ ± SDOM (ng m^{-3})		
	SS 3.5	Gamble's	Ringer's
<0.1	0.72 (0.22 – 0.93)	3.34 ± 0.7	2.29 (2.0 – 2.6)
1.00 – 0.10	0.91 ± 0.1	0.67 (0.22 – 1.2)	0.16 (0.1 – 0.2)
1.78 – 1.00	2.3 ± 0.3	1.0 (0.9 – 1.1)	0.32 (0.2 – 0.4)
3.18 – 1.78	2.8 ± 0.4	0.57 (0.3 – 1.1)	0.45 (0.3 – 0.6)
5.62 – 3.18	2.0 ± 0.3	0.82 (0.4 – 1.3)	0.29 (0.3 – 0.3)
10 – 5.62	1.7 ± 0.3	0.96 (0.8 – 1.1)	0.20 (0.2 – 0.2)
18.0 – 10	1.8 ± 0.3	0.86 (0.3 – 1.4)	0.20 (0.2 – 0.2)
Total	12.3	8.23	3.92

If the sample population (N) was less than 5, a range is reported. If N was 5 or greater, the standard deviation of the mean is reported.

The H_2O_2 normalized to aerosol mass (activity) measured per size fraction varied with the type of extract solution used. In SS 3.5, the H_2O_2 activity was greater than 0.30 ng μg^{-1} for all size fractions, except in ultrafine particles which had an activity of 0.14 ng μg^{-1} (Fig. 4-4-10). Both

Gamble's and Ringer's extract solutions displayed high H_2O_2 activities in the ultrafine particles; 0.27 and 0.42 ng μg^{-1}, respectively, factors of 2 and 3 larger than the signal in SS 3.5 (Table 4-4-9). In particles >0.1 μm, peroxide formation declines in Gamble's and Ringer's by an average of 53 ± 9 and 83 ± 2 %, respectively, compared to activity in SS 3.5. Based on this limited data set, PRSs do not appear to promote the generation of H_2O_2 in particles larger than 0.1 μm. However, PRSs appear to be able to promote H_2O_2 generation in ultrafine particles extracted with PRSs.

During phase III sampling, the ultrafine aerosol mass collected was larger relative to what was measured in the earlier Phase I and II measurements. In phases I and II, the average aerosol mass recorded for ultrafine particles averaged 34 and 30 μg, respectively. During phase III, the amount of aerosol mass collected increased by a factor of 20 to approximately 600 μg. This could be due to two factors: 1) the re-entrainment of particles into the airstream due to the MOUDI stages being reconfigured resulting in the consolidation of size fractions, and 2) contamination from experiments where diesel particulate matter was generated in a smog chamber located 10 m from the MOUDI sampling point. This last explanation is unlikely however, because the high ultrafine masses were observed on days when chamber experiments and the diesel generator were not run. Re-entrainment of particles has been found to occur under normal MOUDI operation; in the case where stages were removed, this problem may have been exacerbated, resulting in above average amount of ultrafine particle mass collected (Marple et al., 1991).

Combining MOUDI size fractions into traditional aerosol size classifications of coarse, accumulation, and ultrafine allowed for a comparison of H_2O_2 activity trends between phases and previous measurements made at UCLA and coarse mode particles. Aerosols larger than 1.78 μm are coarse mode particles, the accumulation mode is 0.1 – 1.78 μm, and ultrafine particles are 0.1 μm and smaller. The H_2O_2 activity per size classification during the three phases for particles extracted in SS 3.5 is shown in Table 4-4-8. Comparing trends in the MOUDI between phases shows that in general, size fractions corresponding to the coarse mode have higher peroxide activities in part due to the larger particle masses collected. Peroxide activity in the coarse mode ranges from 0.39 to 0.48 ng μg^{-1} and shows little sample to sample variation. Accumulation particles are similar in phase I and II, and nearly double in phase III. Ultrafine particle H_2O_2 activity displays variations between phases and samples within specific phases, and in all cases is not measurable in phase II. Comparing peroxide activity measured in MOUDI-collected particles to those collected in previous samples with virtual impactors reveals similarities in the coarse mode. The average MOUDI-based peroxide

activity in phase I-III, and those collected with a virtual impactor, are 0.41 and 0.38 ng μg^{-1}, respectively. Fine mode particles collected with a virtual impactor have a peroxide activity that is 0.37 ng μg^{-1}, compared to an average of 0.29 ng μg^{-1} measured in MOUDI-collected particles. Because the MOUDI size fractions corresponding to the coarse mode are similar to the coarse mode collected by virtual impactors, little difference is expected. In the same vein, the MOUDI size fraction corresponding to the fine mode does not include particles in the range of 1.78 – 2.5 μm and as a result, the peroxide activity is expected to be lower in MOUDI-collected fine mode particles. While there appears to be significant H_2O_2 activity in ultrafine particles (phase I), more measurements would be required to substantiate these preliminary results. Too often, H_2O_2 measurements in the ultrafine particles are below the detection limit or very close to, it resulting in sample-to-sample variations that skew the average.

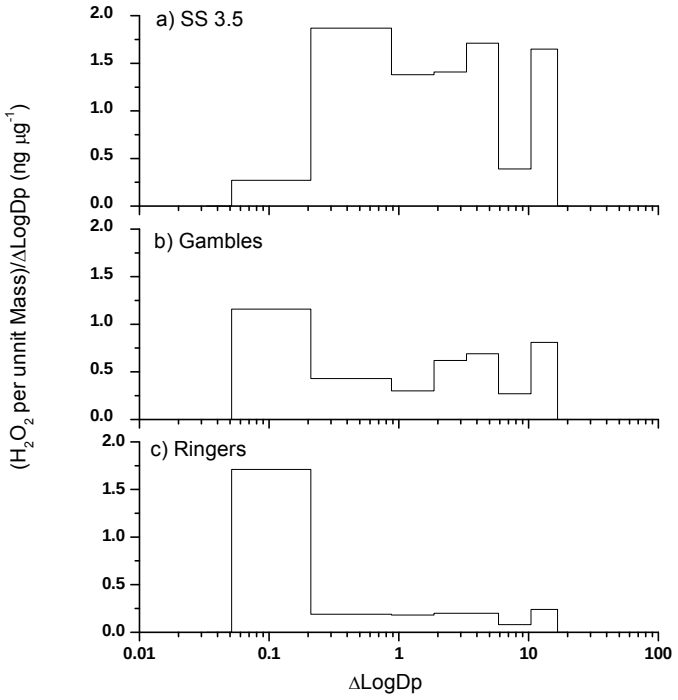

Figure 4-4-10 Average H_2O_2 activities found per size fraction normalized to ΔLogD. Data and associated statistical information are presented in Table 4-4-8.

Table 4-4-8 Average H_2O_2 activity found per size fraction

Size Range (μm)	$[H_2O_2]$/ Mass ± SDOM (ng m^{-3})		
	SS 3.5	Gamble's	Ringer's
<0.1	0.07 (0.02 – 0.18)	0.29 ± 0.07	0.43 (0.41 – 0.45)
1.00 – 0.10	0.39 ± 0.06	0.27 (0.09 – 0.39)	0.08 (0.08 – 0.09)
1.78 – 1.00	0.47 ± 0.09	0.11 ± 0.04	0.05 (0.04 – 0.05)
3.18 – 1.78	0.35 ± 0.05	0.07 (0.04 – 0.13)	0.04 (0.04 – 0.05)
5.62 – 3.18	0.35 ± 0.05	0.15 (0.08 – 0.23)	0.05 (0.04 – 0.06)
10 – 5.62	0.41 ± 0.04	0.20 (0.04 – 0.29)	0.06 (0.05 – 0.07)
18.0 – 10	0.44 ± 0.05	0.18 (0.08 – 0.37)	0.05 (0.04 – 0.06)

N is total sample population used to determine the average. When N < 5, a range is used and shown in parentheses. Error is reported as standard deviation of the mean.

Table 4-4-9 Average H_2O_2 activity estimated per aerosol size classification in SS 3.5

Mode and Sampling Instrument	Size Range (μm)	Sample Period	H_2O_2 Activity (ng μg^{-1})
Coarse (MOUDI)	18 – 1.78	Phase I	0.48 ± 0.06
		Phase II	0.37 ± 0.03
		Phase III	0.39 ± 0.03
Coarse (Virtual Impactor)	≥2.5	Previous Expt's	0.38
Accumulation (MOUDI)	1.78 – 0.1	Phase I	0.24 ± 0.06
		Phase II	0.23 ± 0.05
		Phase III	0.43 ± 0.06
Ultrafine (MOUDI)	≤0.1	Phase I	0.41 (0.15 – 0.63)
		Phase II	<MDL
		Phase III	0.07 (0.02 – 0.18)
Fine Mode [accumulation + ultrafine] (MOUDI)	1.78 - ≤ 0.1	Phase I	0.33
		Phase II	<MDL
		Phase III	0.25
Fine (Virtual Impactor)	≤ 2.5	Previous Expt's	0.37

All data reported is H_2O_2 activity found when using SS 3.5 as the extract solution. Size range describes what size fractions were included in determining the average H_2O_2 activity. To estimate the fine mode when using the MOUDI, the average of H_2O_2 activity in the accumulation and ultrafine mode particles was used. Averages for all coarse and fine mode particles sampled with virtual impactors at UCLA are also shown. Errors are reported as standard deviation of the mean; if the sample size is less than 5, a range is given. <MDL indicates samples that were below the detection limit.

A similar comparison can be made between peroxide activities measured in physiologically relevant solutions (PRSs) used to extract MOUDI and VI-collected particles at different times (Table 4-4-10). In MOUDI size fractions corresponding to the coarse and accumulation mode, H_2O_2 activity measured in SS 3.5 extracts were the largest, followed by Gamble's then Ringer's solutions. Peroxide activity in the coarse and accumulation modes extracted in SS 3.5 were 2.5 times larger than what was measured in Gamble's solution. The opposite trend was observed for ultrafine peroxide activity which registered a larger activity in Ringer's extract solution. Coarse mode peroxide activity in SS 3.5 is similar between MOUDI- and VI-collected particles and shows the same trend in regard to the PRS solutions, in that peroxide activity decreases relative to SS 3.5. Fine mode H_2O_2 activity in both MOUDI- and VI-collected particles has several distinguishing trends. First, when the accumulation and ultrafine peroxide activities (MOUDI) are averaged they yield similar values, which represent fine mode peroxide activity. In contrast, VI-collected fine mode particle results demonstrate that when Ringer's is used as an extract, the H_2O_2 activity is nearly 220% more than what was measured in SS 3.5. Likewise, peroxide activity measured in Gamble's solution is greater than that measured in SS 3.5, by 50%. The elevation of peroxide activity due to the use of PRSs was

observed in ultrafine particles collected by the MOUDI, in which SS 3.5 proved to reduce peroxide activity relative to Ringer's solution. However, only two measurements were made with Ringer's solution and more measurements would be needed to conclude that Ringer's solution increases peroxide activity in ultrafine particles.

Table 4-4-10 Average H_2O_2 activity found in phase III, comparing extraction solutions.

Mode and Sampling Instrument	Size Range (mm)	Extract	H_2O_2 Activity (ng μg^{-1})
Coarse (MOUDI)	18 – 1.78	SS 3.5	0.39 ± 0.03
		Gamble's	0.15 ± 0.03
		Ringer's	0.05 ± 0.00
Coarse (Virtual Impactor)	≥2.5	SS 3.5	0.38
		Gamble's	0.05
		Ringer's	0.11
Accumulation (MOUDI)	1.78 – 0.1	SS 3.5	0.43 ± 0.06
		Gamble's	0.17 ± 0.05
		Ringer's	0.07 (0.04 – 0.09)
Ultrafine (MOUDI)	≤0.1	SS 3.5	0.04 ± 0.02
		Gamble's	0.29 ± 0.07
		Ringer's	0.43 (0.41 – 0.45)
Fine Mode [accumulation + ultrafine] (MOUDI)	1.78 - ≤ 0.1	SS 3.5	0.23
		Gamble's	0.23
		Ringer's	0.25
Fine (Virtual Impactor)	≤ 2.5	SS 3.5	0.24
		Gamble's	0.49
		Ringer's	0.75

All data reported is H_2O_2 activity found when using SS 3.5 as the extract solution. Size range describes what size fractions were included in determining the average H_2O_2 activity. Errors reported as standard deviation of the mean. If the sample size is less than 5 a range is reported in parentheses.

5. Characterization of Source Materials and Test Aerosols

5.1. NIST SRM 1649a

A series of measurements was conducted to determine the H_2O_2 generation activity of SRM 1649a, a widely characterized particulate matter reference material. SRM 1649a is an urban dust standard reference material (SRM) that was collected in the Washington, DC area in 1976–1977

using a bag house specially designed for the purpose by the National Bureau of Standards (now the National Institute of Standards and Technology).

A small quantity of the material was deposited on a filter with a spatula and subjected to analysis in the same manner as ambient samples, by allowing it to extract for two hours in water adjusted to pH 3.5. About double the usual quantity of material was tested. No generation of H_2O_2 above the background was observed. In this particular case, the detection limit was about 0.08 ng/μg of dust. This result is consistent the results reported above, which indicate that the ability of PM to generate H_2O_2 decays with time. It is also consistent with the hypothesis that H_2O_2 generation is linked to labile species in particles.

5.2 Diesel Particulate Matter Phase I: Stockton

Diesel particulate matter (DPM) was sampled from two heavy-duty diesel engines during five days in October, 2005. Two in-use trucks were tested, one with an older 1977 engine and one with a 1992 vintage engine. Both trucks were run on a chassis dynamometer located at the California Air Resources Board's facility in Stockton, CA. The chassis dynamometer allows DPM to be collected with an engine run under different loads which will change the chemical and physical properties of DPM (Kittleson et al., 1998). As far as we are aware, no work has been done investigating the ability of DPM to generate H_2O_2.

Several studies have shown that DPM has the potential to induce oxidative stress through the generation of reactive oxygen species (ROS) (Li et al., 2003, Park et al., 2006, Cho et al., 2004, Dellinger et al., 1999). The relative small size of diesel generated particles results in higher probabilities of being deposited in lower lung regions (Li et al., 2003). It is speculated that ROS formation occurs through the redox reactions of transition metals and/or quinones and semi-quinones (Park et al., 2006, Cho et al., 2004). The H_2O_2 content of freshly generated DPM from a stationary diesel engine source was measured, along with transition metal content. DPM was generated by two diesel engines of different vintages placed on a chassis dynamometer at the California Air Resources Board's facility in Stockton, CA. DPM exiting the diesel exhaust stack was collected and immediately analyzed for H_2O_2 and metal content at a later time.

5.2.2 Sampling, Analysis and Field blanks

DPM from each engine was collected whilst the engine was operated at various loads defined here as idle, mid and high. 'Engine load' corresponds to the amount of torque placed on the engine which is reflective of engine operating speed and hauling. The idle, mid-, and high modes are

characterized by 0, 25 and 65% loads, respectively. These three modes represent typical driving conditions experienced by a truck hauling cargo. Diesel engines are known to produce carbonaceous particles ranging in size from 0.01 to >1 μm (Mathis et al., 2005). It is also known that DPM composition, which can consist of mixtures of elemental and organic carbon, can vary as a function of engine load. Thus, DPM was sampled from an engine operating at idle, mid-, and high modes (Shi et al., 2000, Virtanen et al. 2004). The effect of engine load on H_2O_2 measured was studied along with metal content.

Diesel engine exhaust was directed to an exhaust stack where temperatures can exceed 450 ºF. A stainless steel sampling line situated perpendicular to the exhaust flow with six equidistant openings accepts portions of the exhaust flow. The sampling line was located 30 cm from the exit of the smoke stack. Sampled exhaust is directed to a BG-2 dilution sampler (Sierra Instruments) which dilutes and cools diesel exhaust with HEPA filtered air at a predetermined dilution ratio which was either 4:1 or 6:1. Diluted diesel exhaust is then passed over stainless steel filter holder containing a 47 mm Teflon filter (Pall Corp.) that collects DPM. At this point, the exhaust temperature has dropped to 70 ºF. Sampling flows were all maintained at 70 Lpm with sampling times kept between 45 and 240 sec.

Engines run on the dynamometer were run under three types of engine modes; idle, mid-, and high. Each mode refers to the amount of torque placed on the engine which simulates different engine loads. The amount of torque placed on the engine is indicated by engine operating speed (rpm); the higher the speed the larger the torque (Table 5-2-1). Reaching mid- and high engine modes for sustainable amounts of time required a warm-up period, usually 40 min.

5.2.4 Sample Extraction

Extraction of diesel particulate matter into our extraction solution was highly problematic. The extraction solution is aqueous, and the very fresh diesel particulate (DPM) sampled in this study was, for the most part, very hydrophobic. After extraction, the solutions were typically slightly gray, but with a substantial quantity of black soot particulate material floating on top of the solution. Additional distinct clumps of particles were visible in the solutions. We attempted to enhance the solubility of the DPM by adding 0.2 mL of ethanol to the loaded filter surface before adding extraction solution, but this had no noticeable effect. We also attempted to "age" one filter by leaving it open to the air overnight, but this also had no noticeable effect. As a result, we feel that all of our data represents the very lower limit for peroxide production by diesel particles.

Table 5-2-1 Different engine modes tested

Mode	Speed (rpm)	Power (hp)	Speed (rpm)	Power (hp)
Engine Vintage	1978		1992	
Idle	<100	0	<100	0
Mid	1800	200	1400	200
High	1800	350	1800	275

Field blanks were run as follows: After each engine mode's run series was completed, the exhaust-sample connection was allowed to cool enough for safe handling, and the sampler was disconnected from the exhaust stack. In the case of the 1992 engine, both blanks were collected at the end of the day as the stack was particularly hot and time was not available to allow the stack to cool after each engine mode. A pre-weighed Teflon filter (Pall Corp.) was loaded into the stainless steel filter housing and connected to the BG-2 diluter in the same manner as samples. Air used to dilute the diesel exhaust was passed over the filter for a period ranging from 45 to 240 seconds, as indicated in Table 5-2-2. After the filter exposure was completed the filter was removed, weighed, and analyzed for H_2O_2 in the same manner as the regular samples. Field blanks designated for metal analysis were stored after weighing.

Five field blanks were analyzed for mass and H_2O_2, and fall into two categories (Table 5-2-2). Two of the filters picked up a substantial quantity of mass, 32 and 60 μg, and recorded the two highest peroxide signals, possibly from residual particles left in the sampling train. The other three filters showed little mass gain and lower peroxide signals, just above the peroxide signal recorded for pure extraction solution (3.8×10^{-8} M). The field blanks were run for as long as, or longer than the samples, and thus were exposed to more dilution air than the actual samples. If particle carryover from one sample run to the next is indeed the explanation for the two blanks that gained appreciable mass, this may also happen for sample runs, and appear in sample masses, and thus both should be accounted for in the analysis and be responsible for some of the observed run-to-run variability in the collected masses. For the analyses below, we subtracted the average H_2O_2 concentration and mass of the 3 field blanks that did not gain appreciable mass; 8×10^{-8} M and 3 μg, respectively.

Table 5-2-2 Field blank results for H_2O_2 analysis

Mode	$[H_2O_2]$ (M) X 10^{-8}	sampling time (sec)	Mass pick up (μg)
1978 Engine			
Idle	5.8	240	7
Mid	15.2[a]	120	60
High	7.7	120	<2
Ave	9.6		
1992 Engine			
After all modes had been tested	11, 16[a]	120, 45	3, 32

[a] These samples were not included in calculating the average H_2O_2 concentration used to correct observed H_2O_2 levels due to the large amount of mass picked up.

5.2.3 Results

The 1978 vintage engine displayed significant H_2O_2 levels in DPM collected while the engine was in the idle mode. DPM exhaust mass loadings were too large and the BG-2 dilution factor was increased from 4:1 to 6:1, thus avoiding back pressure build up that led to filters tearing rendering them unusable for any analysis. On average, idle mode H_2O_2 levels were 1.1×10^{-5} and 2.2×10^{-6} M for the 4:1 and 6:1 dilutions, respectively (Table 5-2-6). The amount of DPM mass collected for the idle mode runs averaged 947 and 404 mg for the 4:1 and 6:1 dilutions, respectively. Mass normalized H_2O_2 levels ranged from 2.0 – 3.1 and 1.0 – 1.5 ng μg^{-1} for the 4:1 and 6:1 dilution ratios, respectively. The upper limit of this range was much higher than what has been observed in ambient particulate matter (about 0.5 ng μg^{-1}). Mid-mode H_2O_2 levels were very near or below the field blank H_2O_2 levels for all samples analyzed. This occurred despite the large masses collected, averaging 983 ± 57 μg. High-mode DPM had relatively low H_2O_2 activity ranging from 0.11 – 0.16 ng μg^{-1} and was determined from a 4:1 dilution ratio. In general, as engine modes cycle from idle to high there is considerably less H_2O_2 activity (ng of H_2O_2 per μg of DPM mass) detected.

All three 1992 vintage engine modes were tested in a single day at a 6:1 dilution ratio to avoid potential issues arising from back pressure issues that could have lead to filter failure. Idle-

mode H_2O_2 per unit DPM mass ranged from 0.25 – 0.4 ng μg^{-1} and decreased in the mid- and high-modes, similar to the trend that was observed for the 1978 vintage engine.

Table 5-2-6 H_2O_2 and DPM mass levels for all engines and modes tested.

Engine Mode	N	BG-2 Dilution	Average Measured $[H_2O_2]$ (M) X 10^{-8}	Corresponding Field Blank $[H_2O_2]$ (M) X 10^{-8}	Average DPM Mass Collected (μg)	Corresponding Mass Found on Field Blank (μg)	H_2O_2 per unit DPM mass (ng μg^{-1})
1978 Vintage Engine							
Idle	4	4:1	1140 ± 160	5.8	947 ± 433	7	2.0 – 3.1
Idle	2	6:1	216 ± 160	[a]	404 ± 433	[a]	1.0 – 1.5
Mid	7	4:1	5.8 ± 0.7	15.2	983 ± 57	60[b]	0
High	3	4:1	63 ± 9	7.7	818 ± 29	<2	0.11 – 0.16
High	4	6:1	8.5 ± 2	[a]	240 ± 35	[a]	negligible
1992 Vintage Engine							
Idle	4	6:1	12 ± 2	[c]	31 ± 21	[c]	0.25 – 0.4
Mid	3	6:1	14 ± 4	11	83 ± 30	3	0.13 – 0.2
High	2	6:1	18, 15	16	288, 521	32[b]	0.02 – 0.09

[a] No field blank was run for this engine mode
[b] Due to high mass gains the H_2O_2 concentration found was omitted from average calculations
[c] Both blanks were recorded after all sampling had been completed (see text)

For the idle mode 1978 engine, the normalized peroxide levels are high compared to all other diesel tests we have run (see also below), and are also high compared to ambient PM (about 0.5 ng/μg for the fine mode). For all other engine modes, normalized peroxide levels are fairly uncertain due to their small peroxide signals relative to the blanks; smaller than the typical averages for this quantity for ambient data.

5.3 Diesel Phase II

Several measurements of diesel exhaust were collected from a diesel generator. Diesel particles were produced by a four-stroke, air-cooled direct injection 4.8-kW diesel generator (L70V6, Yanmar Corporation). The generator supplied power to four electrical appliances, each of which pulled 1.42 kW, equivalent to about a 30% load per appliance. The 5 kW generator has been verified to produce PM that is well within the range observed for PM emissions from heavy duty diesel trucks in terms of elemental and organic carbon content, primary particle size, size distribution and

fractal dimension of agglomerates (Chung et al., 2008). It was run on California low-sulfur diesel fuel, and allowed to warm up for 10 minutes prior to collection of any sample. For most of the measurements presented here, diesel engine exhaust was directed to a chamber, which dilutes and cools diesel exhaust with HEPA filtered air (Chung et al., 2008). Diluted diesel exhaust is then collected with stainless steel filter holder containing a 47 mm Teflon filter (2-μm pores, Pall Corporation). Sampling flows were all maintained at 29 LPM with sampling times kept between 10 to 15 min. Field blanks were run by loading an unused Teflon filter into the filter holder and drawing air over it for 30 seconds. Some particles were collected 80 cm away from the generator's exhaust outlet without dilution. Particles were sampled into an open-faced filter or via a short line from the Teflon chamber directly to the filter holder. In two experiments, diesel particles were aged either by oxidizing propene in the chamber or by exposing the diluted diesel exhaust to sunlight. The diesel generator is run at high load to maximize the fraction of elemental carbon, except where specified otherwise. Diesel particles were also mixed, both internally and externally, with secondary organic aerosols generated in the chamber (described below).

Consistent with the Stockton study, the diesel particles exhibited relatively low activity. As was also observed in the diesel particles collected at the ARB's Stockton lab, the particles are very hydrophobic, and do not solubilize well in the extraction solution. An average of 48% of the mass remained on the filters, but this may underestimate the extent of the problem because particles also float on top of the solution. Several extractions were performed using dipalmitoyl phosphatidyl choline (DPPC), a lung surfactant, to try and address this issue, but DPPC did not solubulize particles unless it was sonicated. As sonication of aqueous solutions generates H_2O_2 (Hasson and Paulson, 2003), we did not pursue this approach.

Diesel particle activities ranged from <MDL to 0.37 ng H_2O_2 per μg extracted aerosol mass (Table 5-3-1). For the two experiments in which particles were aged for 2-3 hours (9/5 and 9/27), the activity increased somewhat upon exposure to sunlight and photochemical oxidants. Note that the Stockton data should be compared with Column 4 of Table 5-3-1, ng H_2O_2/μg aerosol mass, as extracted aerosol mass (below) was not recorded for the Stockton data. The observed activities are in very good agreement with those observed at ARB's Stockton lab, where activities ranged from 0.02 to 0.16 ng H_2O_2/μg aerosol mass for high engine loads. The one idle measurement does not agree with the Stockton results, as its H_2O_2 level at 2 hours was the same as that of the field blank. This sample showed activity later, generating up to 1.8 ng/μg after 23 hours in the extraction solution (as always, after blank correction).

Table 5-3-1 Summary of diesel chamber and direct exhaust measurements using commercially available California low-sulfur diesel fuel.

Date	Sample Type	Organic Species Added	Engine load	Aged in sunlight	H_2O_2 per mass (ng mg^{-1})	Percent of Aerosol Mass Extracted	H_2O_2 per extracted mass (ng mg^{-1})
20-Jan-09	Chamber	none	0%	no	0.00	NM	—
23-Mar-09	Direct	none	0%	no	0.37	NM	—
23-Mar-09	Direct	none	60%	no	0.09	NM	—
1-Sep-06	Chamber	none	90%	no	0.12	70	0.17
1-Sep-06	Chamber	none	90%	no	0.04	47	0.09
5-Sep-06	Chamber	propene	90%	yes	0.15	54	0.28
27-Sep-06	Chamber	none	90%	no	0.05	53	0.09
18-Feb-09	Chamber	none	100%	no	0.00	NM	—
23-Mar-09	Direct	none	100%	no	0.11	NM	—
5-Sep-06	Chamber	propene	90%	yes	0.19	55	0.34
27-Sep-06	Chamber	none	90%	yes	0.13	49	0.26

5.4 Secondary Organic Aerosols

SOA experiments were conducted in a 34-m^3 outdoor Teflon chamber. Ozone and NO_x concentrations were measured by gas-phase ozone analyzer (Dasibi 1001-RS) and NO_x analyzer (Thermo Electron Model 14B/E), respectively. Particle concentrations were monitored by a scanning mobility particle sizer (SMPS, TSI-3936L10). Gas-phase concentrations of parent hydrocarbons were measured by a gas chromatograph with a flame ionization detector (GC-FID, HP 5890).

Experiments considered in this study involved SOA production from the ozonolysis of α-pinene and β-pinene in the dark, as well as photochemical reaction of NO_x with α-pinene and toluene under natural sunlight. A few experiments were conducted in the presence of ammonium sulfate seed particles. Ozone was generated using a mercury lamp system (laboratory built); ozone concentrations were typically in the range of 200-500 ppb. NO_x came from the generator as a co-pollutant with the diesel particles, or NO was added separately from a cylinder. During seeded experiments, seed particles were generated by atomizing 0.5% ammonium sulfate solutions using a nebulizer at a flow rate of 5 LPM for about 20 min. Liquid samples of α-pinene and β-pinene (Sigma Aldrich) were evaporated into the chamber in a stream of purified air, which was also used to fill the chamber. During dark ozonolysis experiments, cyclohexane (used as the hydroxyl radical

scavenger) was introduced into the chamber in a similar manner. The concentrations of α–pinene or β-pinene were typically around 500 ppb, and the concentrations of cyclohexane were typically around 200 ppm.

Prior to an experiment, the chamber was flushed with purified air for 24-48 hr. During an experiment, the chamber was initially filled with purified air for about 2 hr. After that, cyclohexane and ozone or NO_x were added to the chamber. In seeded experiments, seed particles were added at the same time. After stabilizing for about 1 hour, α-pinene or β-pinene was introduced to the chamber. For ozonolysis experiments, the reaction was initiated by the injection of α-pinene or β-pinene. For photochemical experiment, reaction was initiated by removing the cover of the chamber. SOA was collected onto 47-mm Teflon filters (Pall Life Sciences) at the end of the experiments. Samples were collected by drawing air from the chamber at 29 L min^{-1} for 10 to 15 min. Field blanks were collected by drawing air from the chamber for 30 sec. Filters were weighed before and after each sampling using a microbalance (ME 5, Sartorius Inc.) under controlled relative humidity (40–45%) and temperature (22–24 ^{0}C) conditions. Particle mass concentrations were determined from the mass change on the filter and the total volume of air sampled.

Secondary organic aerosols were generated by oxidizing an organic in the chamber in the presence of NO_x. Gasses, and sometimes particles, are allowed to mix in a covered chamber. Once mixing was complete, the covers were removed, initiating photochemical oxidation of the mixture. As photochemistry progresses, condensable species are generated, and in the absence of pre-existing particles, secondary organic aerosol (SOA) will appear as freshly nucleated particles. These can later be mixed with diesel particles to make an external mixture of diesel and SOA. Alternatively, internally mixed particles can be generated by adding diesel particles to the chamber together with the gasses, and the secondary organic aerosol will condense on the pre-existing particles (if present in sufficient number), suppressing nucleation.

5.4.1 Toluene

Two chamber experiments were performed in which toluene was oxidized to generate secondary organic aerosol. The results are shown in Table 5-4-1, together with the results for the biogenic alkene investigated, α-pinene (discussed below). In both cases the particles generated were internal mixtures of secondary organic aerosol and particles from the diesel generator, in one case running on low-sulfur diesel, and the other on commercial biodiesel. Diesel particles made up about 70% of the total particle mass.

The toluene secondary organic aerosols showed relatively low activity, 0.22-0.26 ng H_2O_2/μg aerosol mass. 74-94 % of the aerosol mass was extracted from these filters. These activities are much lower than those observed for the α-pinene SOA, but it should be noted that in contrast to the α-pinene secondary organic aerosol, the apparently low activity diesel particles (above) make up the majority of the mass in the toluene-diesel internally mixed SOA investigated.

5.4.2 Biogenic Aerosols

Sixteen chamber experiments have been performed in which α-pinene or β-pinene was oxidized to generate secondary organic aerosols. The results are shown in Table 5-4-1, together with the results for toluene (above). Five experiments generated pure α-pinene secondary organic aerosol samples, and the other three were used to produce internal or external mixtures with diesel particles.

Table 5-4-1 H_2O_2 generation efficiencies for secondary organic aerosol with diesel particles and ambient aerosols for comparison.

Aerosol Generating System	**2 hour H_2O_2 /PM mass (ng/ug)**		**~20 hour H_2O_2/PM mass (ng/ug)**		**Number of measure-ments**
	mean	Std. Deviation	mean	Std. Deviation	
UCLA	0.38	0.18			>50
110 Freeway Site	0.48	0.33			30
β-pinene+O_3 + seeds	1.08				1
β-pinene+O_3/OH	4.96		16.42		1
β-pinene+ O_3	4.21		7.38		1
α-pinene+ O_3	0.69	0.44	0.90		5
α-pinene + O_3/OH	0.91	0.37	3.23	0.53	2
α-pinene +NOx/ O_3/OH	2.30	1.70			2
Diesel+α-pinene +NOx/ O_3/OH	1.53	0.25			4
Diesel+toluene+NOx/ O_3/OH	0.24	0.03			2
Diesel+propene+NOx/ O_3/OH	0.19				2
Diesel+NOx/ O_3/OH	0.13				2
Diesel High Load	0.08	0.06	0.81	0.50	7
Biodiesel High Load	0.34	0.16	0.94	.	5

5.5 Source Materials Intercomparison

Table 5-4-1 shows a summary of H_2O_2 levels associated with biogenic (α-pinene and β-pinene) and anthropogenic (toluene) SOA, diesel, biodiesel and several mixtures, and these results are shown graphically in Figures 5-5-1 and 5-5-2. The average fine mode values from UCLA and the 110 freeway site described in Arellanes et al., 2006 are also shown for reference. The data show results for extraction at 2 hours for all samples, and at 20 ± 3 hours for some samples. Additional peroxide is generated in the additional extraction time, but much more for some (such as conventional diesel) aerosols than others (such as SOA from α-pinene reacting with O_3). There is some sample-to-sample variability even for aerosols that were generated under relatively controlled conditions.

The comparison of the different types of source aerosols indicates that the α-pinene and β-pinene SOA have higher activities than either the diesel aerosols or ambient aerosols. Even though the conventional diesel signal increases by nearly a factor of 10 at 20 hours extraction relative to the H_2O_2 level after 2 hours, it is still eclipsed by the biogenic aerosols in all but one case. The biodiesel tested is much more active than the conventional diesel initially, but they have very similar H_2O_2 generation by 20 hours. Low solubility that increases with time may explain the low initial H_2O_2 production from conventional diesel, and also the initial difference between diesel and biodiesel (biodiesel is more oxygenated than conventional diesel, thus its PM emissions should be, and appears to be, generally more soluble than conventional diesel PM. The only anthropogenic SOA tested, from toluene oxidation, appears at this initial stage to have relatively low activity.

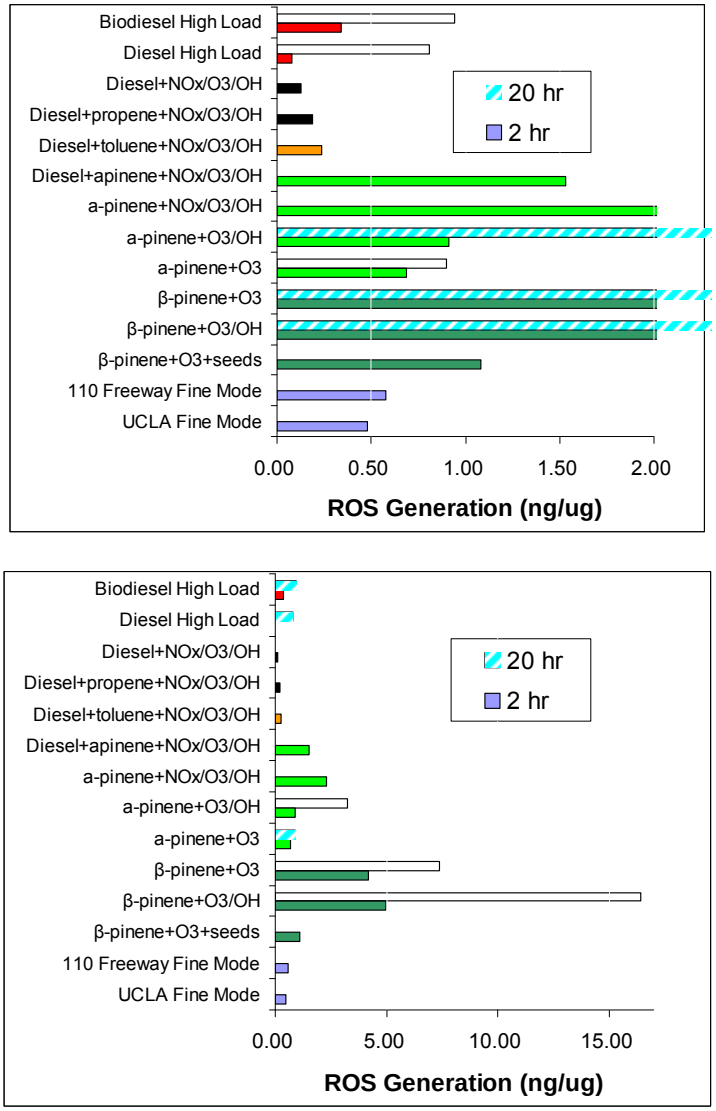

Figure 5-5-1. Comparison of H_2O_2 generation by diesel and SOA particles. The figures are the same, but the scales are different to allow visualization of different parts of the plots. The solid bars indicate H_2O_2 associated with particles after 2 hours of extraction, and the striped bars after 20 hrs of extraction. Biogenic SOA is much more active than other types of aerosols, with β–pinene exhibiting the highest activity.

6. Riverside Field Studies

6.1 Riverside I Study

6.1.1 Introduction

This section presents results of a particle sampling campaign that was conducted in Riverside, California. Riverside experiences some of the highest levels of SOA in Southern California, as it is a downwind receptor site for smog in the Los Angeles basin (Na et al., 2004, Sardar et al., 2005). The intent of this study was to investigate H_2O_2 in SOA-dominated aerosols. However, due to the VI contamination of the fine mode samples (section 3), it is difficult to address the SOA question with the Riverside data. Instead we have performed more targeted studies on SOA, described above. The SOARS sampling site, however, receives not only (presumably) high levels of SOA, but it is also impacted by fresh emissions from activity on campus and the nearby 60 freeway. The freeway is 0.6 km from the site, and is upwind during the day. Sampling was conducted over a two week period in August 2005, during which samples were collected several times a day and analyzed for H_2O_2, mass, and metal content. Analysis of H_2O_2 content in the aerosol- and gas-phase was conducted on site while additional aerosols samples collected were measured for metal and aerosol mass off-site at UCLA.

6.1.2 Sampling and Analysis

Aerosol sampling at Riverside was performed in conjunction with a major collaborative sampling referred to as the Secondary Organic Aerosols at Riverside Study (SOARS). Samples were collected on the campus of U.C. Riverside, located 90 km from downtown Los Angeles, 25 km downwind of an agricultural region (Chino dairy farms) and in close proximity (0.6 km) to the heavily traveled 60 freeway and downwind of various manufacturing sites.

Sampling was conducted during daylight hours, between August 1st and 10th, 2005, on the campus of U.C. Riverside in a moderately used parking lot. Fine and coarse mode aerosols were collected with two virtual impactors operating in parallel, and gas phase samples were collected simultaneously with a stripping coil. Sampling was initiated between 7:00 and 8:30 AM and continued throughout the day at 60 to 90 min intervals up to 6:30 PM. Teflon filters (47 mm, 2 μm pore, Pall Corporation) housed in stainless steel filter holders were used to collect particles. One pair of fine and coarse mode filters were subjected to on-site H_2O_2 analysis while the other pair of fine and coarse mode filters were stored in sealed Petri-dishes and analyzed at a later date for aerosol

mass and metal content. Gas samples were analyzed immediately after collection. After a sampling event, Teflon filters were removed promptly and extracted using 4 mL of stripping solution (0.1 mM Na_2EDTA, pH 3.5) for 2 hrs, with gentle agitation. The particle extract was analyzed for H_2O_2 via HPLC/fluorimetry, as described in Section 2. To determine particle mass, filters were first tared by placing them in a temperature- and relative humidity-controlled room for 24 hrs, then weighed (± 1 μg, Mettler-Toledo MX-5 microbalance), then used in the field. After returning from the field site, filters were again allowed to re-equilibrate in the weighing room prior to re-weighing.

In preparation for metal analysis, filters were cut in half using a ceramic blade (Specialty Blades). Half filters were digested in 4 mL of an acidic solution (pH 3.5, HNO_3) for 2 hrs, at the same pH as our normal extraction, but with nitric acid for use in the spectrometer. The extract for one half-filter was transferred to a 10 mL high density polyethylene (HDPE) bottle. The extract from the other half-filter was syringe-filtered (25 mm, 0.44 μm pore, Fisher Scientific) and also placed in a HDPE bottle. Filtration was performed to remove portions of particles that do not dissolve in our normal extraction solution. There is also potential for undissolved solids to interfere with the metal measurements. Analyses were performed using inductively coupled plasma – optical emission spectrometer (ICP-OES, Perkin-Elmer, TJA IRIS 1000 Radial) detection. Additionally, filtered extracts were further acidified with 1 mL of 25% (w/v) HNO_3 so that submitted samples had a pH matching the ICP-OES matrix. Each sample was run in triplicate and the raw data was reported in units of ppb or alternatively, assuming the density of 5% HNO_3 is 1 g mL^{-1}, in ng mL^{-1} for submitted 5 mL samples. Filter blanks were run by extracting an unused Teflon filter (Pall Corp.) in the same manner as filters with collected particles for every set of samples submitted. Due to uncertainties in how undigested solids affect the ICP-OES detection capabilities, and subsequently the resulting metal content, results from unfiltered extracts were not presented in subsequent analyses of metals related data. However, for most metals, little difference was observed. Cu, Pb, Fe and V were analyzed in all samples, while other metals including Ca, Zn and Ba were analyzed in sub-sets of samples submitted for metals analysis.

During the Riverside campaign, two types of H_2O_2 blanks were run: filter and field blanks. Filter blanks were run daily by extracting an unused Teflon filter (Pall Corp.) for 2 hrs and analyzing the extract for H_2O_2. Field blanks were run by loading an unused Teflon filter (Pall Corp.) into a stainless steel filter holder and drawing air over it for 30 sec at a flow of 55 Lpm. The filter was removed and extracted and analyzed for H_2O_2. Collection of field blanks began on the fourth sampling day (Aug 4th). In Table 6-1-1, filter and field blanks are shown for comparison. For

unknown reasons, filter blanks were higher than usual, and field blanks were higher than filter blanks, averaging 1.8 ± 0.5 × 10^{-7} M and 2.7 × 10^{-7} M, respectively. Field blanks represented 42 ± 20% of the observed H_2O_2 signal, a number that is skewed due to an unusually high field blank recorded on Aug. 8th.

Table 6-1-1 H_2O_2 concentrations in filter and field blanks.

	Filter Blank		Field Blank	
Date	Measured H_2O_2 in 4 mL of Extract (X10^{-7} M)	Average Percent of Signal	Measured H_2O_2 in 4 mL of Extract (X10^{-7} M)	Average Percent of Signal
8/1	2.53	42±20	[1]	[1]
8/2	2.53	28±5	[1]	[1]
8/3	2.60	19±10	[1]	[1]
8/4	1.77	28±20	[1]	[1]
8/5	1.20	21±20	2.49	44±50
8/8	1.65	23±10	5.18	73±40
8/9	1.05	19±10	1.08	20±10
8/10	1.27	21±10	2.03	33±20
Average	1.82 ± 0.6	25 ± 10	2.70 ± 1.7	42 ± 20

[1] Prior to August 5th no field blanks were recorded. The average percent column represents the average for the corresponding date.

6.1.3 Results

6.1.3.1 Gas and Aerosol Phase Peroxides

Except for a few instances, gas phase H_2O_2 samples were collected concurrently with aerosol measurements (Table 6-1-2, Figure 6-1-1). The average gas phase H_2O_2 concentration at Riverside was 1.0 ± 0.7 ppb. This is similar to results from the UCLA and 110 freeway sites; 1.05 ± 0.6 and 1.17 ± 1.0 ppb, respectively (Arellanes, 2005).

The coarse mode PM mass was high at the Riverside site I, at 98 ± 26 μg/m^3. This compares to an average of 26 ± 15 μg/m^3 at the UCLA site, and 27 ± 33 μg/m^3 at a site located close to the 110 freeway in downtown Los Angeles (Arellanes et al., 2005). It is higher than the 50 ± 26 ng/m^3 observed a few km away in the Riverside II study (below). The Riverside II site is upwind of the 60 freeway, and it is removed from immediate traffic activity. The peroxide generation activity was also higher in absolute terms, at 33 ± 13 ng/m^3, compared to 13 ± 10 ng/m^3 and 20 ± 9 ng/m^3 (respectively) for the UCLA and 110 freeway sites, and 17 ± 8 ng/m^3 for the 2008 Riverside "background site" measurements. Normalized to mass, however, the Riverside coarse mode had lower activities, at 0.36 ± 0.2 ng μg^{-1} (Fig. 6-1-3) and 0.44 ± 0.33 ng μg^{-1} for the 2005 parking lot and

2008 background sites respectively, compared to 0.58 ± 0.3 ng μg^{-1} for the UCLA site and 1.05 ± 0.3 ng μg^{-1} for the 110 freeway site. There was no significant correlation between H_2O_2 and particle mass (Fig 6-1-2), consistent with the notion that chemical composition plays a more significant role in H_2O_2 generation than does particle mass. Coarse mode H_2O_2 levels were moderately correlated to time of day ($r = 0.42$, $p < 5$), with higher levels measured in morning hours then decreasing in the afternoon (not shown).

Table 6-1-2 Average gas and coarse mode aerosol phase H_2O_2 levels.

Site	Gas Phase H_2O_2 (ppb)	H_2O_2 (ng m^{-3})	Mass Conc. ($\mu g\ m^{-3}$)	H_2O_2 Activity (ng μg^{-1})
UCLA (Arellanes et al., 2005)	1.05 ± 0.6	13 ± 10	26 ± 15	0.58 ± 0.3
110 Freeway (Arellanes et al., 2005)	1.17 ± 1.0	20 ± 9	27 ± 33	1.05 ± 0.3
Riverside I	1 ± 0.7	33 ± 13	98 ± 26	0.36 ± 0.2
Riverside II	___	17 ± 8	50 ± 21	0.44 ± 0.3

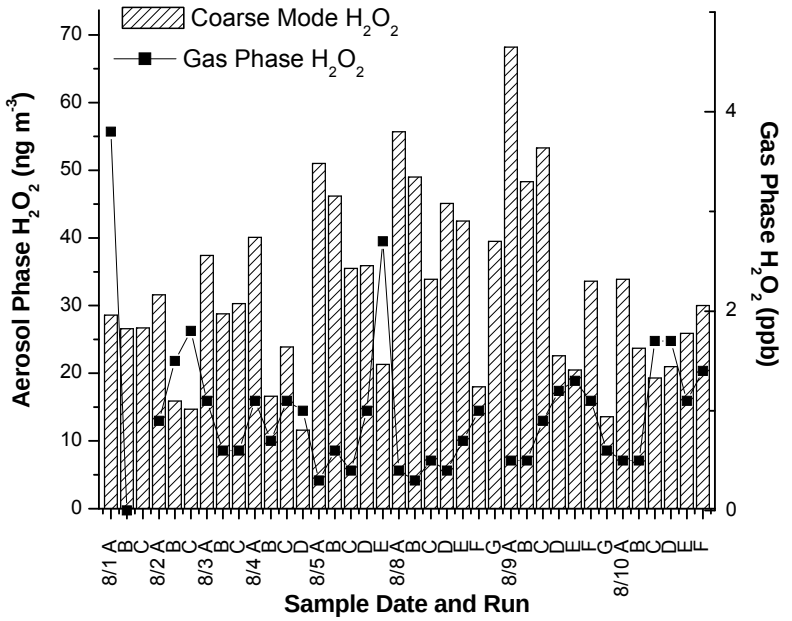

Figure 6-1-1. Coarse mode and gas phase H_2O_2 measurements in a parking lot on the UC Riverside campus. The lack of correlation between the two quantities is consistent with other data indicating that particles generate H_2O_2 in solution.

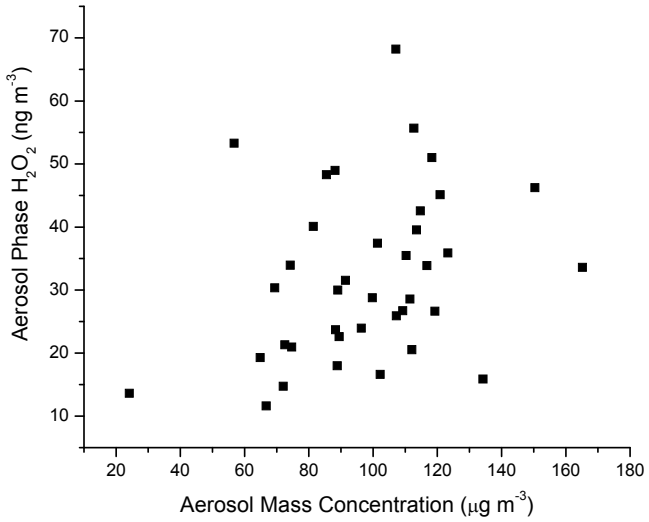

Figure 6-1-2. Coarse mode H_2O_2 measurements plotted against coarse mode aerosol mass. There is no significant correlation, indicating that aerosol chemical composition may play a larger role than aerosol mass in controlling short term variations in this property.

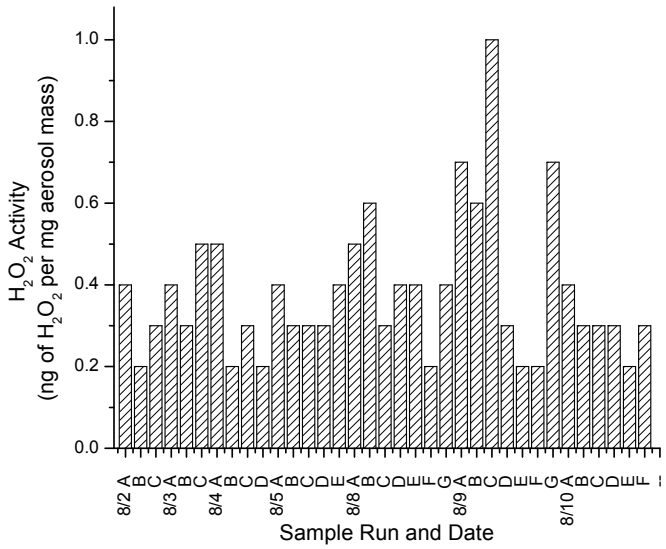

Figure 6-1-3. H_2O_2 generation normalized to aerosol mass.

6.1.3.2 Coarse Mode Metal Content

Metal concentrations in coarse particles are presented in Table 6-1-3. All concentrations presented are for samples that were syringe filtered to remove undissolved solids. Four metals (Fe, Cu, Pb, and V) were measured in all samples. Ca, Zn and Ba were measured in a smaller sub-set of samples. In the coarse mode (Table 6-1-3), Ca is the most abundant metal, which is likely due to a significant contribution from road dust (Singh et al., 2002). Table 6-1-4 shows metal and H_2O_2 concentrations normalized to mass (ng μg^{-1}).

Table 6-1-3 Coarse mode metal, H_2O_2 and mass data.

Sample Date and Run	Metal Concentration (ng m^{-3})						H_2O_2 (ng m^{-3})	Mass Collected (mg m^{-3})
	Fe	Cu	Pb	V	Ca	Zn		
Aug-2 A	89.7	1.8	< MDL	< MDL	5006	NM	37.0	91.4
Aug-2 B	57.0	10.5	< MDL	< MDL	9118	NM	20.8	134.2
Aug-2 C	53.7	< MDL	24.7	< MDL	6268	NM	20.0	72.0
Aug-3 A	43.6	< MDL	< MDL	< MDL	6997	NM	41.9	101.4
Aug-3 B	76.5	7.6	0.6	< MDL	6714	NM	32.7	99.8
Aug-3 C	68.7	< MDL	1.9	< MDL	4943	NM	35.1	69.4
Aug-4 A	59.2	3.0	9.2	< MDL	5107	NM	40.3	81.4
Aug-4 B	69.0	< MDL	< MDL	< MDL	8192	NM	16.8	102.3
Aug-4 C	44.2	< MDL	4.8	< MDL	6838	NM	24.1	96.3
Aug-4 E	30.1	6.1	< MDL	< MDL	3416	NM	11.9	66.7
Aug-5 A	80.3	< MDL	< MDL	< MDL	7195	NM	46.6	118.3
Aug-5 B	91.1	< MDL	< MDL	< MDL	7907	NM	40.0	150.4
Aug-5 C	36.5	< MDL	< MDL	< MDL	6810	NM	31.0	110.3
Aug-5 E	47.7	< MDL	< MDL	< MDL	7404	NM	42.6	123.3
Aug-5 F	50.2	< MDL	< MDL	< MDL	3929	NM	28.4	72.5
Aug-8 A	205.3	188.1	14.0	0.04	NM	41.41	54.5	112.7
Aug-8 B	168.5	152.1	1.3	< MDL	NM	66.06	50.1	88.2
Aug-8 C	162.0	194.4	< MDL	8.5	NM	< MDL	35.0	116.8
Aug-8 E	152.6	56.2	15.4	6.8	NM	< MDL	46.1	120.9
Aug-8 F	147.5	122.9	22.1	1.9	NM	< MDL	43.0	114.7
Aug-8 G	63.3	123.6	11.7	0.1	NM	< MDL	19.0	88.8
Aug-8 H	548.5	96.0	28.2	2.7	NM	90.29	40.2	113.6
Aug-9 A	313.0	135.9	< MDL	17.5	NM	91.93	72.6	107.1
Aug-9 B	278.6	352.6	< MDL	4.6	NM	63.58	52.6	85.5
Aug-9 C	104.4	54.2	< MDL	9.5	NM	48.34	58.0	56.7
Aug-9 E	94.8	< MDL	< MDL	2.5	NM	42.76	27.1	89.4
Aug-9 F	152.1	23.7	< MDL	7.6	NM	90.94	23.1	112.1
Aug-9 G	138.3	60.7	3.7	10.4	NM	65.64	38.3	165.2
Aug-9 H	65.5	122.2	1.3	< MDL	NM	21.88	18.0	24.1
Aug-10 A	115.6	72.0	< MDL	4.1	NM	62.11	33.0	74.2
Aug-10 B	128.6	89.9	17.6	6.0	NM	25.51	22.9	88.3
Aug-10 C	101.4	25.8	< MDL	2.3	NM	3.41	18.5	64.9
Aug-10 E	96.6	123.8	16.6	16.4	NM	< MDL	20.2	74.7
Aug-10 F	< MDL	< MDL	< MDL	8.6	NM	< MDL	24.5	107.2
Aug-10 G	76.5	< MDL	< MDL	11.4	NM	< MDL	28.7	89.0
Average	118.0	92.0	11.5	6.7	6389.6	54.9	34.1	96.7
SDOM	13	14	2	1	303	4	2	5

SDOM represents the standard deviation of the mean
NM indicates no measurement made
<MDL represents below the method detection limit

Table 6-1-4 Coarse mode metal and peroxide concentrations

Sample Date and Run	Metal Activity (ng μg^{-1})						H_2O_2 (ng μg^{-1})
	Fe	Cu	Pb	V	Ca	Zn	
Aug-2 A	1.0	0.0	--	--	54.8	--	0.4
Aug-2 B	0.4	0.1	--	--	67.9	--	0.2
Aug-2 C	0.7	--	0.3	--	87.0	--	0.3
Aug-3 A	0.4	--	--	--	69.0	--	0.4
Aug-3 B	0.8	0.1	0.0	--	67.3	--	0.3
Aug-3 C	1.0	--	0.0	--	71.2	--	0.5
Aug-4 A	0.7	0.0	0.1	--	62.8	--	0.5
Aug-4 B	0.7	--	--	--	80.1	--	0.2
Aug-4 C	0.5	--	0.0	--	71.0	--	0.3
Aug-4 E	0.5	0.1	--	--	51.2	--	0.2
Aug-5 A	0.7	--	--	--	60.8	--	0.4
Aug-5 B	0.6	--	--	--	52.6	--	0.3
Aug-5 C	0.3	--	--	--	61.8	--	0.3
Aug-5 E	0.4	--	--	--	60.0	--	0.3
Aug-5 F	0.7	--	--	--	54.2	--	0.4
Aug-8 A	1.8	1.7	0.1	0.0	--	0.4	0.5
Aug-8 B	1.9	1.7	0.0	--	--	0.7	0.6
Aug-8 C	1.4	1.7	--	0.1	--	--	0.3
Aug-8 E	1.3	0.5	0.1	0.1	--	--	0.4
Aug-8 F	1.3	1.1	0.2	0.0	--	--	0.4
Aug-8 G	0.7	1.4	0.1	0.0	--	--	0.2
Aug-8 H	4.8	0.8	0.2	0.0	--	0.8	0.4
Aug-9 A	2.9	1.3	--	0.2	--	0.9	0.7
Aug-9 B	3.3	4.1	--	0.1	--	0.7	0.6
Aug-9 C	1.8	1.0	--	0.2	--	0.9	1.0
Aug-9 E	1.1	--	--	0.0	--	0.5	0.3
Aug-9 F	1.4	0.2	--	0.1	--	0.8	0.2
Aug-9 G	0.8	0.4	0.0	0.1	--	0.4	0.2
Aug-9 H	2.7	5.1	0.1	--	--	0.9	0.7
Aug-10 A	1.6	1.0	--	0.1	--	0.8	0.4
Aug-10 B	1.5	1.0	0.2	0.1	--	0.3	0.3
Aug-10 C	1.6	0.4	--	0.0	--	0.1	0.3
Aug-10 E	1.3	1.7	0.2	0.2	--	--	0.3
Aug-10 F	--	--	--	0.1	--	--	0.2
Aug-10 G	0.9	--	--	0.1	--	--	0.3
Average	1.3	1.1	0.1	0.1	64.8	0.6	0.4
SDOM [1]	0.1	0.2	0.0	0.01	1.9	0.04	0.0

SDOM represents the standard deviation of the mean

Previous measurements made within the city of Riverside reported that Ca and Fe are the dominant metals (Singh et al., 2002, Chow et al., 1994). Both Chow et al. (1994) and Singh (2002)

conducted extensive particle monitoring and reported metal concentrations in size-fractionated particles. Chow et al. (1994) reported arithmetic average metal concentrations for 24 hour samples. Singh et al. (2002) reported geometric averages. A comparison of metal concentrations obtained in this study with Chow et al. (1994) and Singh (2002) measurements is presented in Table 6-1-5. With the exception of copper, our values are all lower than those of Chow et al. (1994), and with the exception of iron, they are all higher than those of Singh et al. (2002). Coarse mode particles are sensitive to fairly local sources, which, together with differences in sampling dates, may explain the differences.

Table 6-1-5 Average metal concentrations at the Riverside I site in ng per cubic meter.

Metal	PM10			
	Arithmetic Mean		Geometric Mean	
	This Study	Chow et al.	This Study	Singh et al.
Fe	118 ± 17	2950	94	151
Cu	92 ± 18	59	48	3
Ca	6390 ± 415	11960	6180	142
Ba	27 ± 7	82	19	15
Zn	55 ± 8	127	44	4
V	7 ± 1	10	4	1
Pb	12 ± 2	196	7	2

[1] Chow et al. (1994) and Singh et al. (2002) metal averages represent 24 hr averages while measurements made in this study represent 1 to 1.5 hr averages.
[2] Singh reports their averages using a geometric mean; and when making a comparison to those measurements a geometric mean was computed.

Table 6-1-6 shows correlations between aerosol metal concentrations and H_2O_2 generation for both the Riverside I and II studies. In both cases, there was a significant correlation with iron in the particles, with correlation coefficients of 0.48 and 0.65, respectively. A less statistically significant correlation was observed for aluminum at the upwind site, and correlations with Zn and Cu is suggested by the Riverside I (downwind) site, but they were not significant at the 0.05 level. Figure 6-1-4 shows sample-to-sample variations of iron and H_2O_2 generation in the Riverside I data.

Table 6-1-6

Correlation coefficients between H_2O_2 and metals in coarse particles

	upwind site	downwind site
H_2O_2 vs. Fe	**.653(**)**	**.482(**)**
H_2O_2 vs. Al	**.418(*)**	NA
H_2O_2 vs. Cu	-0.007	0.401
H_2O_2 vs. Zn	-0.13	0.509
H_2O_2 vs. Pb	0.135	-0.005
H_2O_2 vs. V	-.395(*)	0.209

** Correlation is significant at the 0.01 level (2-tailed).

* Correlation is significant at the 0.05 level (2-tailed).

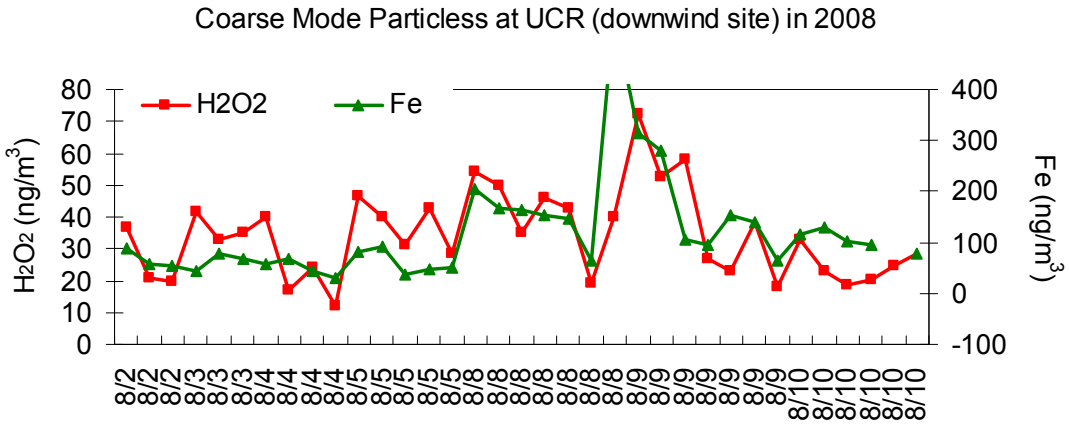

Figure 6-1-4 Coarse mode H_2O_2 levels measured at the Riverside I site. Also shown (with respect to the right hand axis) are iron levels, which correlate with the H_2O_2 levels.

6.2 Riverside II Study

6.2.1 Location and Measurements

The location for these measurements was a trailer located in an isolated section of an orange grove that is part of the UC Riverside agricultural experiment station. The site was 1 km upwind (during all measurements) of the 60 freeway. It is also about 300 m upwind of a moderately travelled surface street. The immediate fetch consists of about 300 m of orange trees that are rarely visited by

motorized vehicles (generally fewer than 10 per day). As such it represents a 'background' site for an area with high levels of particulate pollutants. Influences of very local sources are minimal.

6.2.2 Sampling and Analysis

Sampling was conducted on the June-August 2008 dates shown in Figure 6-2-1. The sampling was terminated early due to the state funding freeze. Because H_2O_2 signals were relatively low, 1 set of 4 hour samples were collected each day. These measurements were made in conjunction with measurements of ultrafine particles that were part of another study, and which will be reported elsewhere. As described above (Section 6.1), measurements of H_2O_2 generation was conducted onsite, and aerosol mass and metals measurements were obtained from paired samples that were stored and analyzed later at UCLA.

6.2.3 Results

Coarse mode aerosol masses at the Riverside II site were also elevated relative to the UCLA and 110 freeway sites, but not as much as the Riverside I site, averaging 50 ± 21 $\mu g/m^3$. H_2O_2 levels ranged between 7 and 35 ng m^3, averaging 17 ± 8 $\mu g/m^3$, similar to the UCLA site which had lower mass loadings but higher activity on a per mass basis (Table 6-1-2) [Is 0.58 ± 0.3 clearly higher than 0.44 ± 0.3?]. Figure 6-2-1 shows iron, aerosol H_2O_2, and aluminum in coarse mode samples from the Riverside II site. They are clearly highly correlated, supporting the notion that transition metals (particularly iron) play a major role in H_2O_2 production by coarse mode aerosols at this site.

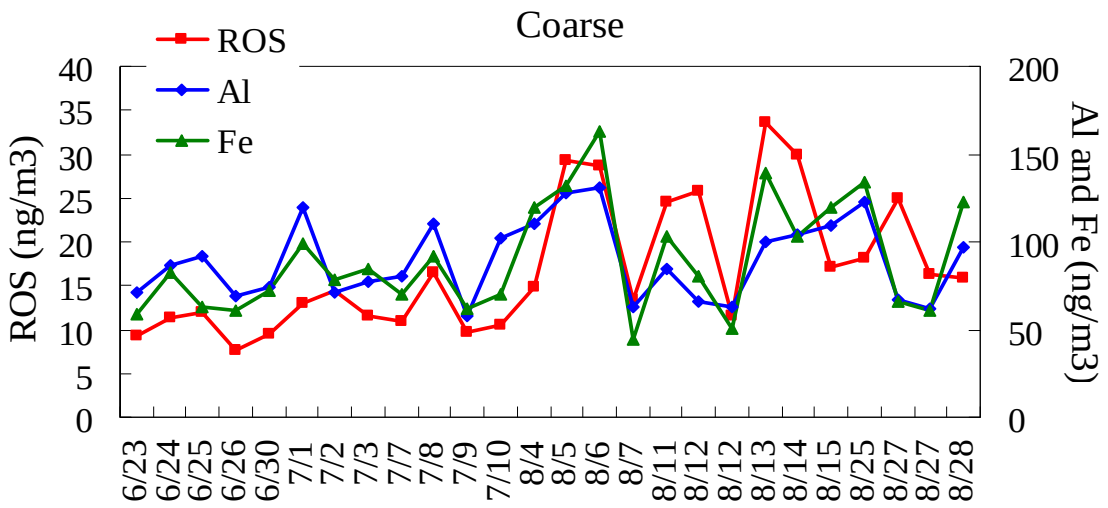

Figure 6-2-1 Coarse mode H_2O_2 levels measured at the Riverside II site. Also shown (with respect to the right hand axis) are iron and aluminum levels, which correlate with the H_2O_2 levels.

7. Acknowledgements

We had the benefit of support and input from many individuals and organizations for this work. Foremost among them is the ARB staff, under the able organization of Ralph Propper, our contract manager. ARB lent us the MOUDI impactor and arranged for the heavy duty diesel truck tests at the Stockton lab. Postdoc Daniel Curtis worked on the project briefly and performed the set up for the Riverside II campaign. The measurements at the first Riverside field study were a part of the SOARS I field campaign that was organized by Prof. J. Jimenez of the University of Colorado at Boulder, and facilitated locally by Prof. Paul Ziemann. The Riverside II measurements were made possible by Michael Kleinman of UC Irvine, who graciously allowed us to work in his trailer. PhD students Hwajin Kim, Leila Lackey, and Albert Chung have all contributed to diesel and chamber measurements made at UCLA.

8. List of Abbreviations

AS	Ammonium Sulfate
CA	California
DPM	Diesel particulate matter
EDTA	Ethylenediaminetetraacetic acid
EtOH	Ethanol
HO_2	Hydroperoxy radical
H_2O_2	Hydrogen Peroxide
HPLC	High Performance Liquid Chromatograph
ICP-OES	Inductively coupled plasma- optical emission spectrometer
L	Liter
Lpm	Liter per minute
M	Molar (moles/liter)
MDL	Method detection limit
MOUDI	Micro orifice uniform deposition impactor
O_2^{-}	Superoxide anion
PM	Particulate Matter
PM10	All particulate matter with diameter less than 10 microns
PM2.5	All particulate matter with diameter less than 2.5 microns
PRS	Physiologically relevant solution
RH	Relative Humidity
ROS	Reactive Oxygen Species
SDOM	Standard deviation of the mean
SOA	Secondary organic aerosol
SS 3.5	Stripping solution adjusted to pH 3.5 (water with 0.1 mM EDTA)
SS 7.4	Stripping solution adjusted to pH 7.4 (water with 0.1 mM EDTA)
UV	Ultraviolet
VI	Virtual Impactor

9. References

Alexis, N.; Barnes, C.; Bernstein, L. I.; Berstein, J. A.; Tarlo, S. M.; Williams, B. P., Health Effects of Air Pollution. Environmental and Occupational Respiratory Disorders **2004,** *114*, (8), 1116-1123.

Anastasio, C., B.C. Faust and C.J. Rao (1997). "Aromatic carbonyl compounds as aqueous-phase photochemical sources of hydrogen peroxide in acidic sulfate aerosols, fogs, and clouds. 1. Non-phenolic methoxybenzaldehydes and methoxyacetophenones with reductants [phenols]." Environmental Science and Technology **31**:218-232.

Arellanes, C.; Paulson, S. E.; Fine, P. M.; Sioutas, C., Exceeding of Henry's Law by Hydrogen Peroxide Associated with Urban Aerosols. Environmental Science and Technology **2006,** *40*, 4859-4866.

Arellanes, C. (2008). The Measurement of Reactive Oxygen Species in Ambient Aerosols Sampled in the Los Angeles Basin. Department of Atmospheric and Oceanic Sciences. Los Angeles, University of California, Los Angeles. **PhD:** 180.

Bast, A. and R. J. A. Goris (1989). "Oxidative Stress: Biochemistry and Human Disease." Pharmaceutisch Weekblad Scientific **11**: 199-206.

Bierkens, J. (2000). "Applications and pitfalls of stress-proteins in biomonitoring." Toxicology **153**(1-3): 61-72.

Brouckaert, P. and W. Fiers (1996). Tumor necrosis factor and the systemic inflammatory response syndrome, in Pathology Of Septic Shock. Pathology of Septic Shock **216:** 167-187.

Brown, D. M., K. Donaldson, P. J. Born, R. P. Schins, M. Dehnhardt, P. Gilmor, L. A. Jimenez and V. Stone (2004). "Calcium and ROS-Mediated Activation of Transcription Factors and TNF-alpha Cytokine Gene Expression in Macrophages Exposed to Ultrafine Particles." American Journal of Physiol. Lung Cell. Mol. Physiol. **286**(L344-L353).

Chebbi, A. and P. Carlier (1996). "Carboxylic acids in the troposphere, occurrence, sources, and sinks: a review." Atmospheric Environment **30**: 4233 - 4249.

Cho, A. K., E. DiStefano, Y. You, C. E. Rodriguez, D. A. Shmmidt, Y. Kumagai, A. H. Miguel, A. Eiguren-Fernandez, E. Kobayashi, E. Avol and J. R. Froines (2004). "Determination of four quinones in diesel exhaust particles, SRM 1649a, and atmospheric PM2.5." Aerosol. Sci. Technol. **38**: 68-81.

Chow, J. C., J. G. Watson, E. M. Fujita, Z. Lu, D. R. Lawson and L. L. Ashbaugh (1994). "Temporal and spatial variations of PM2.5 and PM10 aerosol in the Southern California air quality study." Atmospheric Environment **28**: 2061-2080.

Chung, A., A.A. Lall, and S.E. Paulson (2008), Particulate Emissions by a Small Non-Road Diesel Engine: Biodiesel and Diesel Characterization and Mass Measurements using the Extended Idealized Aggregates Theory. *Atmos. Environ.* DOI:10.1016/j.atmosenv.2007.11.050.

Chung, M. Y., R. A. Lazaro, D. Lim, J. Jackson, J. Lyon, D. Rendulic and A. S. Hasson (2006). "Aerosol-Borne quinones and reactive oxygen species generation by particulate matter extracts." Environmental Science & Technology **40**: 4880-4886.

Chung, M. Y., C. Maris, U. Krischke, A. W. Ho and S. E. Paulson (2003). "An Investigation of the Relationship Between Total Non-Methane Organic Carbon and the Sum of Speciated Hydrocarbons and Carbonyls Measured by Standard GC/FID." Atmospheric Environment **37**: S159-S170.

Chung, M. Y., S. Muthana, P. N. Rodhelen and A. S. Hasson (2005). "Measurements of Effective Henry's Law Constants for Hydrogen Peroxide in Concentrated Salt Solutions." Atmospheric Environment **39**: 2981-2989.

Crim, C. and W. J. Longmore (1995). "Sublethal Hydrogen Peroxide inhibits Alveolar Type II Cell Surfactant Phosolipid Biosynthetic Enzymes." American Journal of Physiology **12**: L129-L135.

Deguillaume, L., M. Leriche, K. Desboefs, G. Mailhot, C. George and N. Chaumerliac (2005). "Transition metals in atmospheric liquid-phases: sources, reactivity and sensitive parameters." Chemical Reviews **105**: 3388-3431.

Deguillaume, L.; Leriche, M.; Monod, A.; Chaumerliac, N., The role of transition metal ions on HOx radicals in clouds: a numerical evaluation of its impact on multiphase chemistry. *Atmospheric Chem. Phys.* **2004,** *4*, 95 - 110.

Dellinger, B., W. A. Pryor, R. Cueto, G. L. Squadrito, V. Hedge and W. A. Deutsch (2001). "Role of Free Radicals in the Toxicity of Airborne Fine Particulate Matter." Chem. Res. Toxicol. **14**: 1371-1377.

Desboefs, K., A. Sofikitis, R. Losno, J. L. Colin and P. Ausset (2005). "Dissolution and Solubility of Trace Metals from Natural and Anthropogenic Aerosol Particulate Matter." Chemosphere **58**: 195-203.

Donaldson, K., V. Stone, P. J. A. Born, L. A. Jimenez, P. S. Gilmour, R. P. F. Schins, A. M. Knaapen, I. Rahman, S. P. Faux, D. M. Brown and W. MacNee (2003). "Oxidative Stress and Calcium Signaling in the Adverse Effects of Environmental Particles (PM_{10})." Free Radical Biology & Medicene **34**(11): 1369-1382.

EPA Toxic Release Inventory. http://www.epa.gov/tri/

Erel, Y., S. O. Pehkonen and M. R. Hoffmann (1993). "Redox chemistry of iron in fog and stratus clouds." Journal of Geophysical Research **98**(D10): 18423-18434.

Ervens, B., G. C. Williams, G. V. Buxton, G. A. Salmon, M. Bydder, F. Wilkinson, F. Dentener, P. Mirabel, R. Wolke and H. Herrmann (2003). "CAPRAM2.4: and extended and condensed tropospheric aqueous phase mechanism and it application." Journal of Geophysical Research **108-D14**: 4426.

Fenton, H. J. H. (1894). "Oxidation of tartaric acid in presence of iron." Journal of the Chemical Society, Transactions **65**:899-910.

Fine, P. M.; Shen, S.; Sioutas, C., Inferring the sources of fine and ultrafine particulate matter at downwind receptor sites in the Los Angeles Basin using multiple continuous measurements. *Aerosol Science and Technology* **2004,** *38 (S1)*, 182-195.

Finlayson-Pitts, B. J. and J. N. J. Pitts (2000). Chemistry of the Upper and Lower Atmosphere. San Diego, Academic Press.

Flynn, C. M. (1984). "Hydrolysis of inorganic iron(III) salts." Chem. Rev. **84**: 31-41.

Friedlander, S. K. and E. K. Yeh (1998). "The Submicron Atmospheric Aerosol as a Carrier of Reactive Chemical Species." Applied Occupational and Environmental Hygiene **13**: 416-420.

Geiser, T., M. Ishigaki, C. vanLeer, M. A. Matthay and V. C. Broaddus (2004). "H2O2 inhibits alveolar epithelial wound repair in vitro by induction of apoptosis." American J. Physiol. Lung Cell. Mol. Physiol. **287**: L448-L453.

Gurtner, G. H., L. S. Farrukh, N. F. Adkinson, A. M. Sciuto, J. M. Jacobson and J. R. Micheal (1987). "The role of arachidonate mediators in peroxide-induced lung injury." American Rev. Respir. Dis. **136**: 2207-2213.

Hartkamp, H. and P. Bachhausen (1987). "A Method for the Determination of Hydrogen Peroxide in Air." Atmospheric Environment **21**: 2207-2213.

Hasson, A. S., A. W. Ho, K. T. Kuwata and S. E. Paulson (2001b). "Production of stabilized Criegee intermediates and peroxides in the gas phase ozonolysis of alkenes. 2. Asymmetric and biogenic alkenes." Journal of Geophysical Research [Atmospheres] **106**:34143-34153.

Hasson, A. S., G. Orzechowska and S. E. Paulson (2001a). "Production of stabilized Criegee intermediates and peroxides in the gas phase ozonolysis of alkenes. 1. Ethene, trans-2-butene, and 2,3-dimethyl-2-butene." Journal of Geophysical Research [Atmospheres] **106**:34131-34142.

Hasson, A. S. and S. E. Paulson (2003). "An investigation of the relationship between gas phase and aerosol borne hydroperoxides in urban air." J. Aerosol Sci. **34**: 459-468.

Heikes, B. G., G. L. Kok, J. G. Walega and A. L. J. Lazrus (1987). "Hydrogen peroxide, ozone, and sulfur dioxide measurements in the lower troposphere over the eastern United States during fall." Journal of Geophysical Research [Atmospheres] **92**:915-931.

Hellpointner, E. and S. Gab (1989). "Detection of methyl, hydroxymethyl and hydroxyethyl hydroperoxides in air and precipitation." Nature **337**:631-634.

Hewitt, C. N. and G. L. Kok (1991). "Formation and Occurrence of Organic Hydroperoxides in the Troposphere: Laboratory and Field Observations." Journal of Atmospheric Chemistry **12**: 181-194.

Hinds, W. C. (1982) Aerosol Technology Wiley: New York.

Holm, B. A., B. B. Hudak, L. Keicher, C. Cavanaugh, R. R. Baker, P. Hu and S. Matalon (1991). "Mechanisms of H2O2-mediated injury to type II cell surfactant mess or 0110 olism and protection with PEG-catalase." American Journal of Physiology. **261**: C751-C757.

Hung, H. F. and C. S. Wang (2001). "Experimental determination of reactive oxygen species in Taipei aerosols." J. Aerosol Sci. **32**: 1201-1211.

Imrich, A., Y. Y. Ning, H. Koziel, B. Coull and L. Kobzik (1999). "Lipopolysaccharide priming amplifies lung macrophage tumor necrosis factor production in response to air particles." Toxicology and Applied Pharmacology **159**(2): 117-124.

Jackson, A. V. and C. N. Hewitt (1999). "Atmosphere Hydrogen Peroxide and Organic Hydroperoxides: A Review." Chemical Reviews in Environmental Science and Technology **29**(2): 175-228.

Jung, H., B. Gou, C. Anatasio and I. M. Kennedy (2006). "Quantitative measurements of the generation of hydroxyl radicals by soot particles in a surrogate lung fluid." Atmospheric Environment **40**: 1043-1052.

Junkermann, W., M. Fels, P. Pietruk, F. Slemr and J. Hahn (1993). "Peroxide measurements at remote mountain field sites (Wank-1780 m. and 1175 m.): seasonal and diurnal variations of hydrogen peroxide and organic peroxides." Photo-oxid.: Precursors Prod., Proc. EUROTRAC Symp. '92, 2nd 180-184.

Kanapilly, G. M., O. G. Raabe and C. H. T. Goh (1973). "Measurement of in vitro dissolution of aerosol particles for comparison to in vivo dissolution in the lower respiratory tract after inhalation." Health Phys **24**: 497-507.

Kehrer, J. P. (1993). "Free radicals as mediators of tissue injury and disease." Critical Reviews in Toxicology **23**:21-48.

Khwaja, H. A. (1995). "Atmospheric concentrations of carboxylic acids and related compounds at a semi urban site." Atmospheric Environment **29**(1): 127-139.

Kieber, R. J.; Skrabal, S. A.; Smith, B. J.; Wiley, J. D., Organic Complexation of Fe(II) and Its Impact on the Redox Cycling of Iron in Rain Environmental Science & Technology **2005,** *39*, 1576-1583.

Kim, S.; Shen, S.; Sioutas, C.; Zhu, Y.; Hinds, W. C., Size Distribution and Diurnal and Seasonal Trends of Ultrafine Particles in Source and Receptor Sites of the Los Angeles Basin. *J. Air & Waste Manage. Assoc.* **2002,** *52*, 297-307.

Kittleson, D. B., Engines and Nanoparticles: A Review. *Journal of Aerosol Science* **1998,** *29*, (5/6), 575-588.

Kleeman, M. J., Cass, G. R., Source contribution to the size and composition distribution of urban particulate air pollution. *Atmospheric Environment* **1998,** *32*, 2803-2816.

Kleinman, M. T., C. Sioutas, M. C. Chang, A. J. F. Boere and F. R. Cassee (2003). "Ambient fine and coarse particle suppression of alveolar macrophage functions." Toxicology letters **137**:151-158.

Laskin, D. L. and K. J. Pendino (1995). "Macrophages and inflammatory mediators in tissue injury." Annual Review of Pharmacology and Toxicology **35**:655-677.

Lee, M., B. G. Heikes and D. W. O'Sullivan(2000). "Hydrogen Peroxide and Organic Hydroperoxide in the Troposphere: A Review." Atmospheric Environment **34**:3475-3494.

Li, N., C. Sioutas, A. K. Cho, D. A. Schmitz, C. Misra, J. Sempf, M. Wang, T. Oberley, J. Froines and A. E. Nel (2003). "Ultrafine Particulate Pollutants Induce Oxidative Stress and Mitochondrial Damage." Environmental Health Perspectives **111**: 455-460.

Li, N., M. Venkatesan, A. H. Miguel, R. Kaplan, C. Gujuluva, J. Alam and A. E. Nel (2000). "Induction of heme oxygenase-1 expression in macrophages by diesel exhaust chemicals and quinones via the antioxidant-responsive element." J. Immunol. **165**: 3391-3401.

Li, N., M. Wang, T. D. Oberley, J. M. Sempf and A. E. Nel (2002). "Comparison of the pro-oxidative and pro-inflammatory effects or organic diesel exhaust particle chemicals in bronchial epithelial cells and macrophages." J. Immunol. **169**: 4531-4541.

Li, T.-H. and K. A. Hooper (2000). "An exposure system to study the effects of water-soluble gases on PM-induced toxicity." Inhalation Toxicology **12**: 563-576.

Li, X. Y., P. S. Gilmour, K. Donaldson and W. MacNee (1996). "Free radical activity and pro-inflammatory effects of particulate air pollution (PM_{10}) in vivo and in vitro." Thorax **51**: 1216-1222.

Lightfoot, P. D., R. A. Cox, J. N. Crowley, M. Destriau, G. D. Hayman, M. E. Jenkin, G. K. Moortgat and F. Zabel(1992). "Organic peroxy radicals: kinetics, spectroscopy and tropospheric chemistry." Atmospheric Environment, Part A: General Topics **26A**: 1805-1961.

Mathis, U.; Mohr, M.; Kaegi, R.; Bertola, A.; Boulouchos, K., Influence of diesel engine combustion parameters on primary soot particle diameter. Environmental Science & Technology **2005,** 39, 1887-1892.

Marple, V. A., K. L. Rubow and S. M. Behm (1991). "A Microorifice Uniform Deposition Impactor (MOUDI): Description, Calibration and Use." Aerosol Science and Technology **14**: 434-446.

Morio, L. A., K. A. Hooper, J. Brittingham, T.-H. Li, R. E. Gordon, B. J. Turpin and D. L. Laskin (2001). "Tissue Injury Following Inhalation of Fine Particulate Matter and Hydrogen Peroxide is Associated with Altered Production of Inflammatory Mediators and Antioxidants by Alveolar Macrophages." Toxicology and Applied Pharmacology **177**: 188-199.

Murano, F., S. Boland, V. Bonvallot, A. Baulig and A. Baeza-Squiban (2002). "Human airway epithelial cells in culture for studying the molecular mechanisms of the inflammatory response triggered by diesel exhaust particles." Cell Biol. Toxicol. **18**: 315-320.

Murphy, DM, Cziczo, DJ, Hudson, PK, Thompson, JC, Wilson DK, Kojima, T, Busek, P. Particle generation and resuspension in aircraft inlets when flying in clouds. Aerosol Science and Technology: **38**: 400-408.

Na, K., A. A. Sawant, C. Song and D. R. Cocker (2004). "Primary and secondary carbonaceous species in the atmosphere of Western Riverside County, California." Atmospheric Environment **38**: 1345-1355.

Oosting, R. S., L. Van Bree, J. F. Van Iwaarden, L. M. G. Van Golde and J. Verheof (1990). "Impairment of phagocytic functions of alveolar macrophages by hydrogen peroxide." American J. Physiol. **259**: L87-L94.

Park, S.; Nam, H.; Chung, N.; Park, J.-D.; Lim, Y., The role of iron in reactive oxygen species generation from diesel exhaust particles. Toxicology in Vitro **2006,** 20, 851-857.

Pehkonen, S. O., Y. Erel, and M. R. Hoffmann (1992). "Simultaneous spectrophotometric measurement of Fe(II) and Fe(III) in atmospheric water." Environmental Science & Technology **26**: 1731-1736.

Pehkonen, S. O., R. Siefert, Y. Erel, S. M. Webb, and M. R. Hoffmann (1993). "Photoreduction of iron oxyhydroxides in the presence of important organic compounds." Environmental Science & Technology **27**: 2056-2062.

Pope, A. C., R. T. Burnett, M. J. Thun, C. E. Eugenia, D. Krewski, K. Ito and G. D. Thurston (2002). "Lung Cancer, Cardiopulmonary Mortality and Long-term Exposure to Fine Particulate Matter Air Pollution." Journal of American Medical Association **287**: 1132-1141.

Sagai, M.; Lim, H. B.; Ichinose, T., Lung carcinogenesis by diesel exhaust particles and the carcinogenic mechanism via active oxygens. Inhalation Toxicol. **2000,** 12, 215-223.

Sagai, M., H. Saito, T. Ichinose, M. Kodama and Y. Mori (1993). "Biological effects of diesel exhaust particles. I. In vitro production of superoxide and in vivo toxicity in mouse." Free Radical Biology and Medicine **14**: 37-47.

Salvi, S. and S. T. Holgate (1999). "Mechanisms of Particulate Matter Toxicity." Clinical and Experimental Allergy **29**: 1187-1194.

Samet, J.M. (2002). "Air pollution and epidemiology: "déjà vu all over again?"" Epidemiology 13:118-119.

Samet, J., R. Wassel, J. K. Holmes, E. Abt and K. Bakshi (2005). "Research Priorities for Airborne Particulate Matter in the United States." Environmental Science and Technology **39**(14): 299A-304A.

Sander, R. (1999). "Compilation of Henry's Law Constants for Inorganic and Organic Species of Potential Importance in Environmental Chemistry (Version 3)." from http://www.mpch-mainz.mpg.de/~sander/res/henry.html.

Sardar, S. B.; Fine, P. M.; Sioutas, C., Seasonal and Spatial Variability of the Size-Resolved Chemical Composition of Particulate Matter (PM10) in the Los Angeles Basin. Journal of Geophysical Research **2005,** 110, DO7S08.

Schins, R. P. F., J. H. Lightbody, P. J. A. Borm, T. Shi, K. Donaldson and V. Stone (2004). "Inflammatory effects of coarse and fine particulate matter in relation to chemical and biological constituents." Toxicology and Applied Pharmacology **195**:1-11.

See, S. W., Wang, Y. H., Balasubramanian, R., Contrasting reactive oxygen species and transition metal concentrations in combustion aerosols. Environmental Research **2007,** 103, 317-324.

Seinfeld, J. H. and S. N. Pandis (1998). "Atmospheric Chemistry and Physics." John Wiley and Sons: New York City.

Shi, J. P.; Mark, D.; Harrison, R. M., Characterization of Particles from a Current Technology Heavy-Duty Diesel Engine. Environmental Science & Technology **2000,** 34, 748-755.

Siefert, R., S. O. Pehkonen, Y. Erel and M. R. Hoffmann (1994). "Iron photochemistry of aqueous suspensions of ambient aerosols with added organic acids." Geochemica et Cosmochimica Acta **58**(15): 3271-3279.

Sies, H. (1986). "Biochemistry of Oxidative Stress." Angewandte Chemie **25**: 1058-1071.

Singh, M.; Jacques, P. A.; Sioutas, C., Size distribution and diurnal characteristics of particle-bound metals in source and receptor sites of the Los Angeles Basin. Atmospheric Environment **2002,** *26*, 1675-1689.

Sloane, CS, Wolff, GT (1985). Prediction of ambient light-scattering using a physical model responsive to relative-humidity - validation with measurements from Detroit. Atmospheric Environment: 19 (4), 669-680.

Sporn, P. H. S., T. M. Marshall and M. Peters-Golden (1992). "Hydrogen peroxide increases the availability of arachidonic acid for oxidative metabolism by inhibiting acylation into phospholipids in the alveolar macrophage." American J. Respir. Cell Mol. Biol. **7**: 307-316.

Squadrito, G. L., R. Cueto, B. Dellinger and W. A. Pryor (2001). "Quinoid redox cycling as a mechanism for sustained free radical generation by inhaled airborne particulate matter." Free Radical Biology & Medicene **31**(9): 1132-1138.

Srendi-Kenigsbuch, D., T. Kambayshi and G. Strassman (2000). "Neutrophils augment the release of TNF alpha from LPS-simulated macrophages via hydrogen peroxide." Immunology Letters **71**(2): 97-102.

Tolbert, M. A., M. Klein, K. B. Metzger, J. Peel, W. D. Flanders, K. Todd, J. A. Mulholland, P. B. Ryan and H. Frumkin (2000). "Interim results of the study of particulates and health in Atlanta (SOPHIA)." Journal of Exposure Analysis and Environmental Epidemiology **10**:446-460.

Venkatachari, P., P. K. Hopke, W. H. Brune, R. Xinrong, R. Lesher, J. Mao and M. Mitchell (2007). "Characterization of Wintertime Reactive Oxygen Species Concentrations in Flushing, New York." Aerosol Science and Technology **41**: 97-111.

Venkatachari, P., P. K. Hopke, B. D. Grover and D. J. Eatough (2005). "Measurement of Particle Bound Reactive Oxygen Species in Rubidoux Aerosols." Journal of Atmospheric Chemistry **50**: 49-58.

Vidrio E, Jung H., Anastasio C. (2008). Generation of hydroxyl radicals from dissolved transition metals in surrogate lung fluid solutions. Atmospheric Environment: **18**: 4369-4379.

Virtanen, A. K. K.; Ristimaki, J. M.; Vaaraslahti, K. M.; Keskinen, J., Effect of engine load on diesel soot particles. Environmental Science & Technology **2004,** *38*, 2551-2556.

Utell, M. J. and M. W. Frampton (2000). "Acute health effects of ambient air pollution: the ultrafine particle hypothesis." Journal of Aerosol Medicine **13**:355-359.

Wagner, J. M. and R. A. Roth (2000). "Neutrophil migration mechanisms, with an emphasis on the pulmonary vasculature." Pharmacological Reviews **52**(3): 349-374.

Wehril, B., B. Sulzberger and S. Werner (1989). "Redox processes catalyzed by hydrous oxide surface." Chemical Geology **78**: 167-189.

Wexler, A. S. and R. Sarangapani (1998). "Particles do not Increase Vapor Deposition in Human Airways." Journal of Aerosol Science **29**: 197-204.

Zepp, R. G., Faust, B. C.; Hoigne, J., Hydroxyl radical formation in aqueous reactions (pH 3-8) of iron(II) with hydrogen peroxide: the photo-Fenton reaction. Environmental Science & Technology **1992,** *26*, 313-319.

Zuo, Y. and Y. W. Deng (1997). "Iron(II) catalyzed photochemical decomposition of oxalic acid and the generation of H_2O_2 in atmospheric liquid phases." Chemosphere **35**: 2051-.

Zuo, Y. and J. Hoigne (1992). "Formation of hydrogen peroxide and depletion of oxalic acid in atmospheric water by photolysis of iron(III)-oxalato complexes." Environmental Science & Technology **26**: 1014-1022.